PRONTO: Protontherapy and nuclear techniques for oncology

L.M. Fraile
Grupo de Física Nuclear & IPARCOS
Universidad Complutense
Madrid, Spain

Instituto de Investigación Sanitaria del Hospital
Clínico San Carlos (IdISSC)
Madrid, Spain

Pronto
Protontherapy and nuclear techniques for oncology

gfn UCM
Grupo de Física Nuclear

Acknowledgements and material

- ✓ A lot of material taken from
  - → Bernard Gottschalk, Harvard University
    - https://gray.mgh.harvard.edu/teaching/proton-techniques
  - → Samuel España, Universidad Complutense
  - → Daniel Sánchez Parcerisa, Universidad Complutense
  - → PTCOG [*Particle Therapy Co-Operative Group*]
    - https://www.ptcog.ch/
  - → Katia Parodi - LMU Munich
  - → Harald Paganetti
    - "Proton Therapy Physics", First Edition, CRC Press

Outline

- ✓ Introduction
- ✓ Physical quantities
- ✓ Range in protontherapy
- ✓ Main problems
- ✓ Some detetion techinques to assess range
- ✓ Production of radioistopes and proof of principle
- ✓ PRONTO

At the beginning...

[Gottschalk]

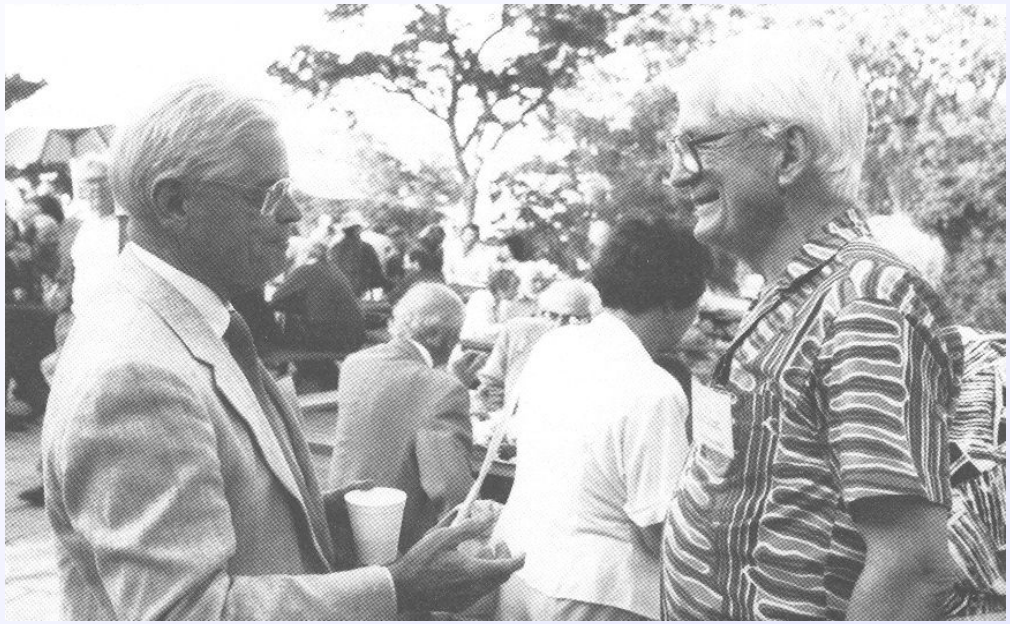

Robert R. Wilson (left) designed the first cyclotron (moved to Cornell before it was actually built). Norman Ramsey was its first Director (right)

Wilson wrote the short paper that triggered proton radiotherapy ("Radiological use of fast protons", Radiology **47** (1946) 487)

- The second Harvard Cyclotron available on 15 June 1949.
- Used for nuclear structure studies
- Upgraded in 1956 and in clinical use in the mid 1960s, after monkey studies (**William Preston** and **Andrew Koehler**).
- First treatments by Dr. Ray Kjellberg, were single fraction "radiosurgery" of intracranial targets.
- Fractionated therapy of larger tumors, began under the supervision of Dr. Herman Suit and Michael Goitein sin 1974.
- The last patient, a one year old infant, was treated 10 April 2002.

A new old problem

Preston and Koehler,
Submitted but never published

[Gottschalk]

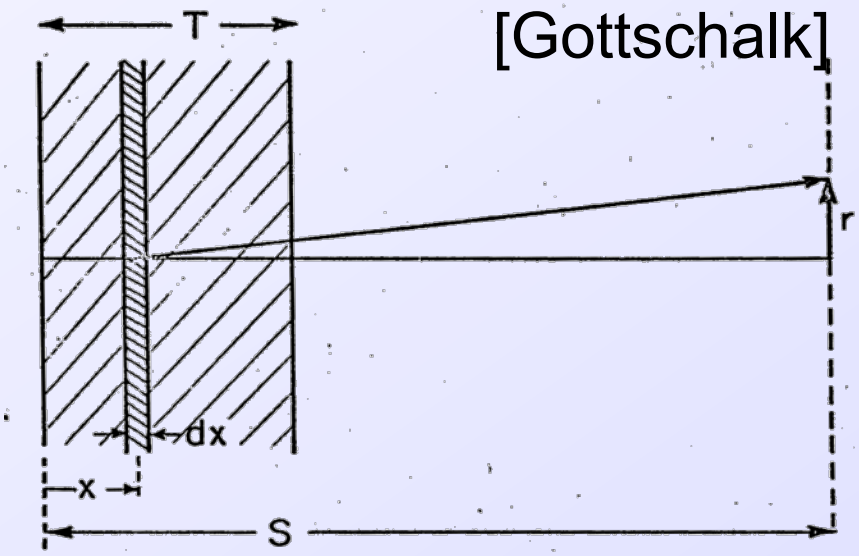

The Effects of Scattering on Small Proton Beams

W. M. Preston and A. M. Koehler

Department of Physics, Harvard University

Cambridge, Massachusetts

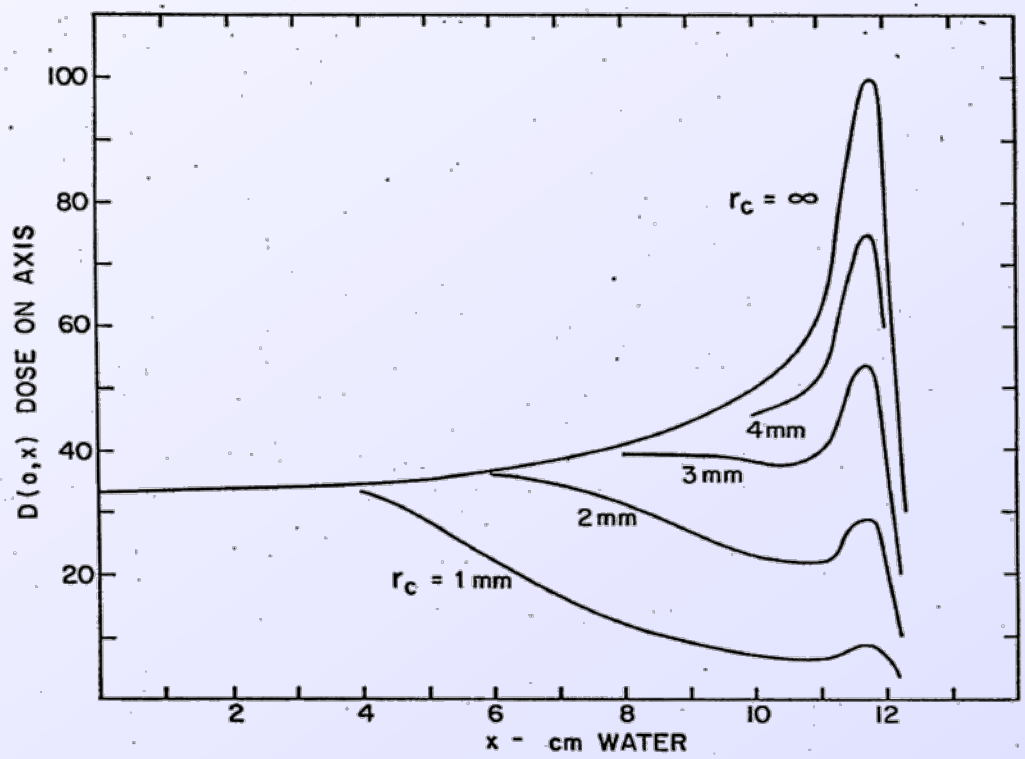

FIGURE 7

FIGURE I

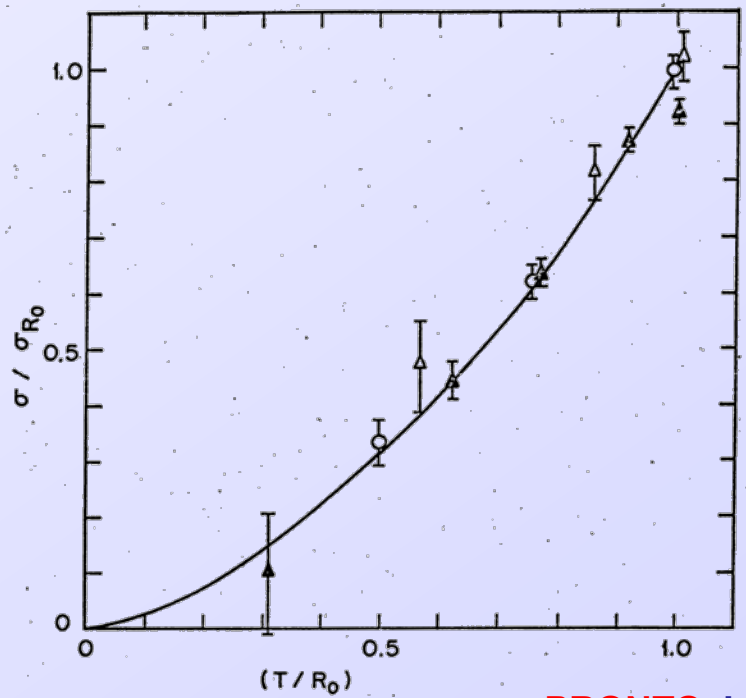

FIGURE 17

The basic concept

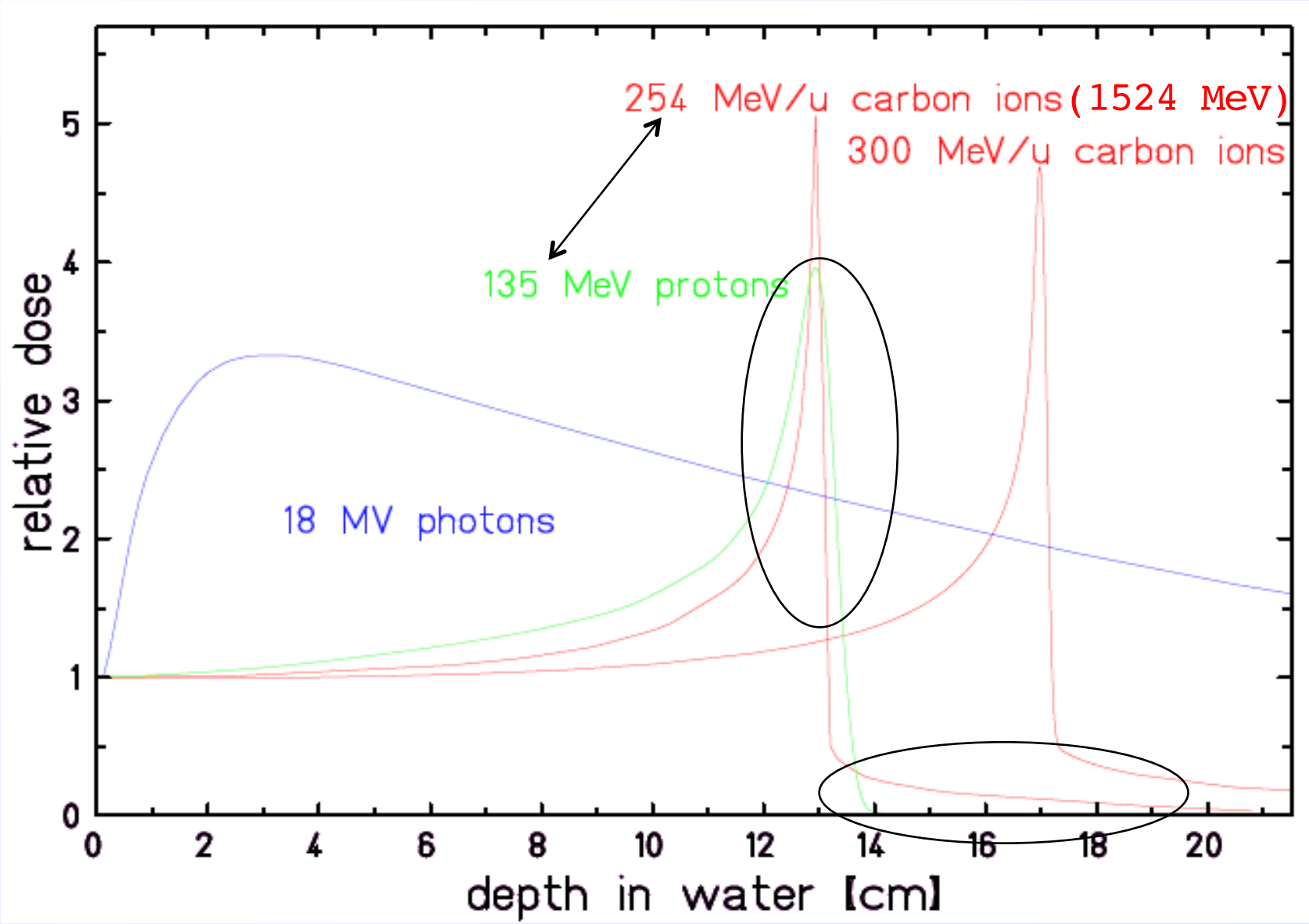

The concept, in practice...

[S-Parcerisa]

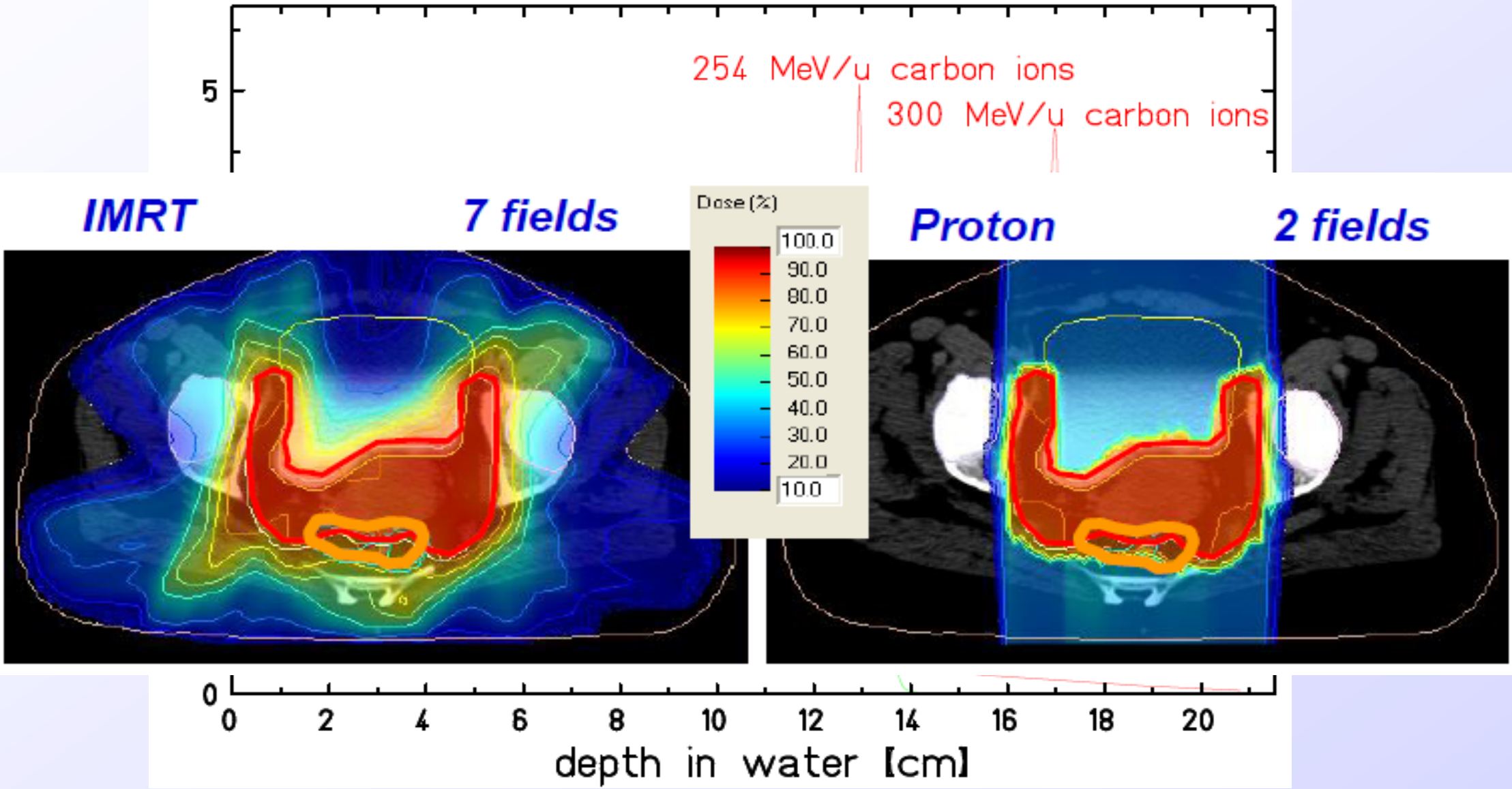

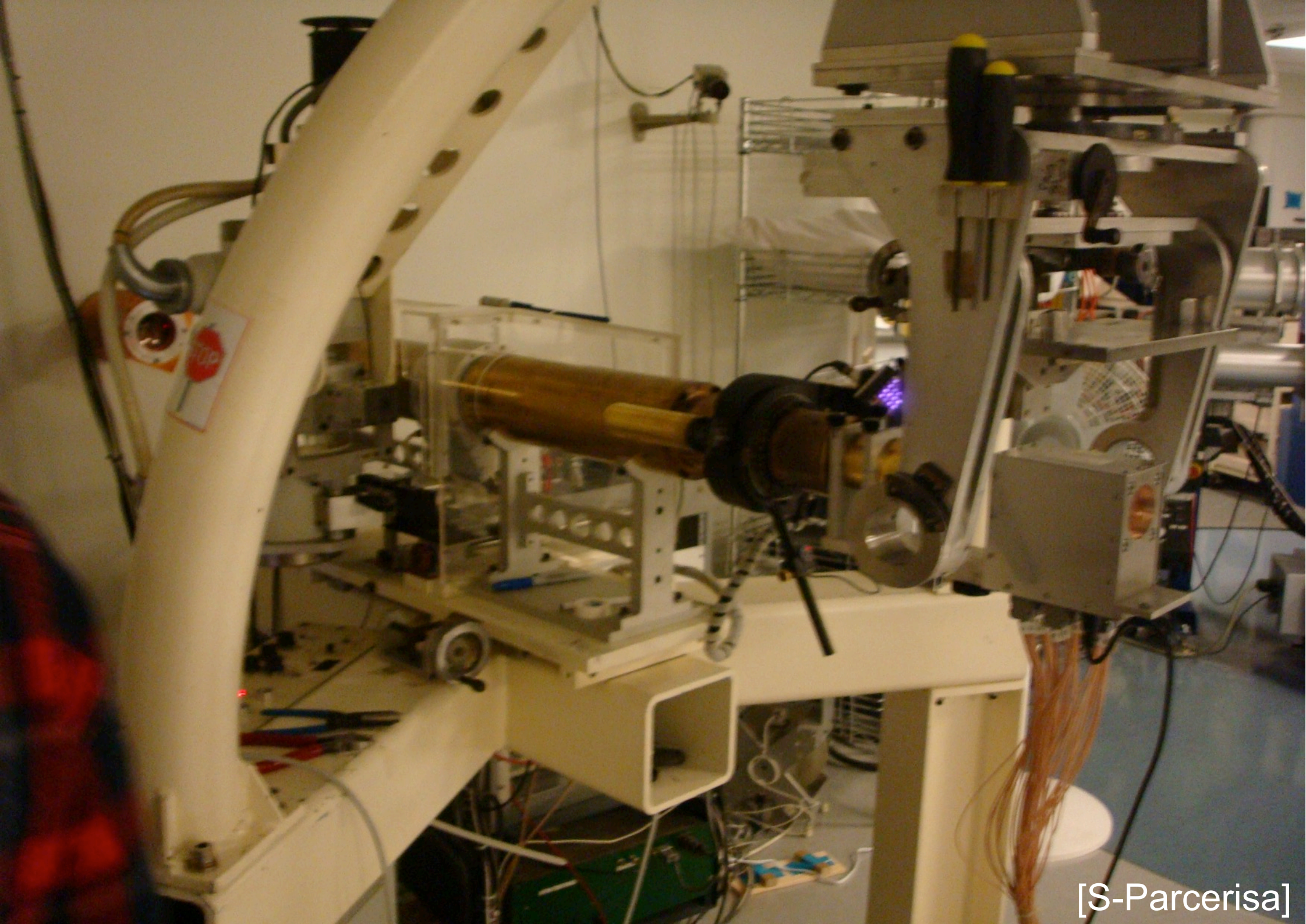
[S-Parcerisa]

An artist view (IBA)

Commercial...

80+ Treatment Rooms to be Operational in Europe by 2020

Number of Treatment Rooms In Each Country

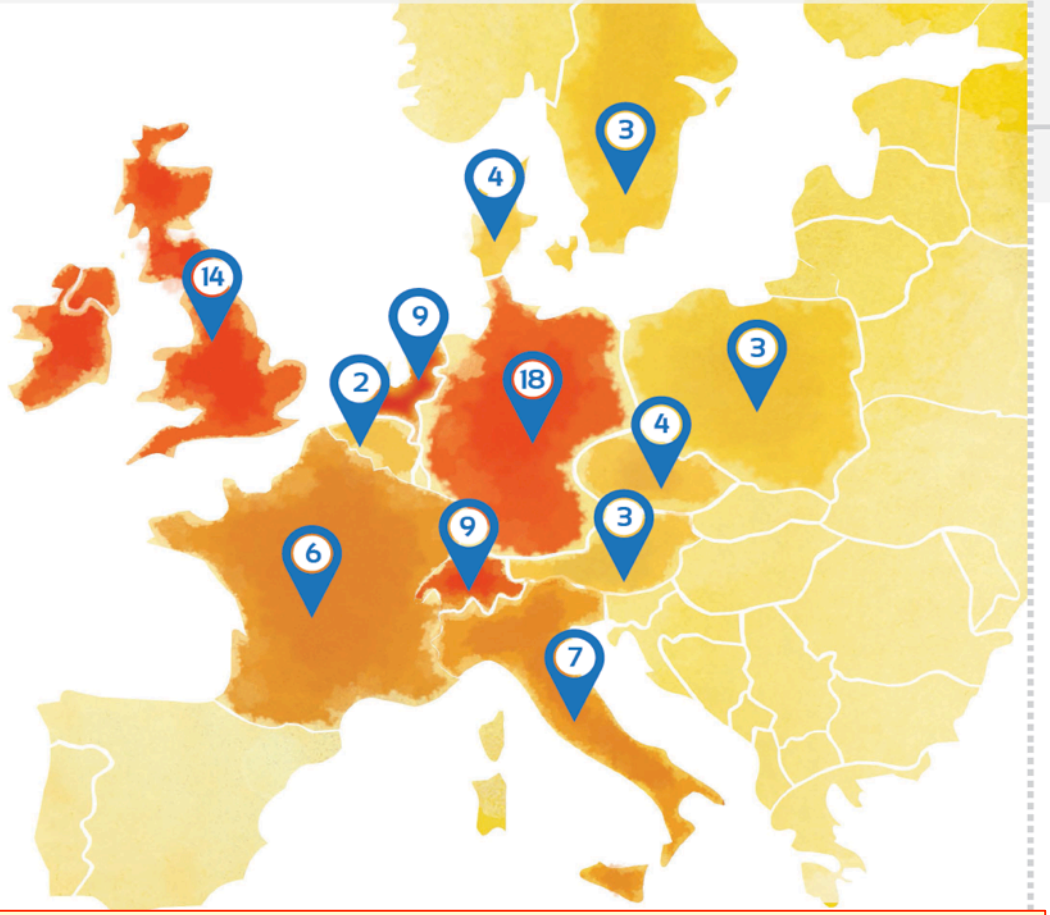

Treatment Rooms are Spread Across 35 Proton Therapy Centres* in 12 European Countries: Germany and UK Leading the Pack

*Planned and operational

Number of Treatment Rooms Per City

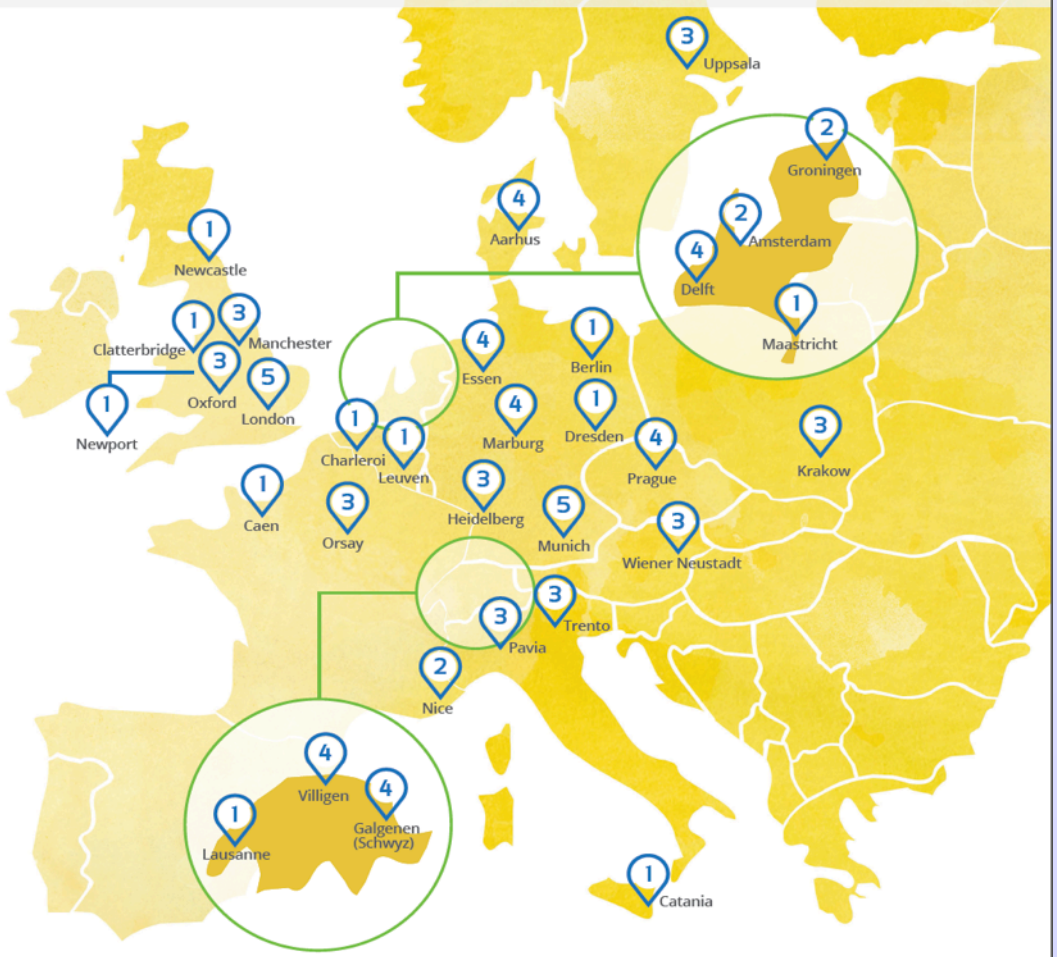

PTCOG end of 2016:

- 56 proton facilities in operation
- 150000 patients treated

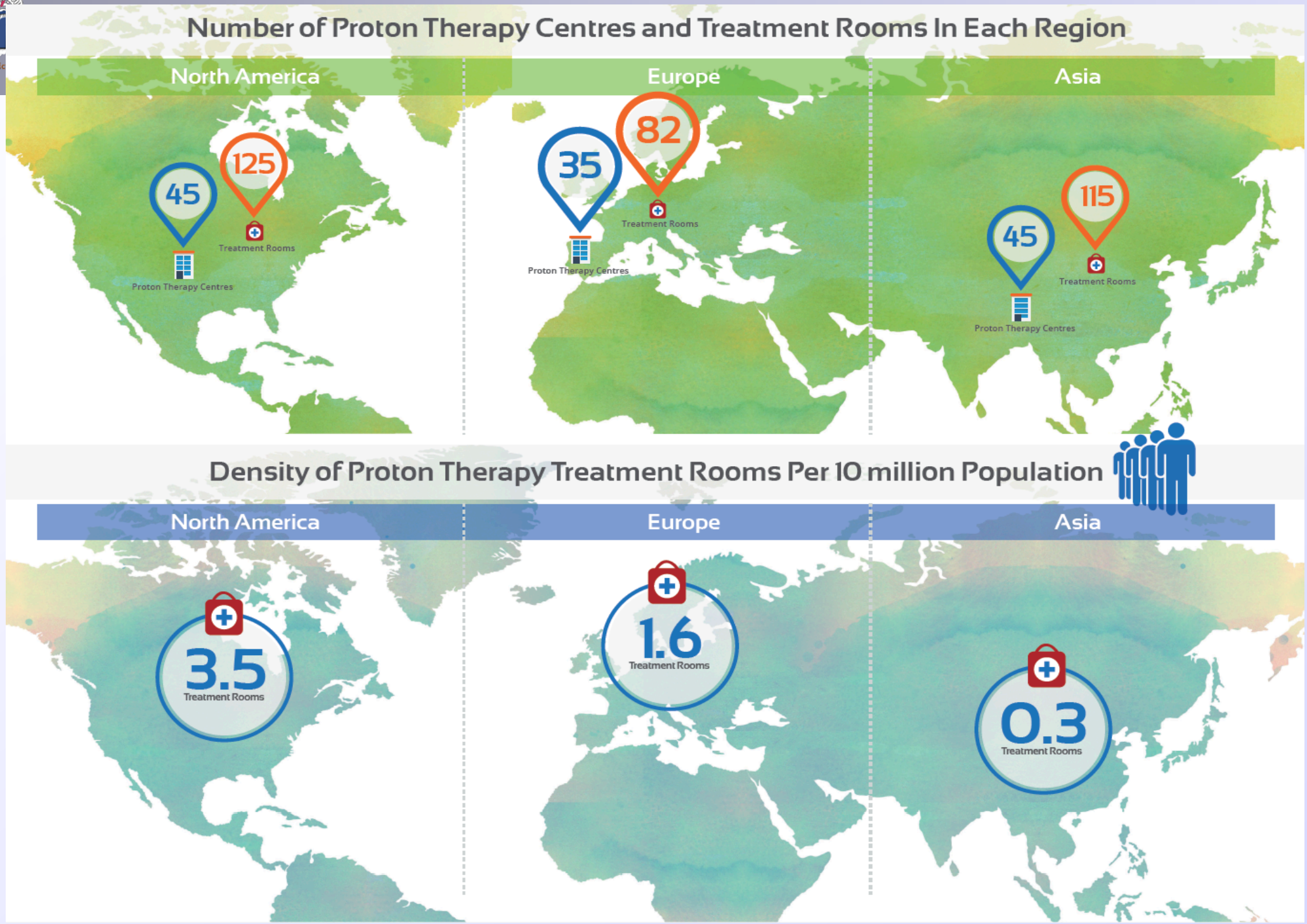
Number of Proton Therapy Centres and Treatment Rooms In Each Region
North America
45
Proton Therapy Centres
125
Treatment Rooms
Europe
35
Proton Therapy Centres
82
Treatment Rooms
Asia
45
Proton Therapy Centres
115
Treatment Rooms
Density of Proton Therapy Treatment Rooms Per 10 million Population
North America
3.5
Treatment Rooms
Europe
1.6
Treatment Rooms
Asia
0.3
Treatment Rooms

Anuncio Quirónsalud

quirónsalud
La salud persona a persona

Red hospitalaria | Cuadro médico | Investigación e innovación | Calidad | Comunicación | El grupo

Inicio | Comunicación | Notas de prensa

Notas de prensa

Quirónsalud pondrá en marcha el primer centro de terapia de protones de España

4 de enero de 2017

Quirónsalud, en su compromiso por mantenerse siempre a la vanguardia de los últimos tratamientos médicos disponibles, invertirá en torno a 40 millones de euros para construir y equipar el primer centro de protonterapia de España, que empezará a tratar a los primeros pacientes a comienzos de 2019. El centro se ubicará en Madrid y estará abierto a pacientes de todas las procedencias, tanto de la sanidad pública como privada, y sus profesionales trabajarán de forma coordinada con los médicos de referencia de los pacientes para garantizar la continuidad de la atención. Además de ofrecer atención de excelencia a pacientes con cáncer, el centro será un espacio de innovación e investigación que contribuirá con sus proyectos a la mejora de los resultados de los tratamientos del cáncer y de la calidad de vida de los pacientes.
La radioterapia de protones es, en la actualidad, el tratamiento de elección en muchos tipos de cáncer debido a su eficacia igual o superior a la radioterapia convencional y sus menores efectos secundarios, eliminados en gran medida. Entre los beneficios de la protonterapia destacan la mínima, incluso nula, radiación en los

Anuncio Clínica Universidad de Navarra (CUN)

HITACHI
Inspire the Next

News Release

FOR IMMEDIATE RELEASE

Hitachi to Install New Proton Beam Therapy System in Spain

Tokyo, December 15, 2017--- Hitachi, Ltd. (TSE:6501) today announced that it has entered into an agreement to provide Clínica Universidad de Navarra (CUN) with its proton beam therapy (PBT) system. The agreement includes PBT system maintenance following completion of the systems' installation.

The PBT System will be installed at CUN's facility in Madrid, Spain and is equipped with state of the art technology including spot scanning capability* for treating certain forms of cancer. The System includes a compact synchrotron accelerator, full rotating gantry with cone beam CT and the option to add an additional gantry treatment room in the future. PBT patient treatment using the new system is expected to start at the hospital in the spring of 2020.

Cancer incidence

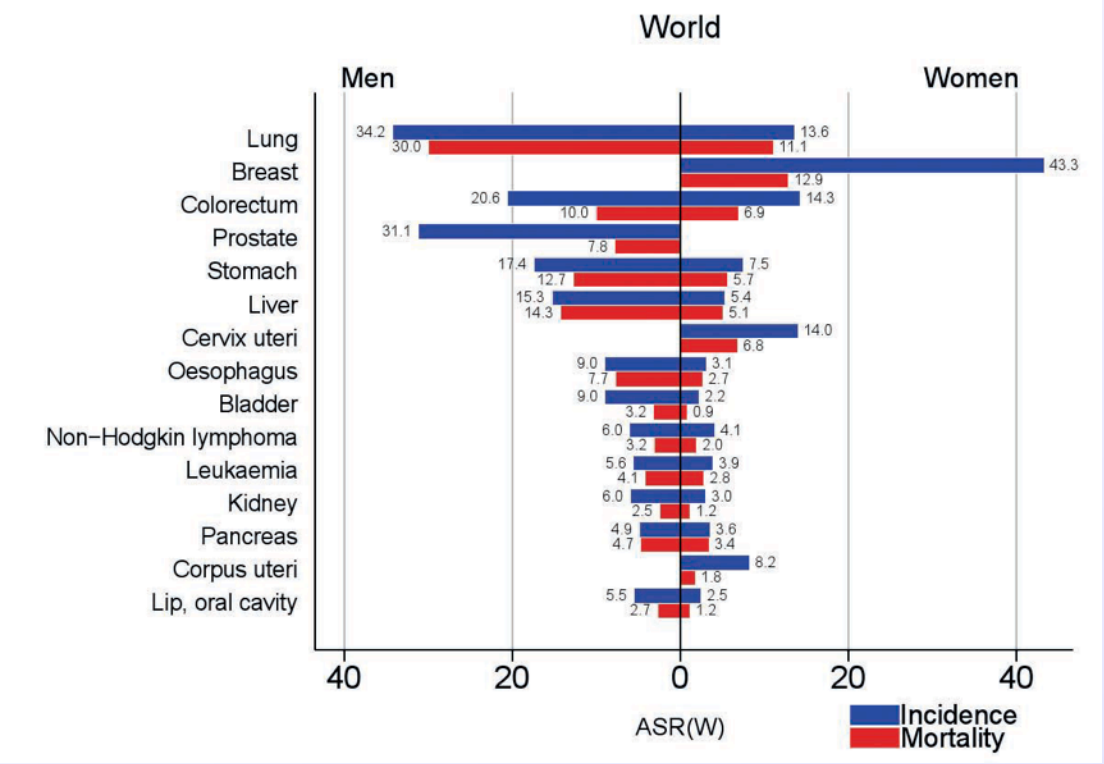

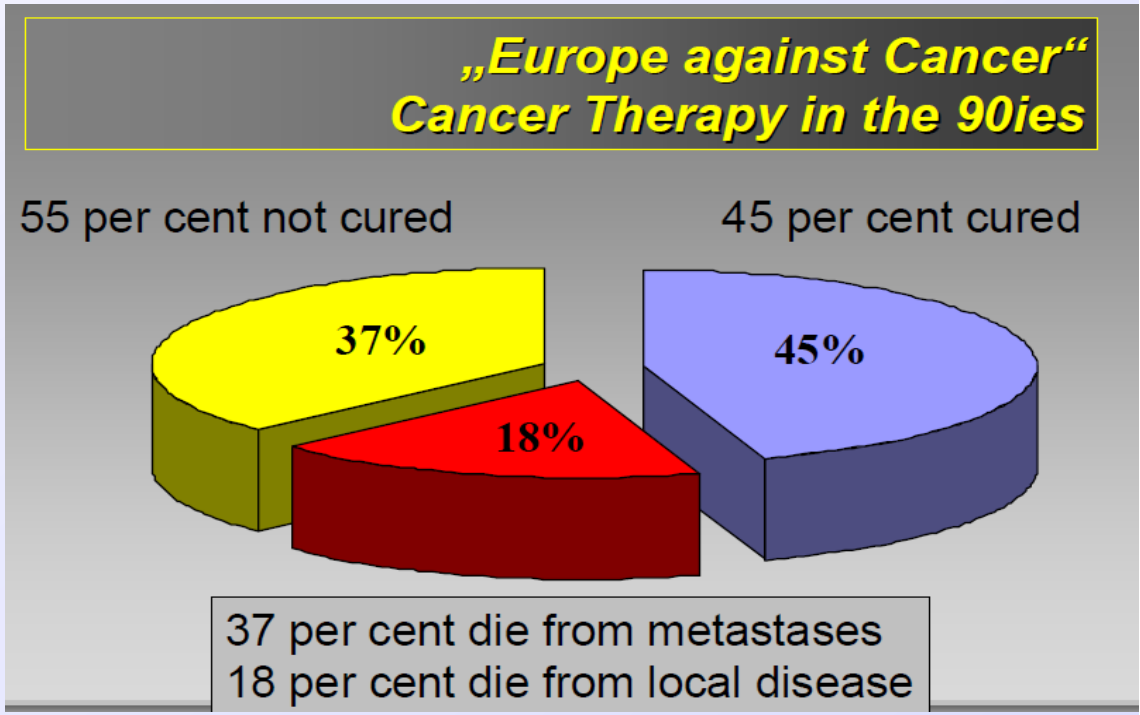

[World Cancer Report 2014]

[S-Parcerisa]

Cancer treatment modalities

More localized

Protons

More systemic

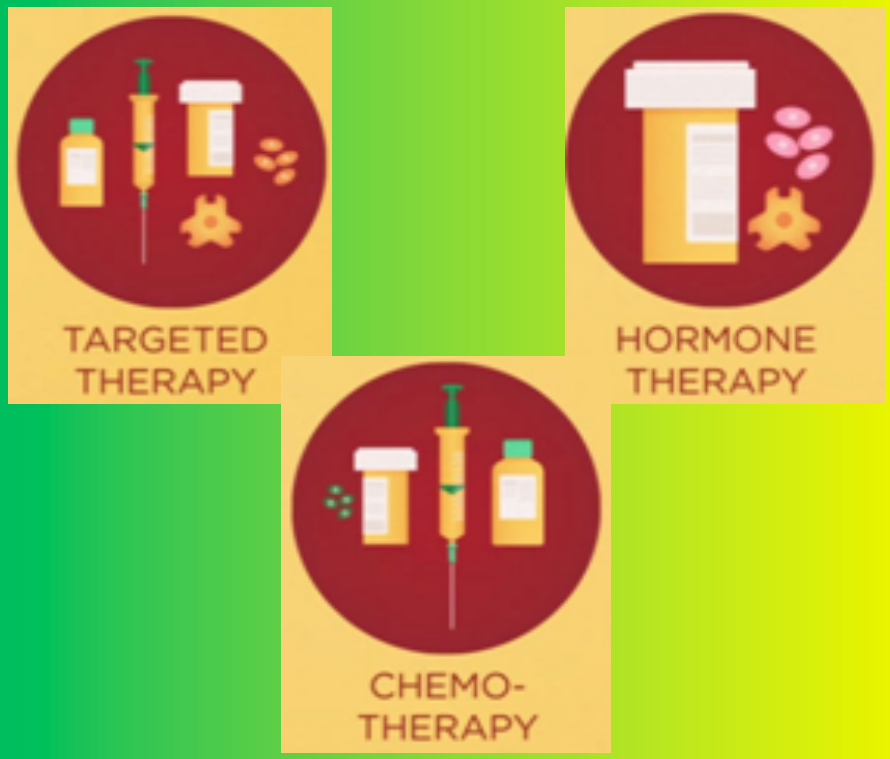

[S-Parcerisa]

Advantages of hadrontherapy

1. Improve local control

→ Dose insufficient to cure the tumor

→ Tumor located near to OAR (organs at risk)

→ With protons:

- optimize dose deposited in the tumor
- without increasing dose to OAR
- Dose escalation

2. Prevention or reduction of radiation-induced site effects

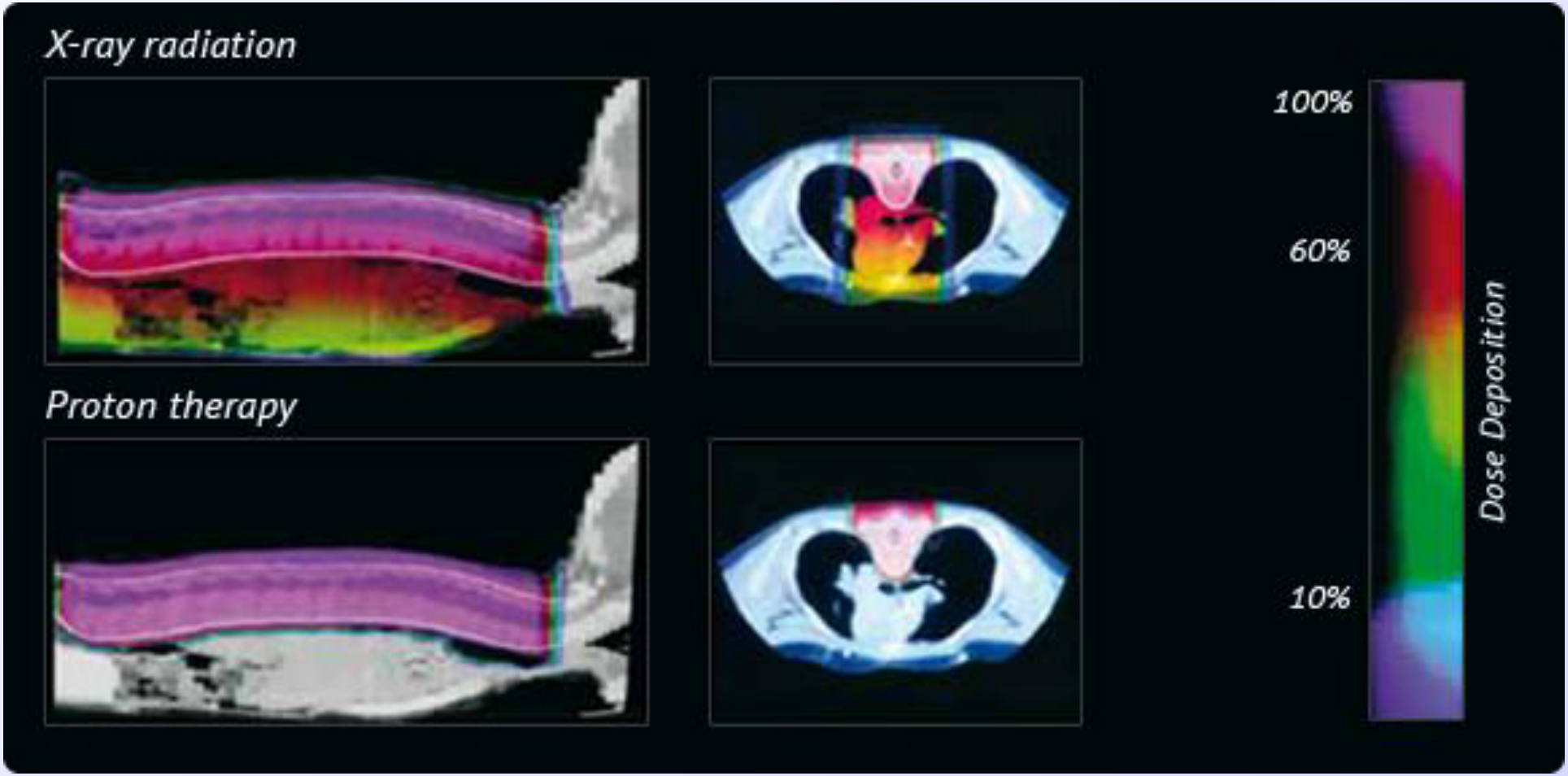

Advantages of hadrontherapy

Reduction of *acute* toxicity (clinical benefit)

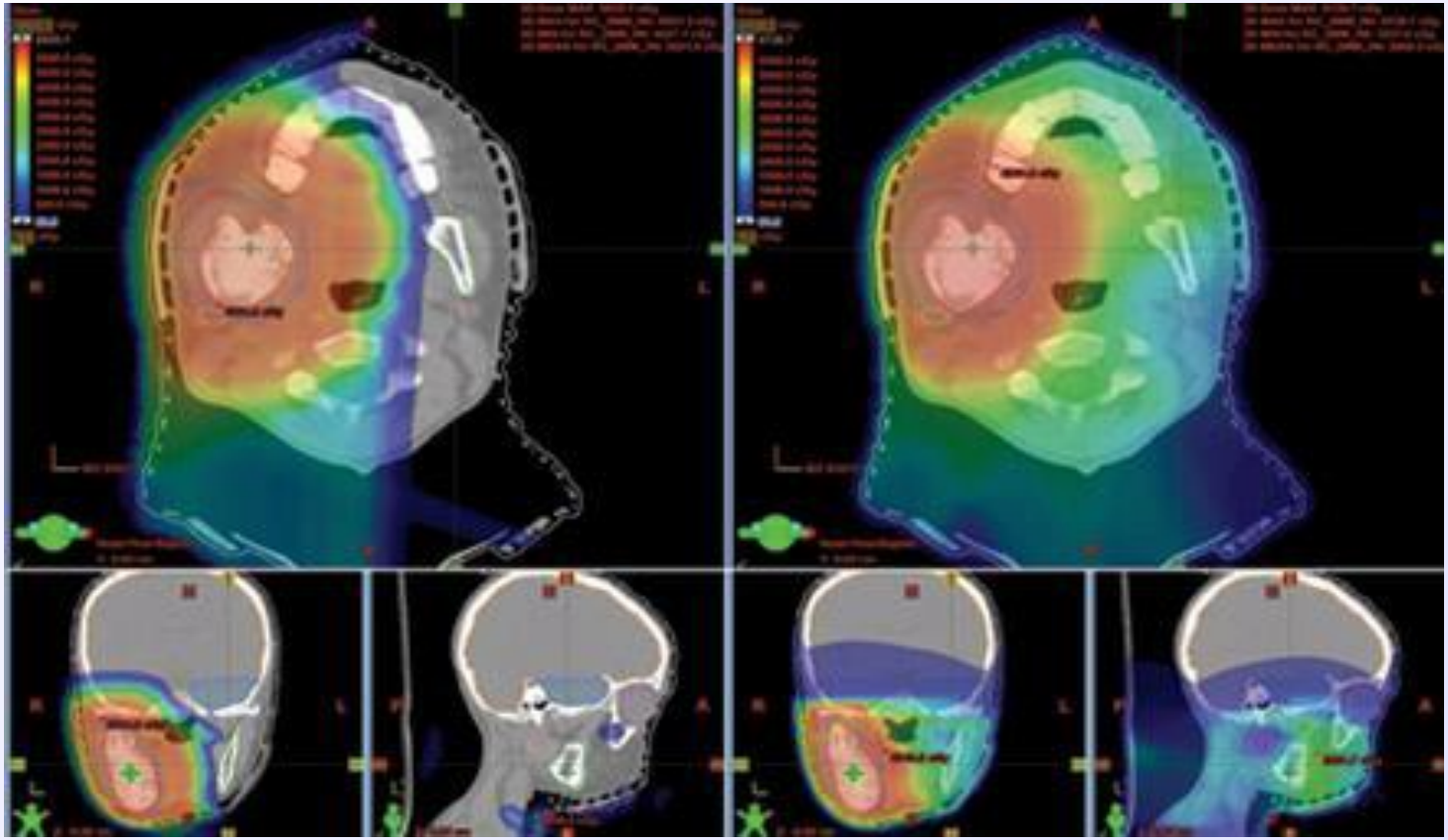

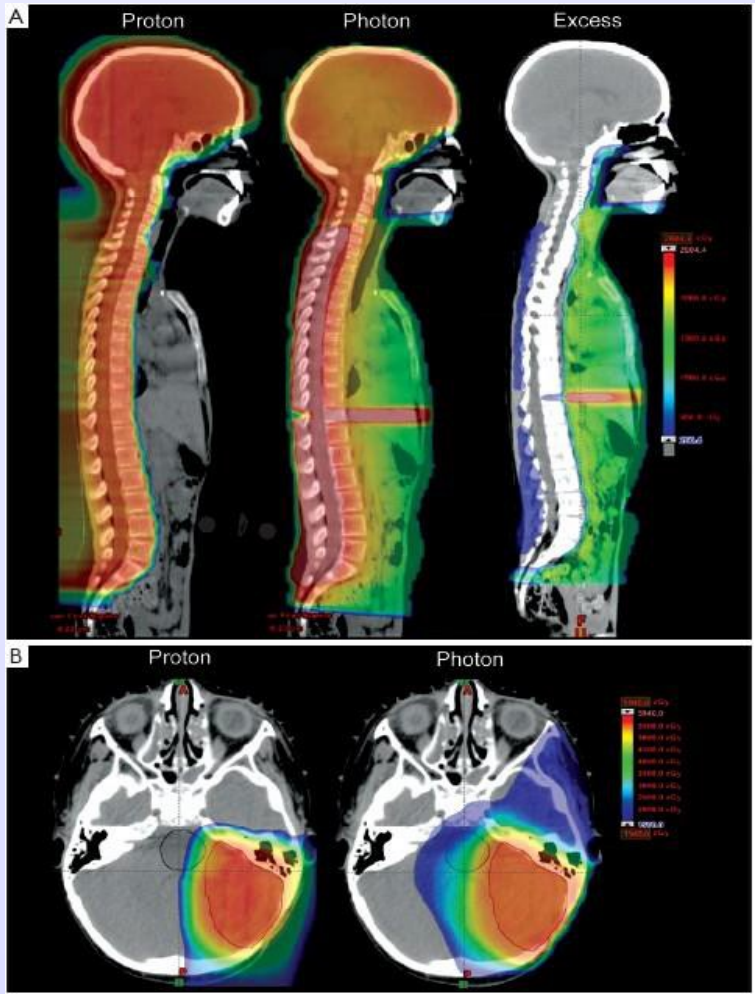

…and reduction of *late* toxicity -->

Why hadrontherapy

- ✓ 3. Operative reason (cost, easiness) (for the same conditions)

Where are protons / ^{12}C used?

- **Radio resistant tumors close to radiosensitive organs**
- **Eye tumors**
- **Base of skull and spine tumors**
- **Pediatric tumors**
- **But also: prostate, lung, gastrointestinal**

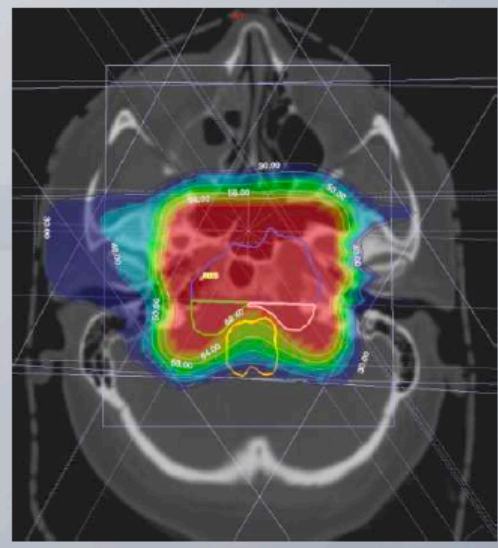

Dose distribution, parameters, uncertainties

Particles

The atomic nucleus of carbon (12 times heavier than the proton) is accelerated to about 70% of the speed of light for use.

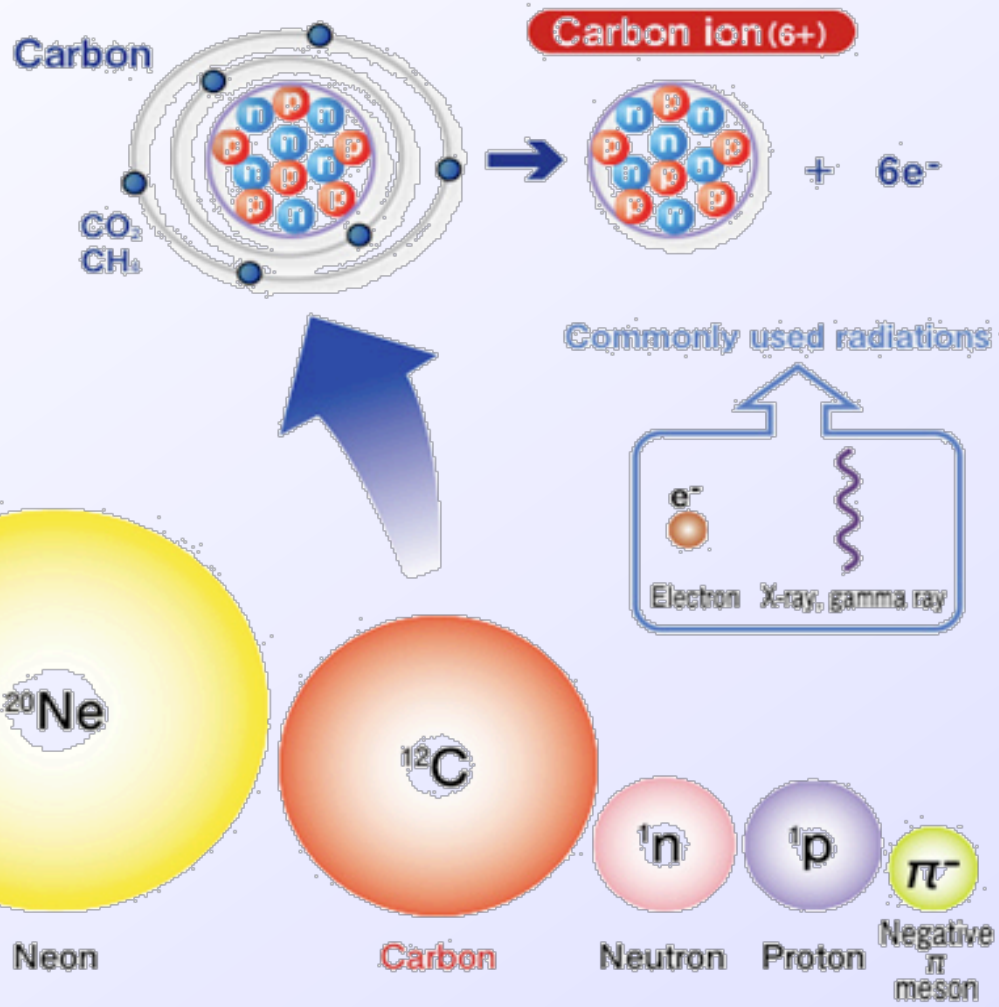

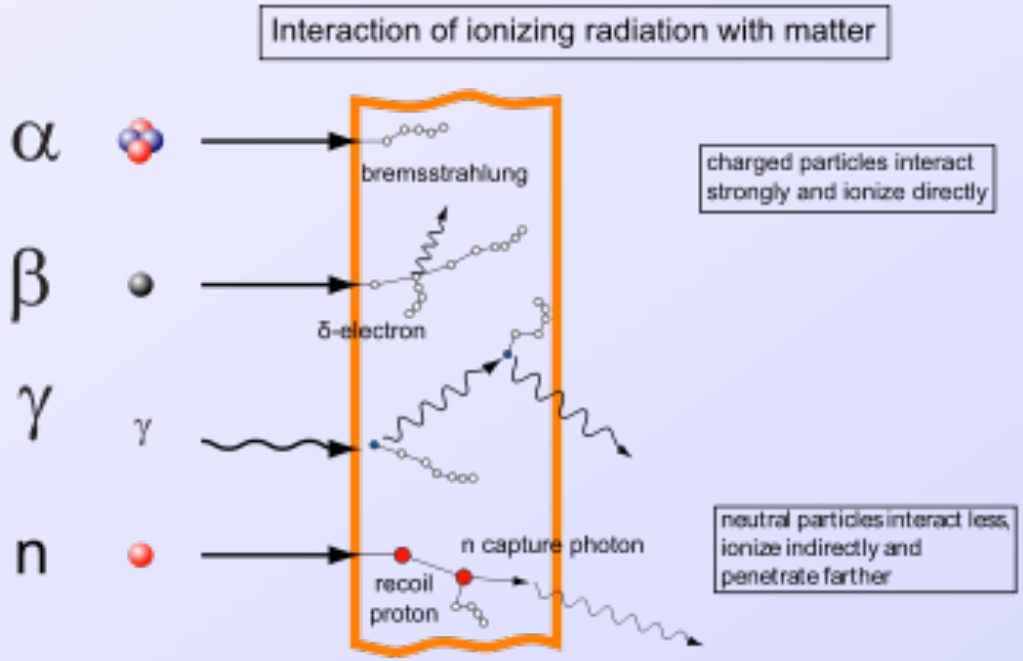

Depth-dose distributions

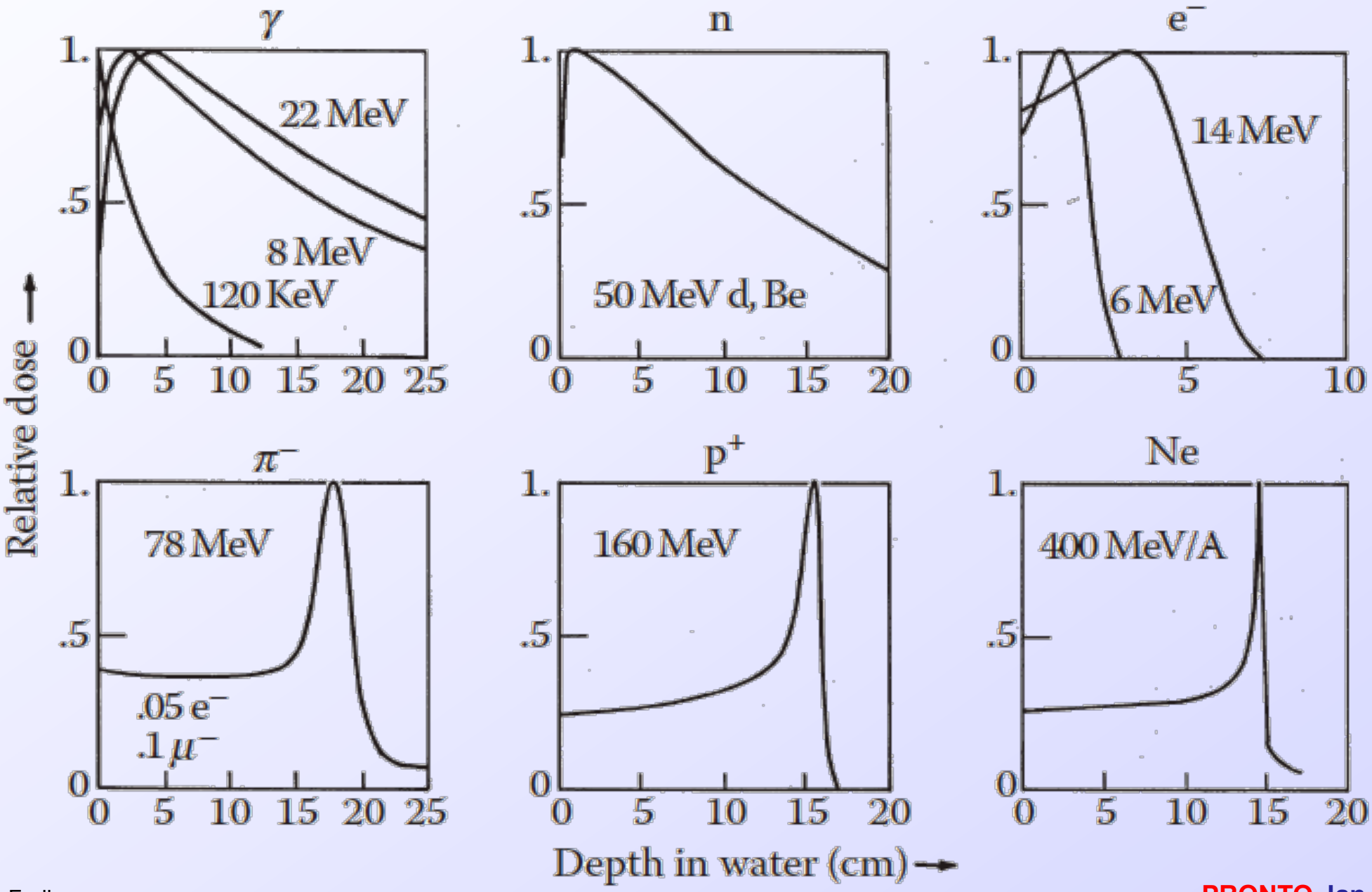

Depth-dose distributions

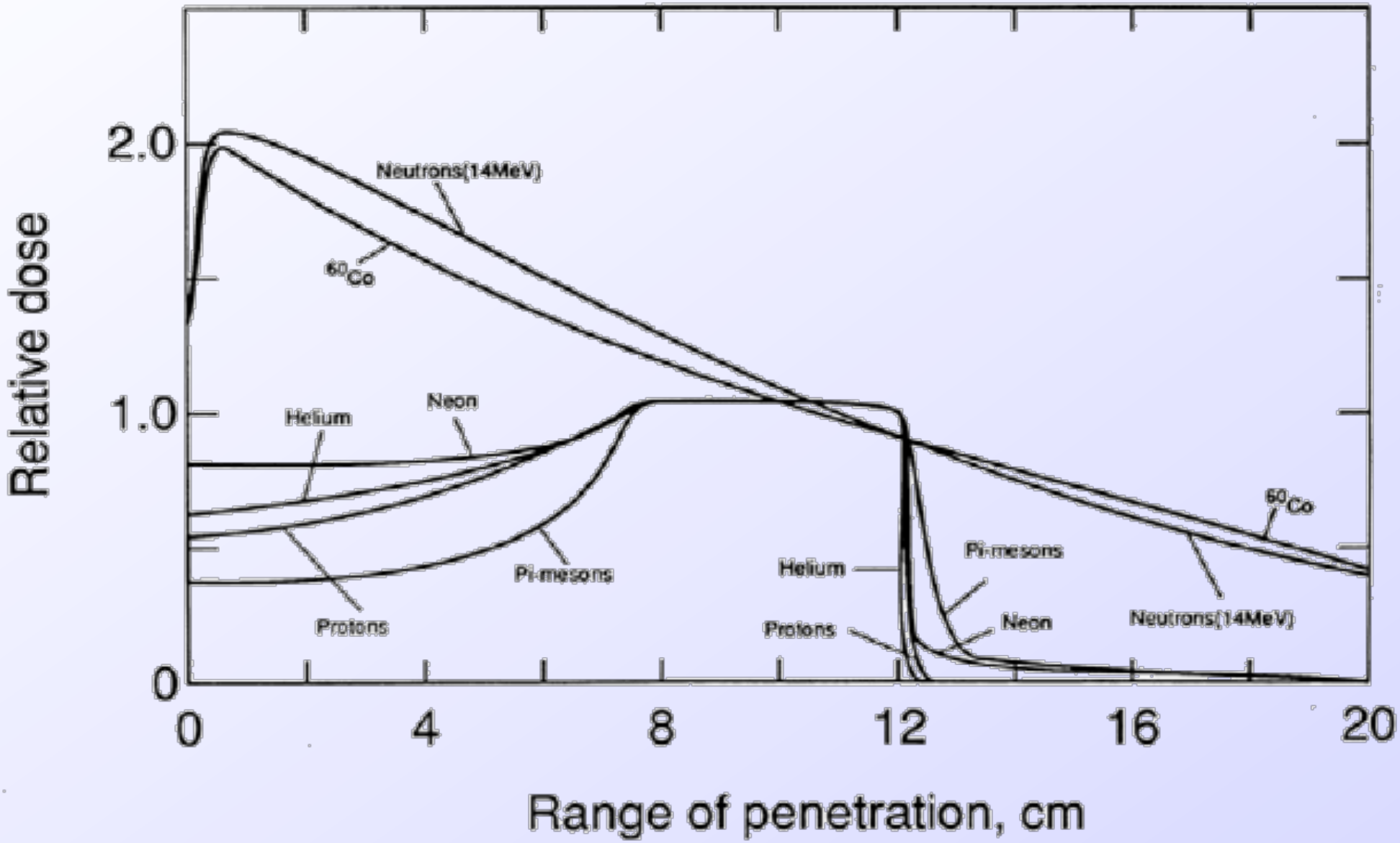

Main quantities

- **Fluence (Φ)** is a quantity which depends on position in the water tank. It is defined as the number of protons, during a given exposure or treatment, crossing an infinitesimal element of area dA normal to x

$$\Phi \equiv \frac{dN}{dA} \quad \frac{\text{protons}}{\text{cm}^2}.$$

- **Stopping power** is the rate at which a single proton loses kinetic energy

$$S \equiv -\frac{dE}{dx} \quad \frac{\text{MeV}}{\text{cm}}$$

- **Mass stopping power** is stopping power "corrected" for density

$$\frac{S}{\rho} \equiv -\frac{1}{\rho}\frac{dE}{dx} \quad \frac{\text{MeV}}{\text{g/cm}^2}$$

- **Physical absorbed dose (D)** at some point in a radiation field is the energy absorbed per unit target mass

$$D \equiv \frac{\text{J}}{\text{kg}}$$

Gray: 1 Gy ≡ 1 J/kg. 1 Gy = 100 rad or "centiGray" (cGy)

A proton radiotherapy treatment might consist of ≈ 70 Gy given in ≈ 35 fractions (2 Gy/session)

[S. España]

Range

- The **range (R)** of a proton beam is defined as the depth of material at which half the protons that undergo only EM interactions have stopped. It is defined by a fluence measurement. However, a dose measurement may be used instead, provided the result is properly interpreted.

[S. España]

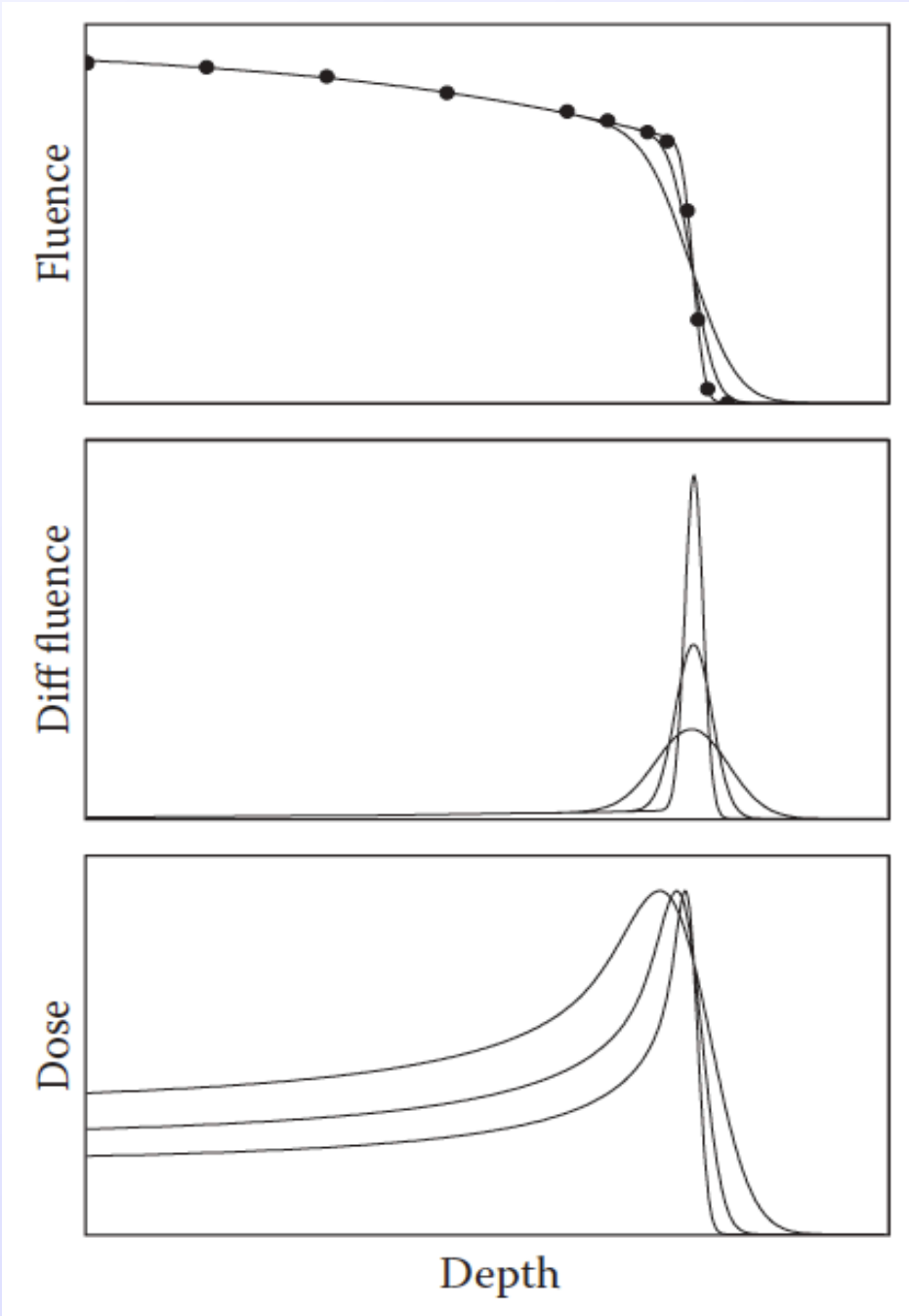

Type of interactions

- ✓ **Energy Loss** - Coulomb interactions with electrons. Defines the range and shape of dose profile along the beam line.
- ✓ **Scattering** - Coulomb interactions with target nuclei. Defines the shape of lateral profile.
- ✓ **Nuclear Interactions** - Inelastic nuclear interaction with target nuclei. Modifies the depth dose and lateral dose distribution.
- ✓ Bremsstrahlung is theoretically possible, but at therapeutic proton beam energies this effect is negligible

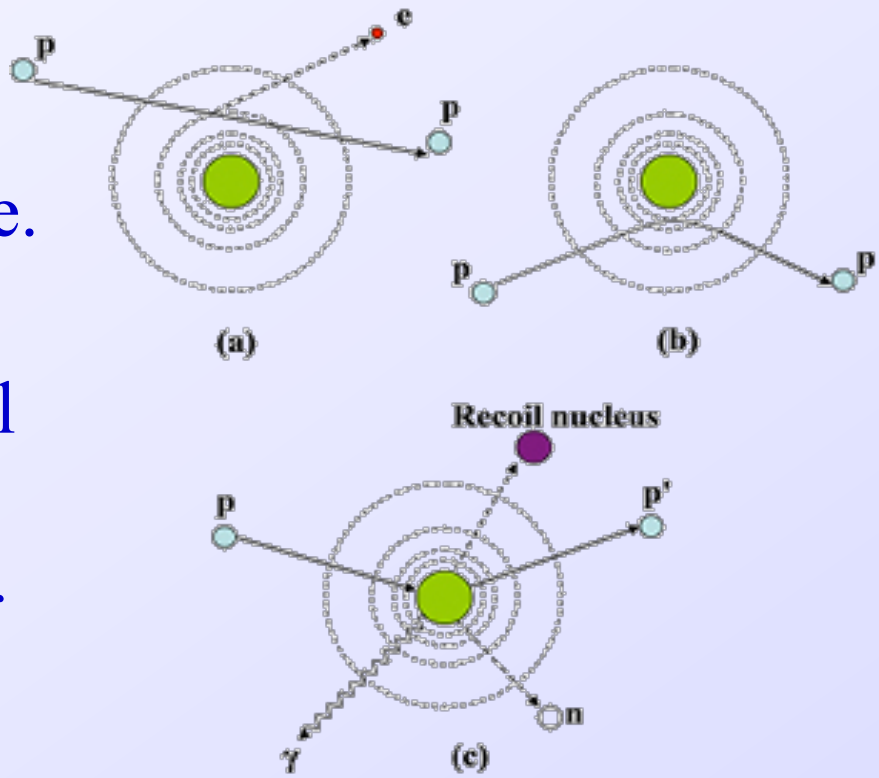

Electromagnetic Interaction with Electrons

- Proton mass (M_p) is 938 MeV/c^2 in comparison M_e = 0.511 MeV/c^2 => No significant depletion.
- Range of secondary electrons is < 1mm => locally absorbed dose.
- Bethe-Bloch equation for protons in the radiotherapy energy regime 3–300 MeV

$$\frac{S_{el}}{\rho} \equiv -\frac{1}{\rho}\frac{dE}{dx} = 0.3072\frac{Z}{A}\frac{1}{\beta^2}\left(\ln\frac{W_m}{I} - \beta^2\right) \quad \frac{\text{MeV}}{\text{g/cm}^2}$$

[S. España]

Stopping Power

$$-dE/dx \sim 1/\beta^2 \simeq 1/v^2$$

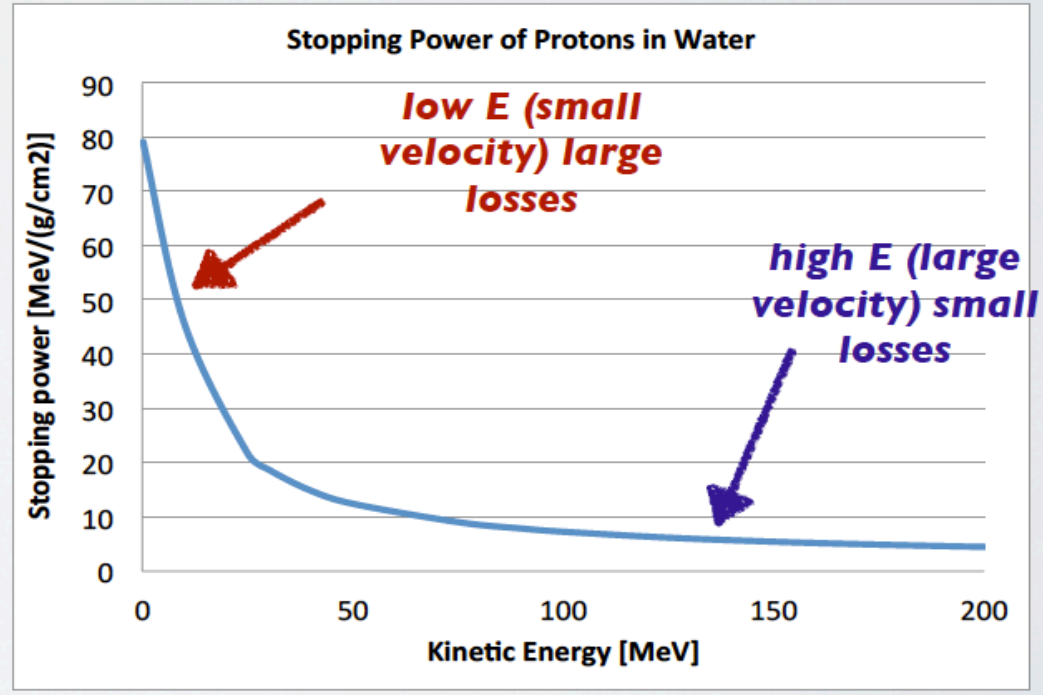

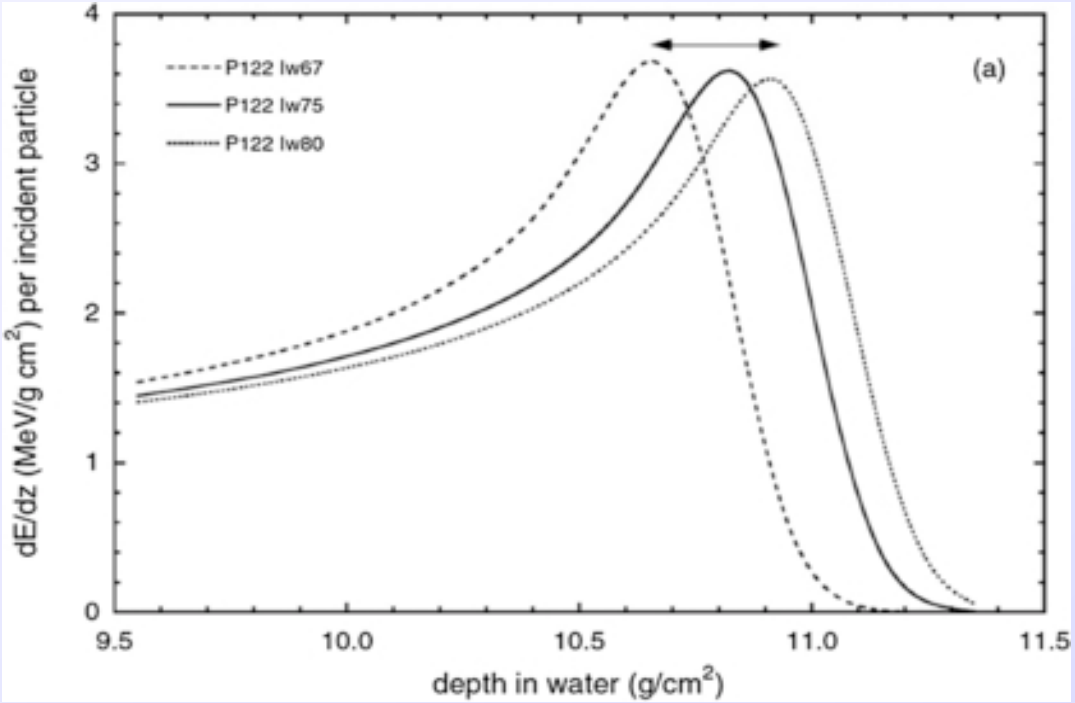

The rate at which the proton loses energy increases as the proton slows down because, in a given proton–electron collision, more momentum is transferred to the electron, the longer the proton stays in its vicinity.

[S. España]

Mean Excitation Energy

- ✓ **I** is the mean excitation energy of the target material. It cannot be calculated to sufficient accuracy. Tables can differ from each other by 1%–2%, due solely to different choices of I .
- ✓ One percent of range at 180 MeV corresponds to ≈ 2 mm range in water. Therefore when the treatment depth itself depends on it, we must rely on measured ranges in water and measured water equivalents of other materials.

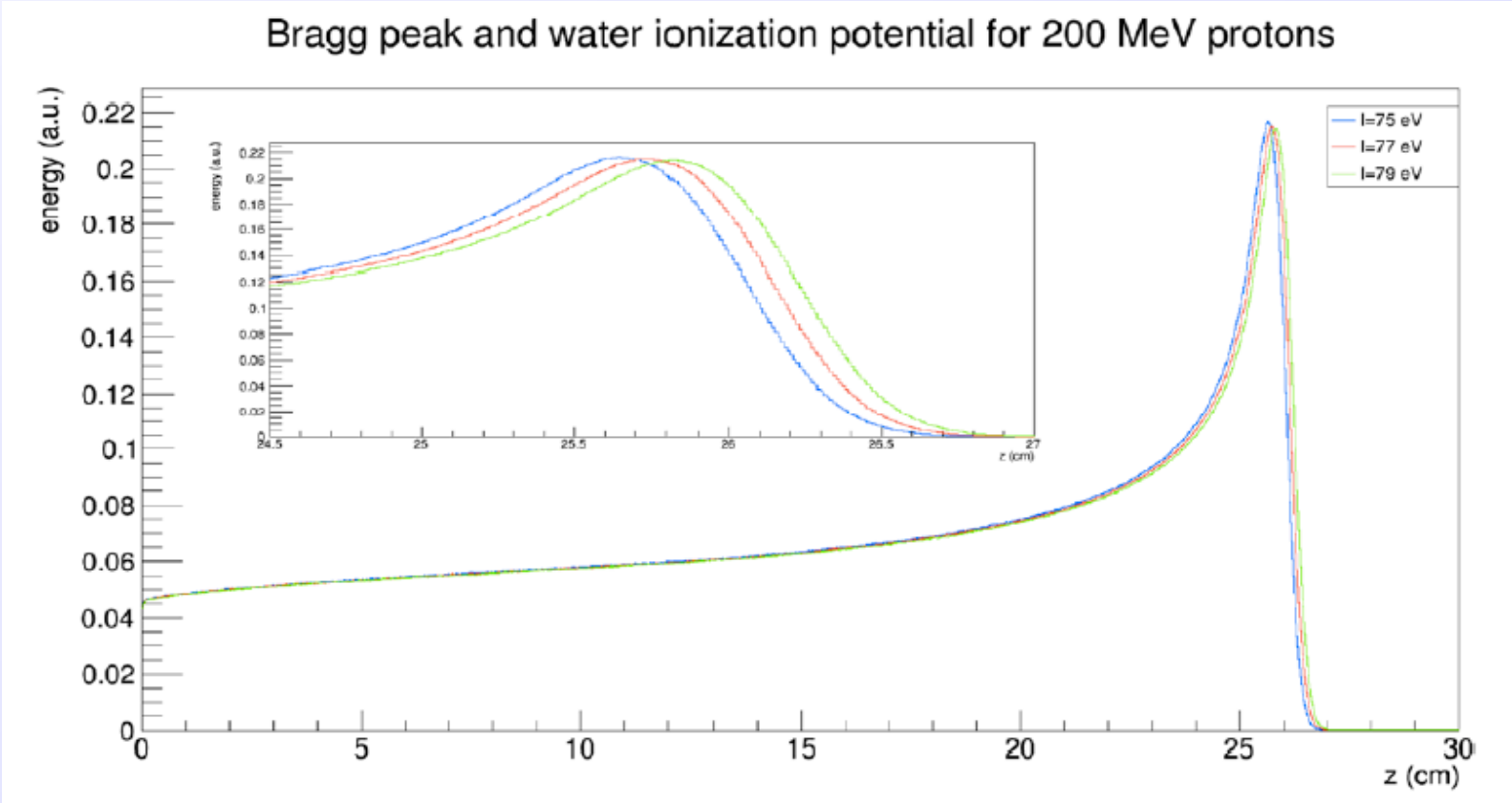

[S. España]

Range of protons in water

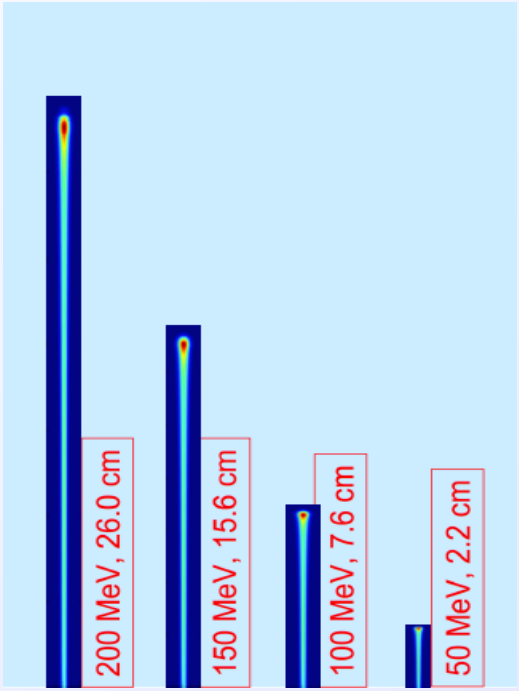

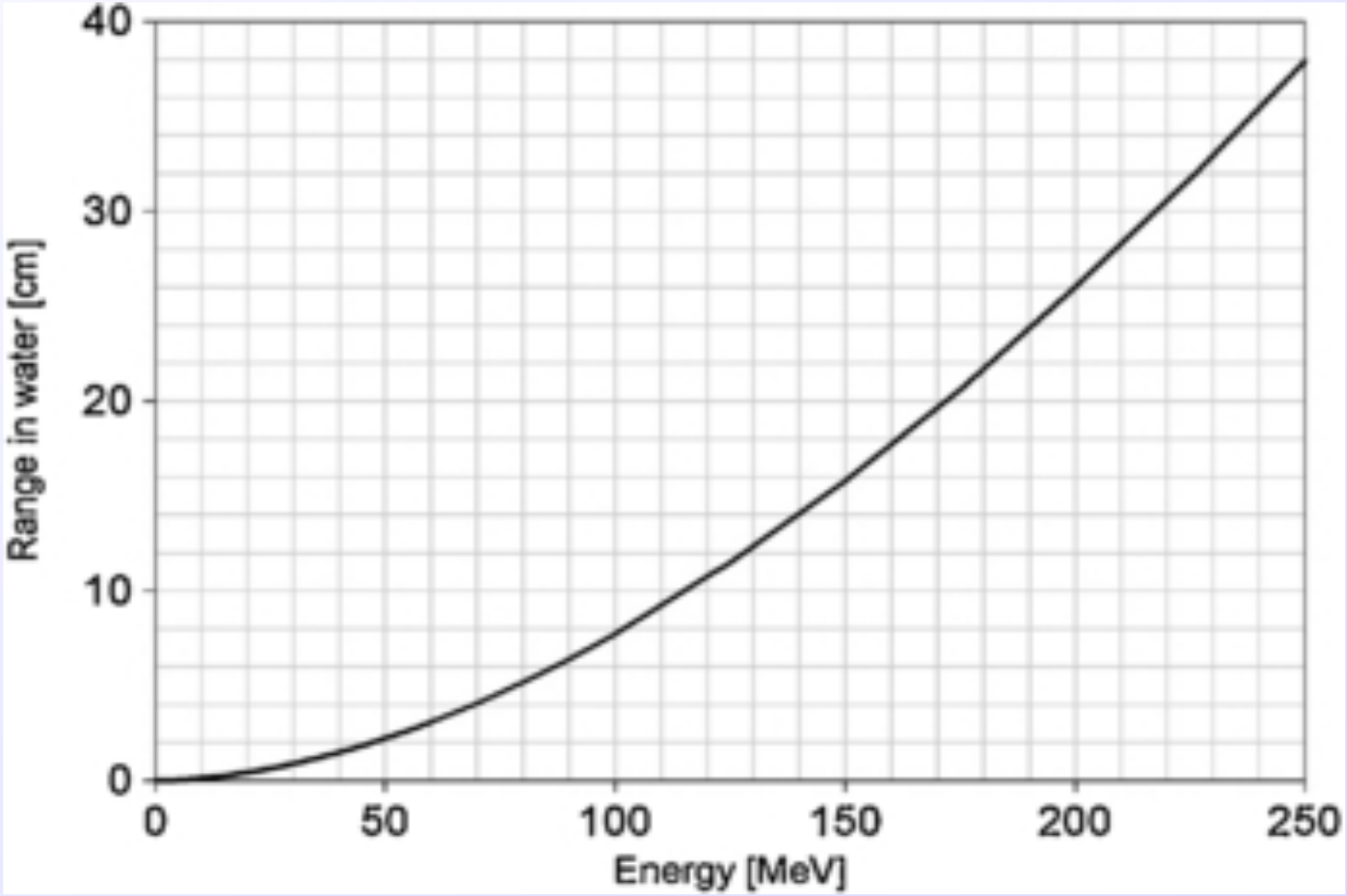

First issue: **range straggling**

- ✓ Protons even if their initial energy is exactly the same, will not all stop at exactly the same depth.

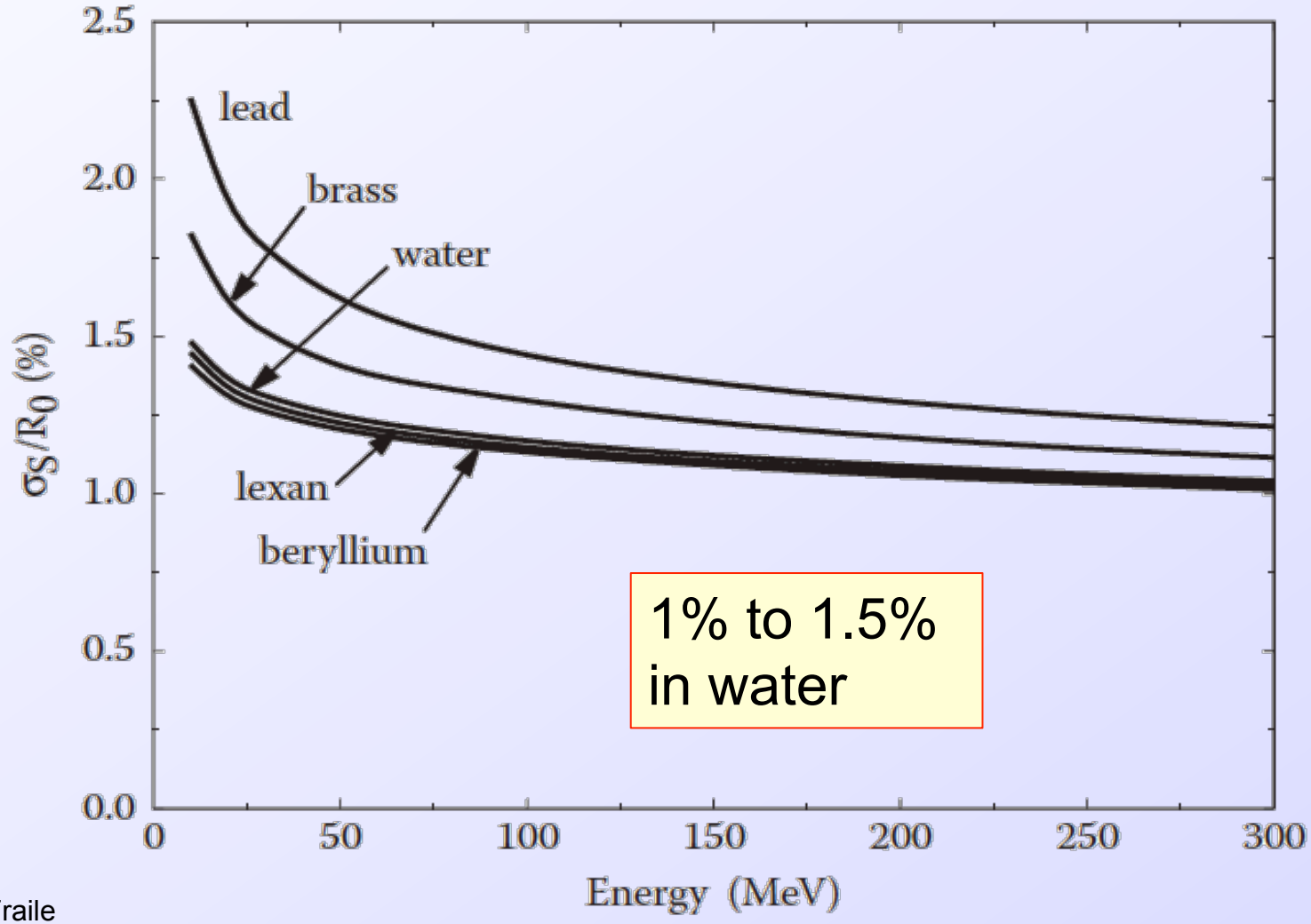

Electromagnetic Interaction with Nuclei

- ✓ Protons are deflected frequently in the electric field of nuclei.
- ✓ Protons predominantly scatter due to elastic coulomb interaction with target nuclei
- ✓ Many small angle deflections (Multiple Coloumb Scattering) -> Lateral distribution
- ✓ For radiotherapy beam broadening can be approximated by a Gaussian distribution.
- ✓ Full description is given by Moliere scattering and later by Highland approximation.
- ✓ Beam broadening can be approximated by a Gaussian distribution.
- ✓ Deviation up to 16 degrees in the very worst case and usually only a few degrees

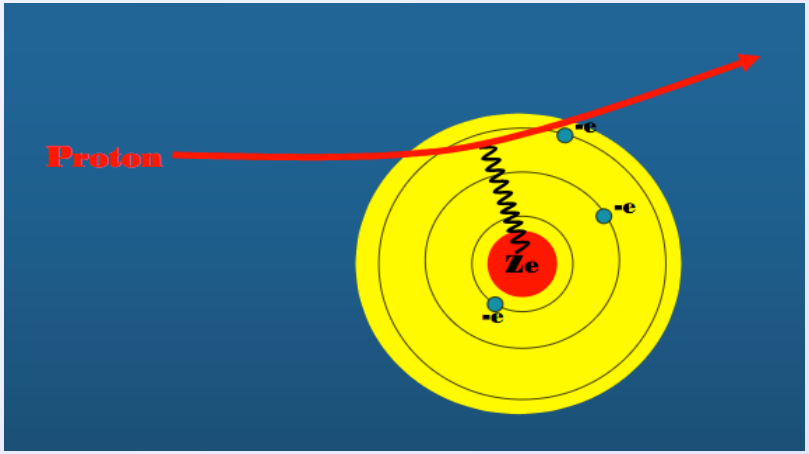

$$\theta_0 = \frac{14.1\ \text{MeV}}{pv}\sqrt{\frac{L}{L_R}}\left[1+\frac{1}{9}\log_{10}\left(\frac{L}{L_R}\right)\right]\text{rad}$$

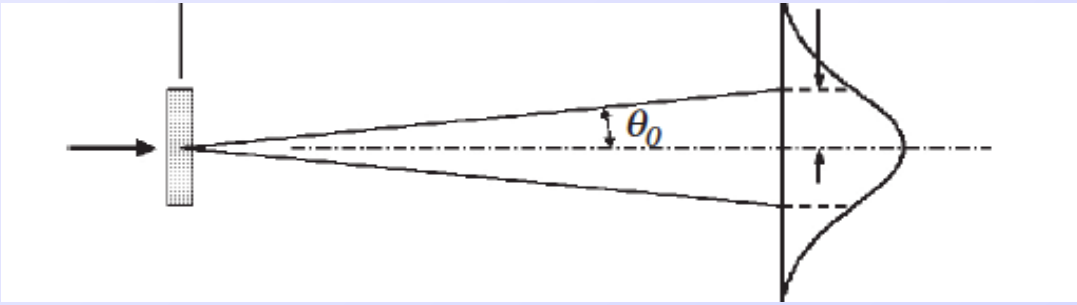

Lateral spread in water

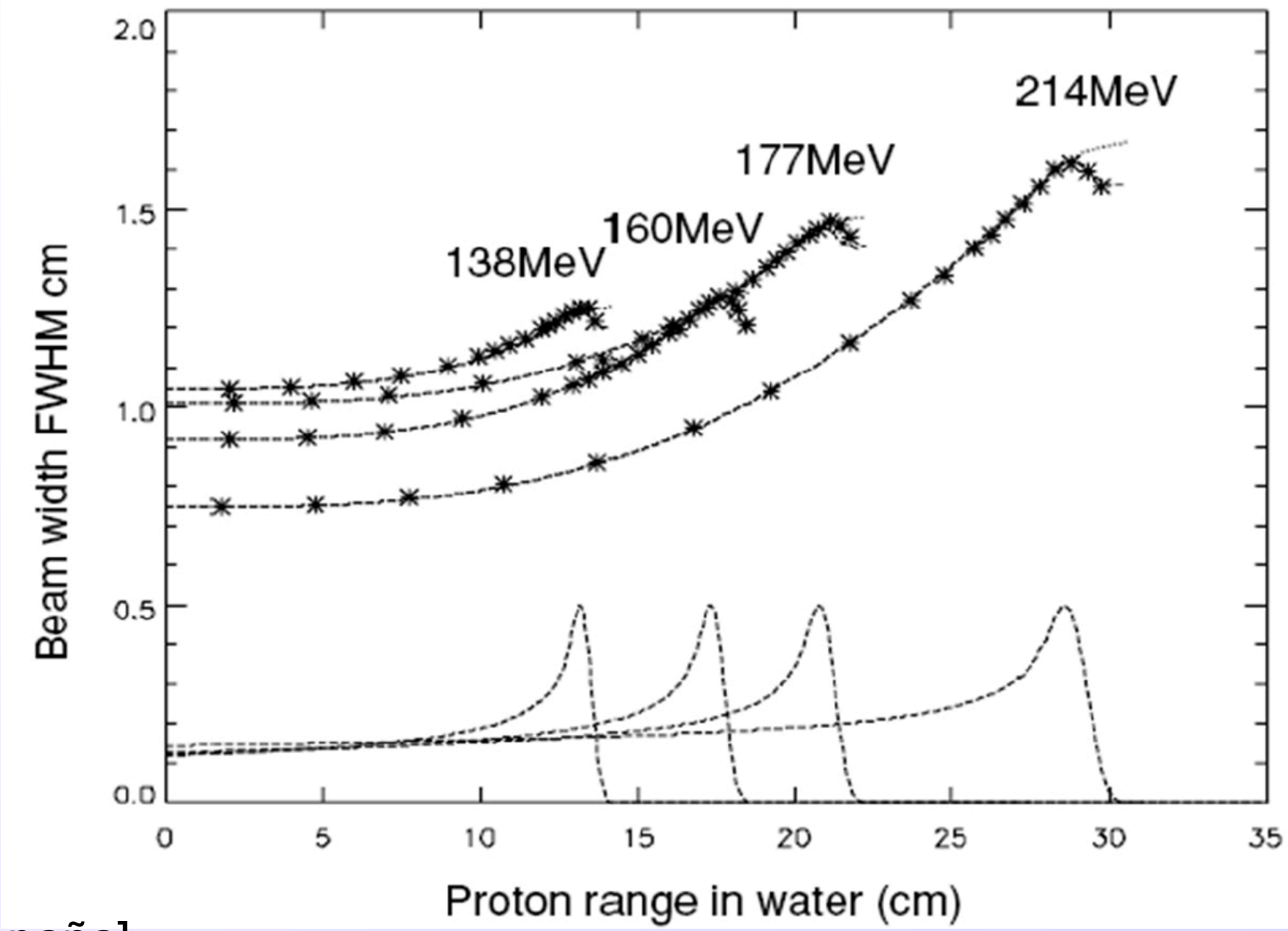

[S. España]

Lateral spread in water

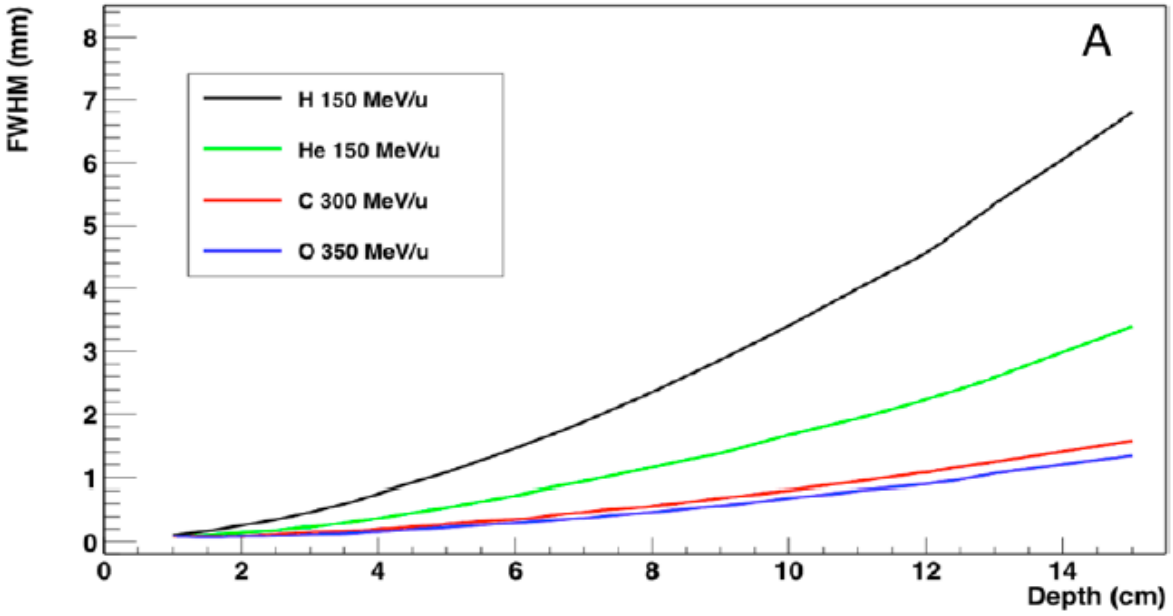

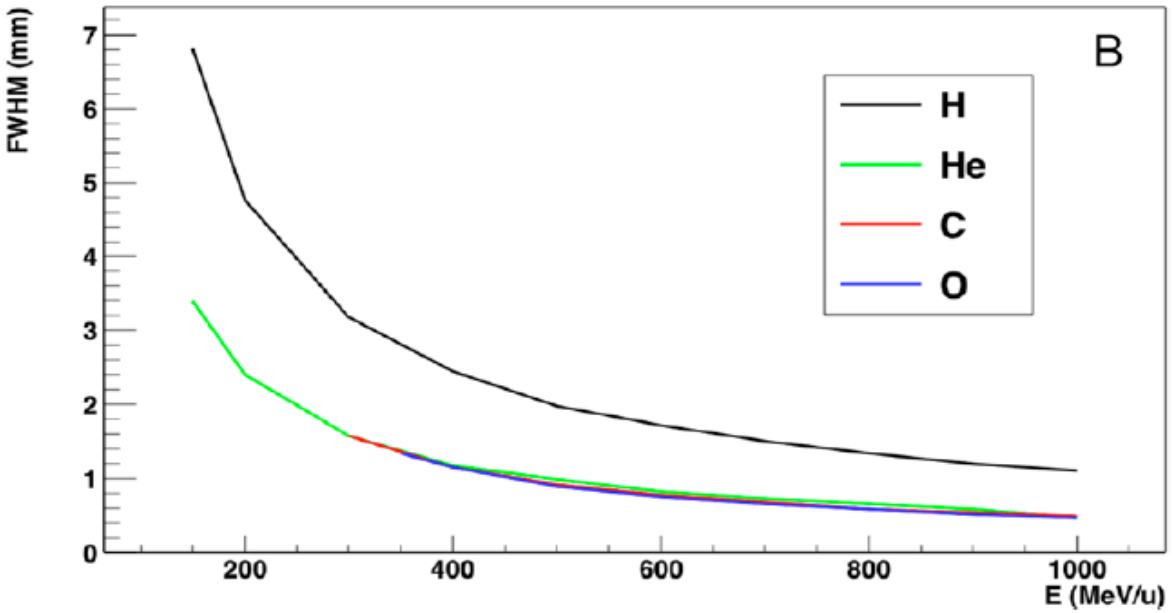

Lateral spread as a function of the depth for beams of different energy, having the same range of 15 cm in water.

Calculation as a function of the energy of different beams after traversing 15 cm in water.

Stopping & Scattering

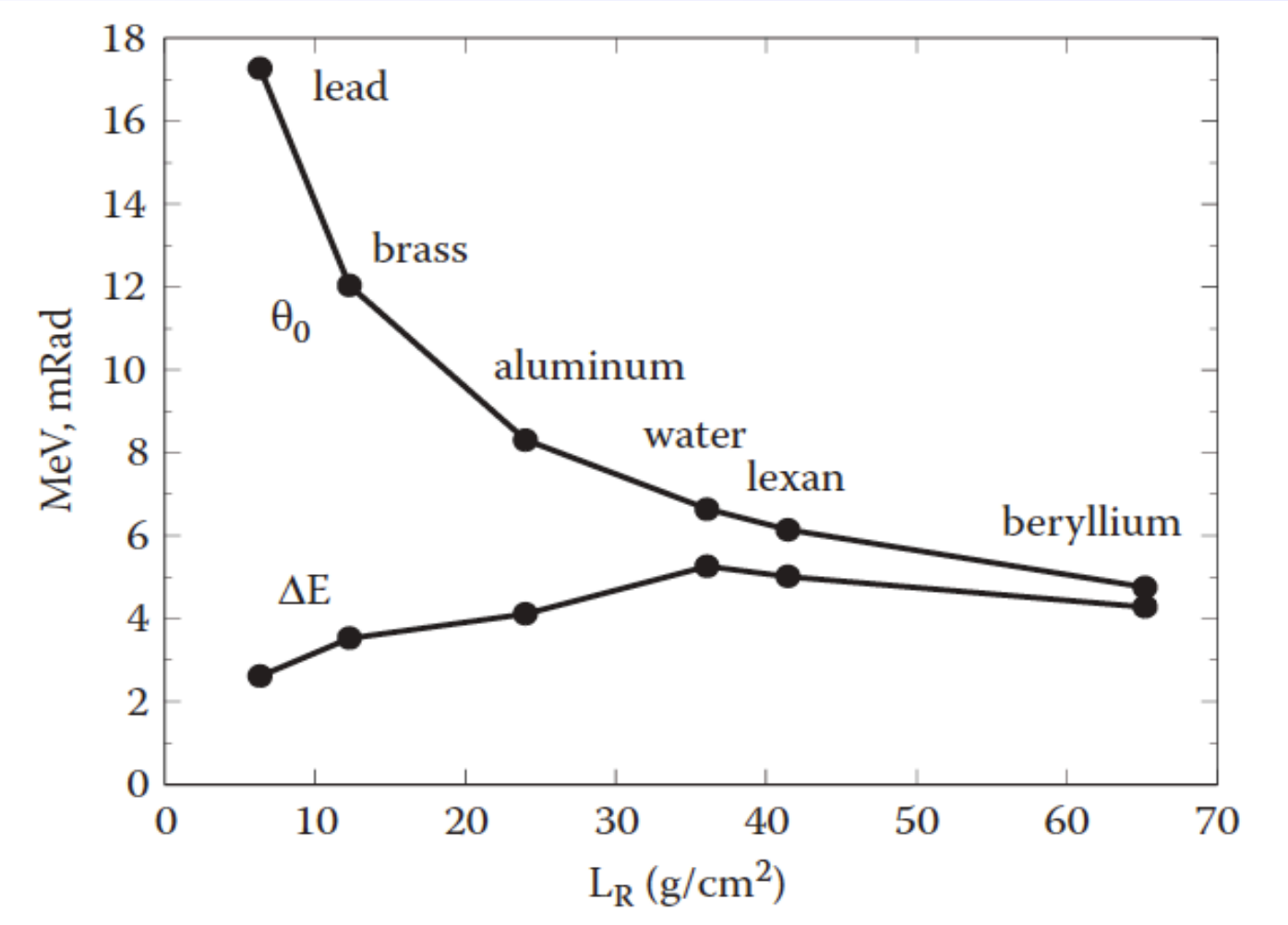

Multiple scattering angle and energy loss for 160-MeV protons traversing 1 g/cm^2 of various materials.

Nuclear Reactions

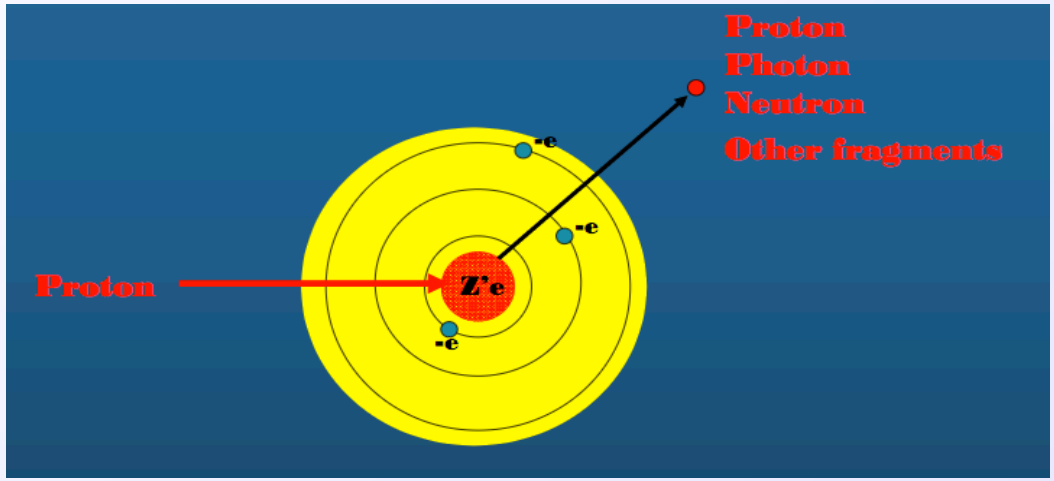

- ✓ Secondaries:
  - →charged (p,d,α,recoil target nuclei) ~ 60% of energy - absorbed locally.
  - →neutral (n,γ) ~ 40% of energy - absorbed in surrounding tissues.
- ✓ Production of unstable recoil particles (activation)
- ✓ About 20% of incident 160 MeV protons have inelastic nuclear interactions with the target nuclei.
- ✓ Only 50% of the carbon ions reach the Bragg peak. These secondaries contribute to the longitudinal spread of the beam.
- ✓ Reduction of primary proton fluence with depth.

Nuclear Reactions

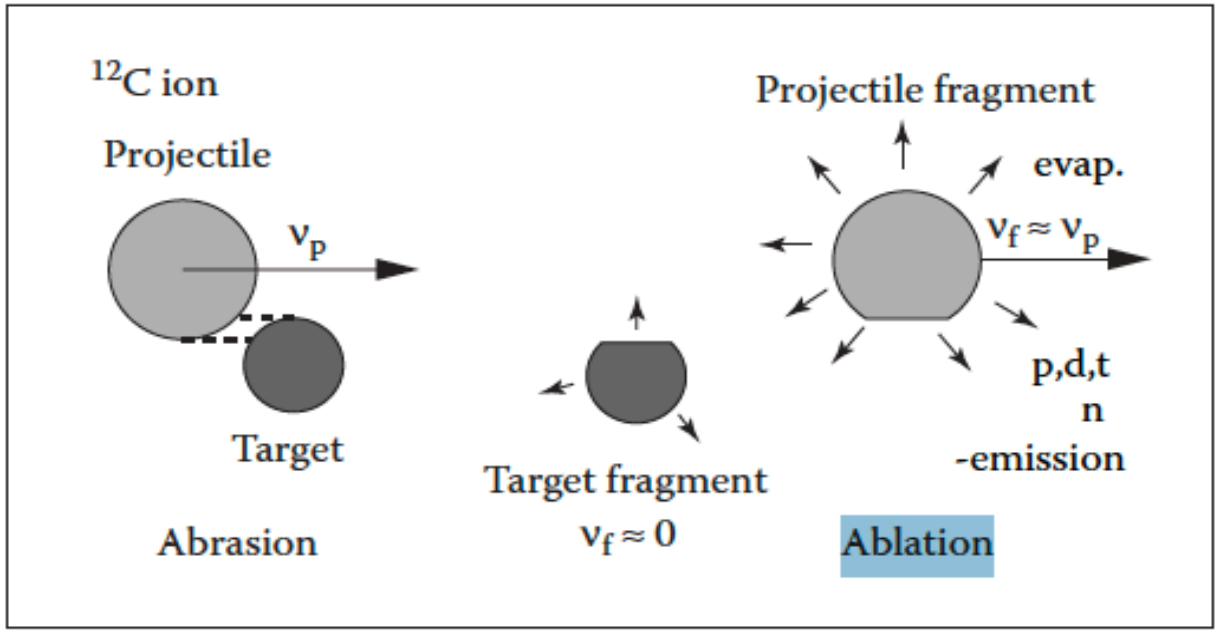

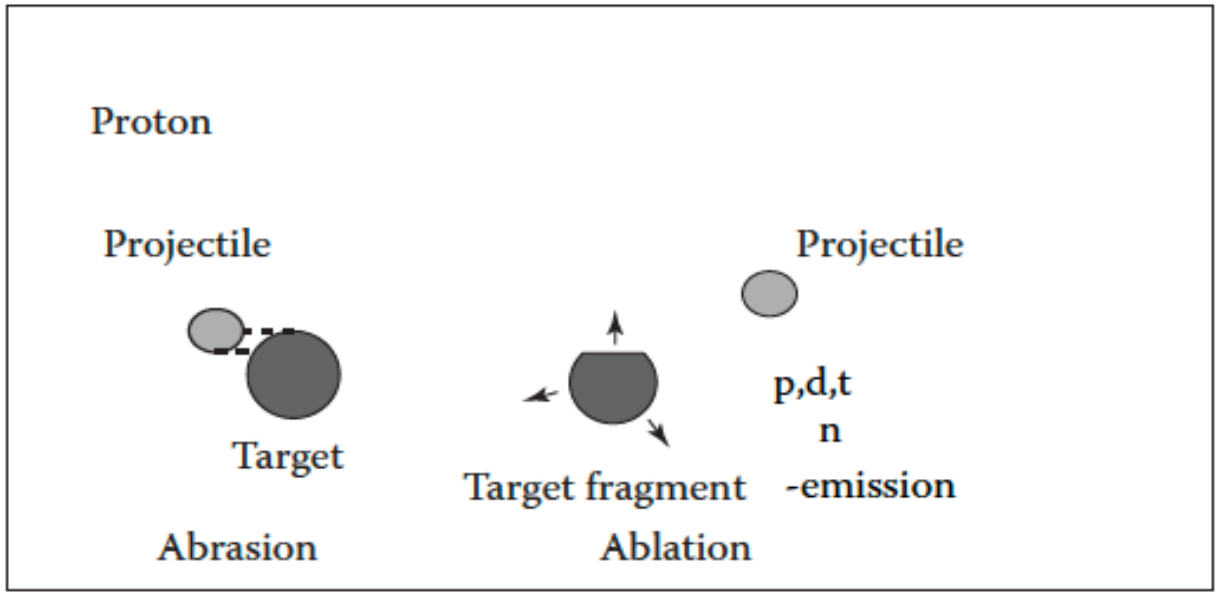

Threshold issues - Coulomb Barrier

To enter the nucleus, protons need to have sufficient energy to overcome the **Coulomb barrier** of the nucleus, which depends on its atomic number.

The **total proton-induced non-elastic nuclear reaction cross section in oxygen** versus proton energy, showing a threshold corresponding to the Coulomb barrier at approximately 6 MeV

[S. España]

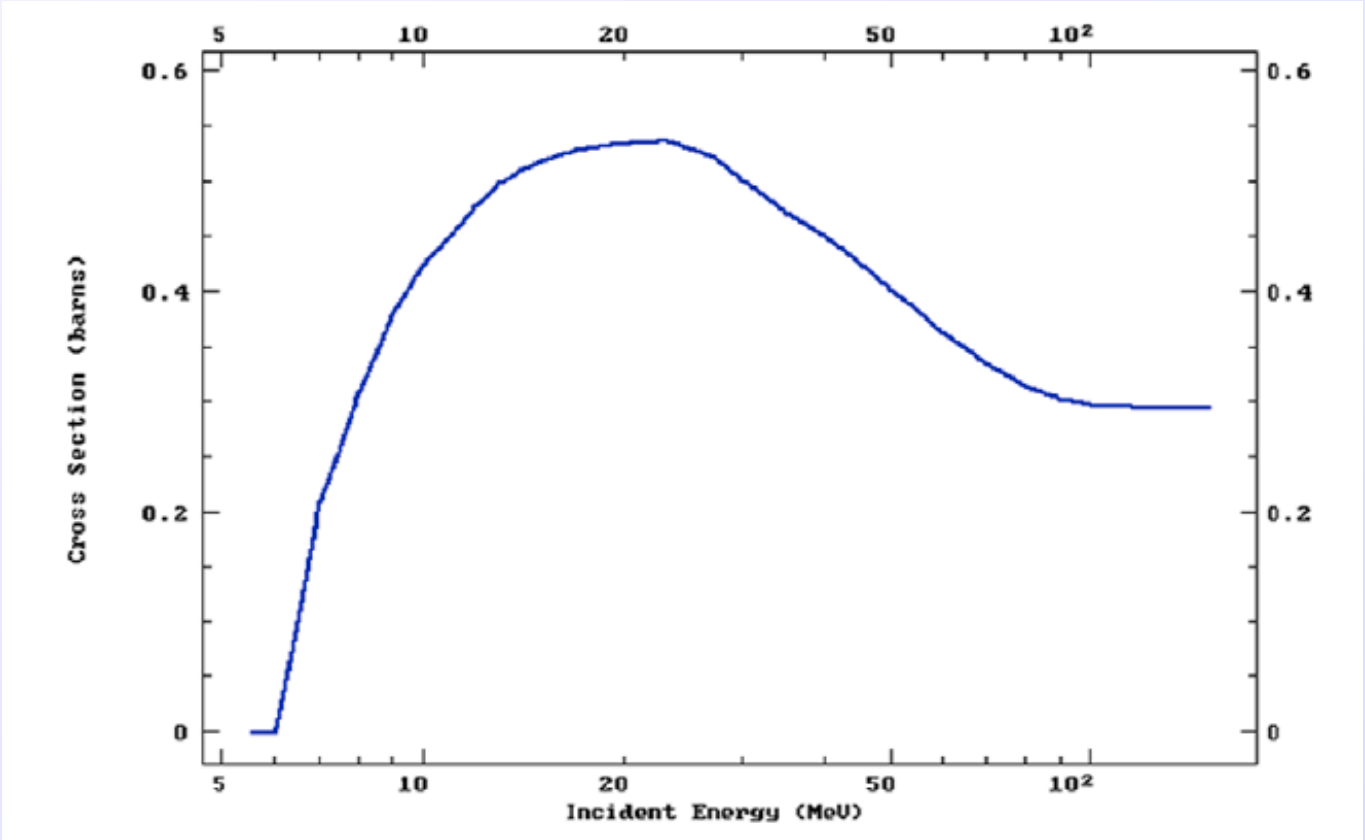

Fluence

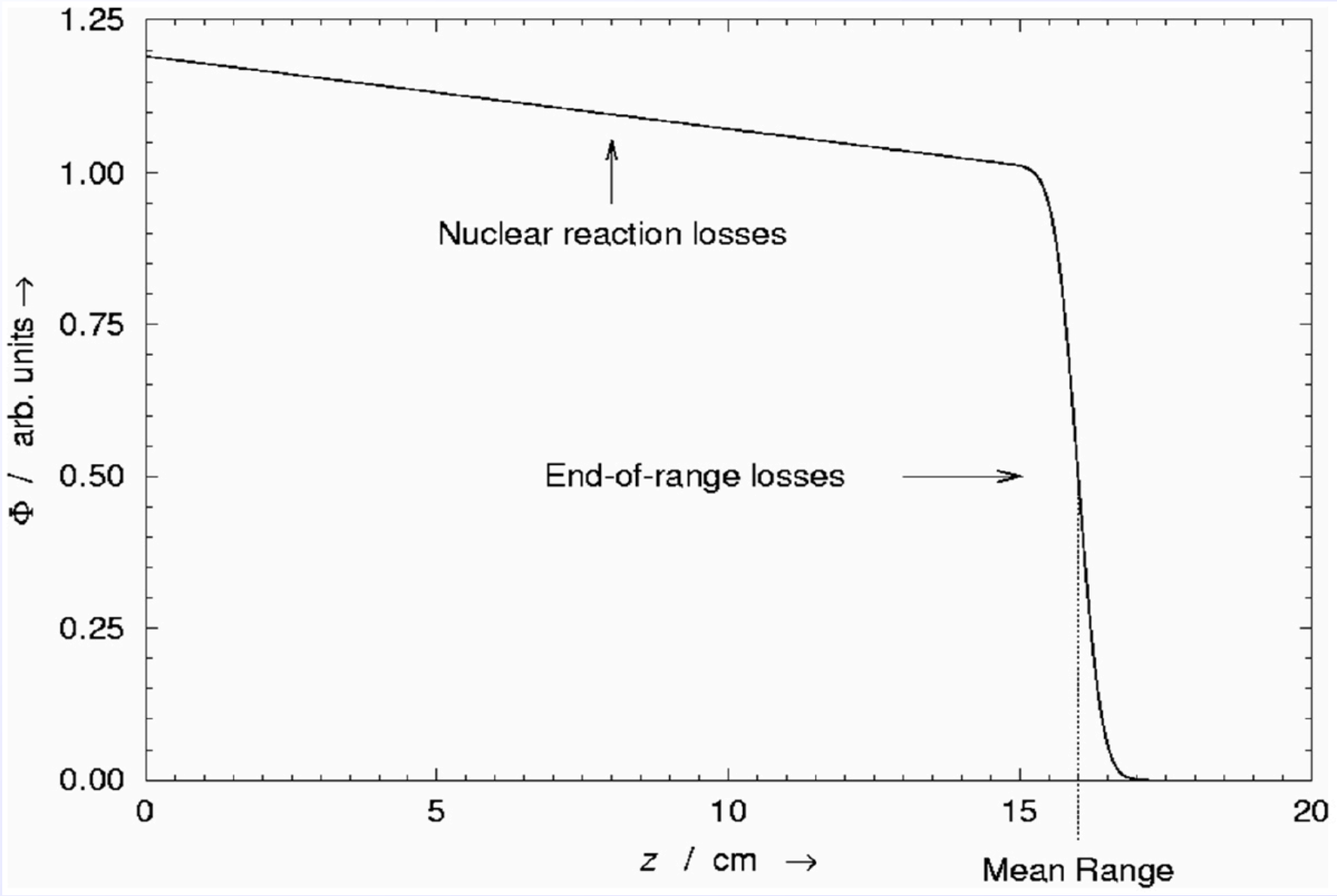
1.25
1.00
0.75
0.50
0.25
0.00
Φ / arb. units →
Nuclear reaction losses
End-of-range losses
0
5
10
15
20
z / cm →
Mean Range

Secondary Particles - Protons

Pristine **160 MeV** proton beam in water

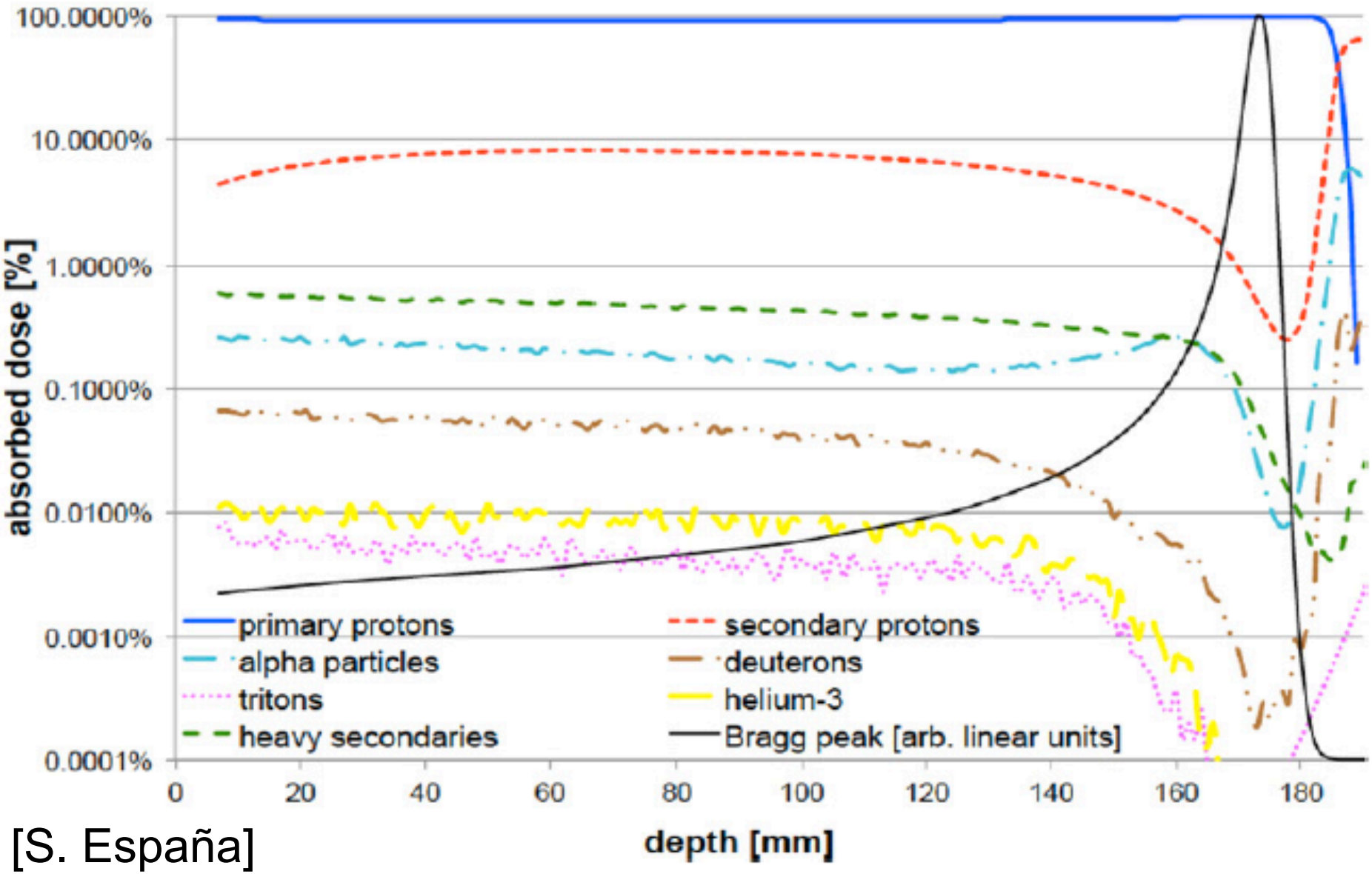

[S. España]

Secondary Particles - Carbon Ions

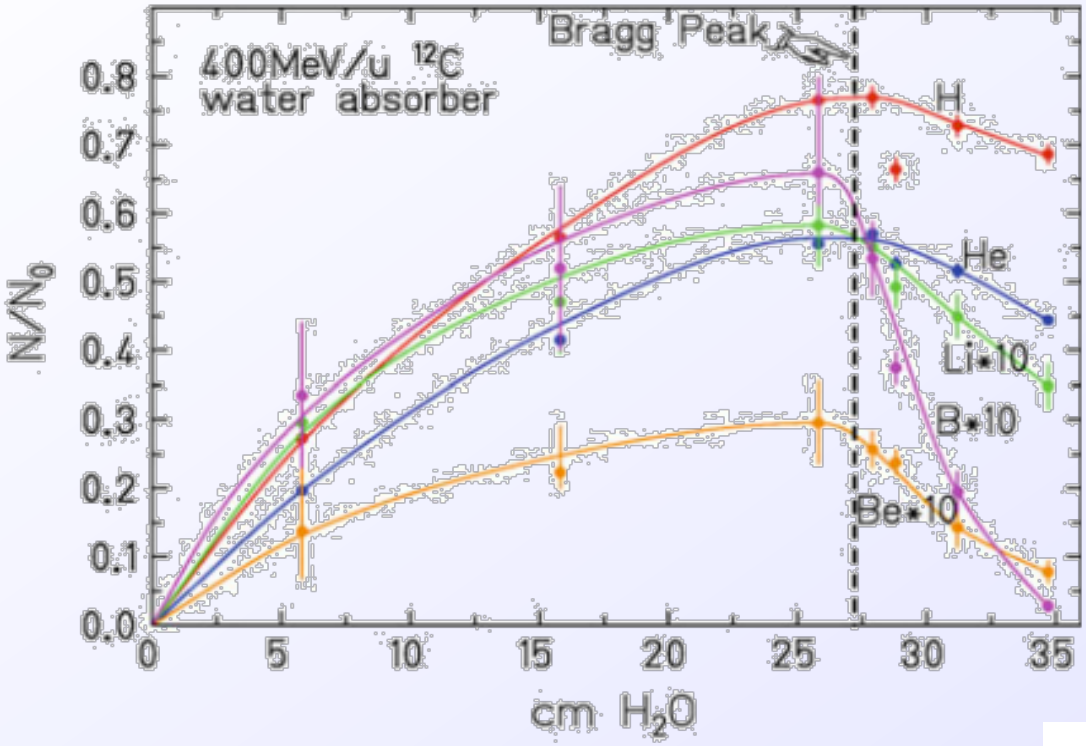

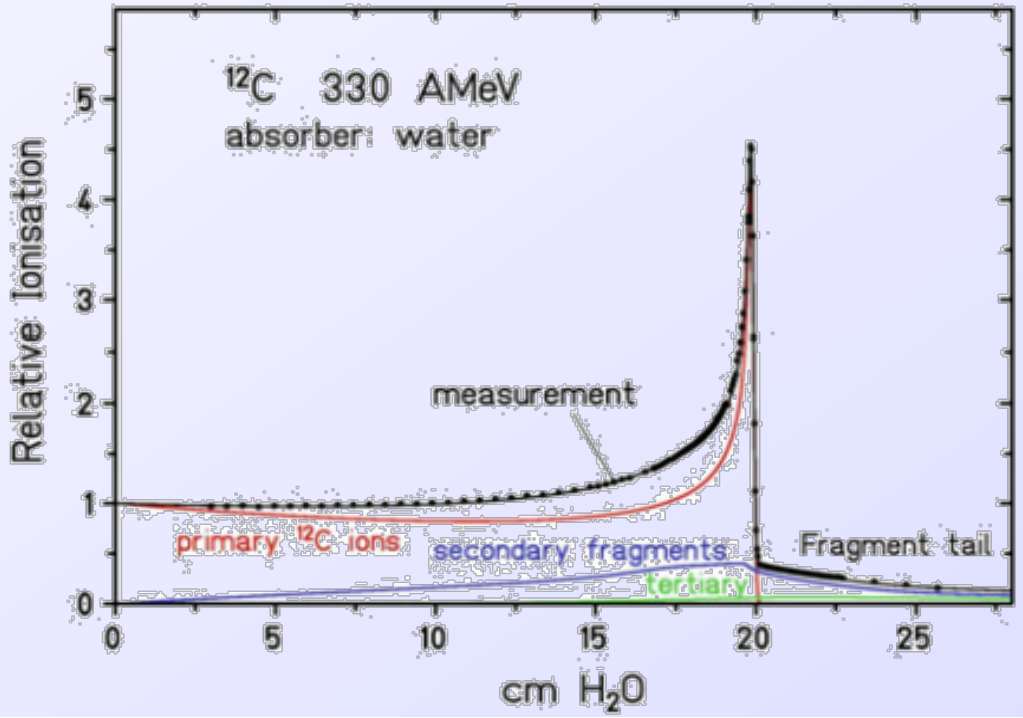

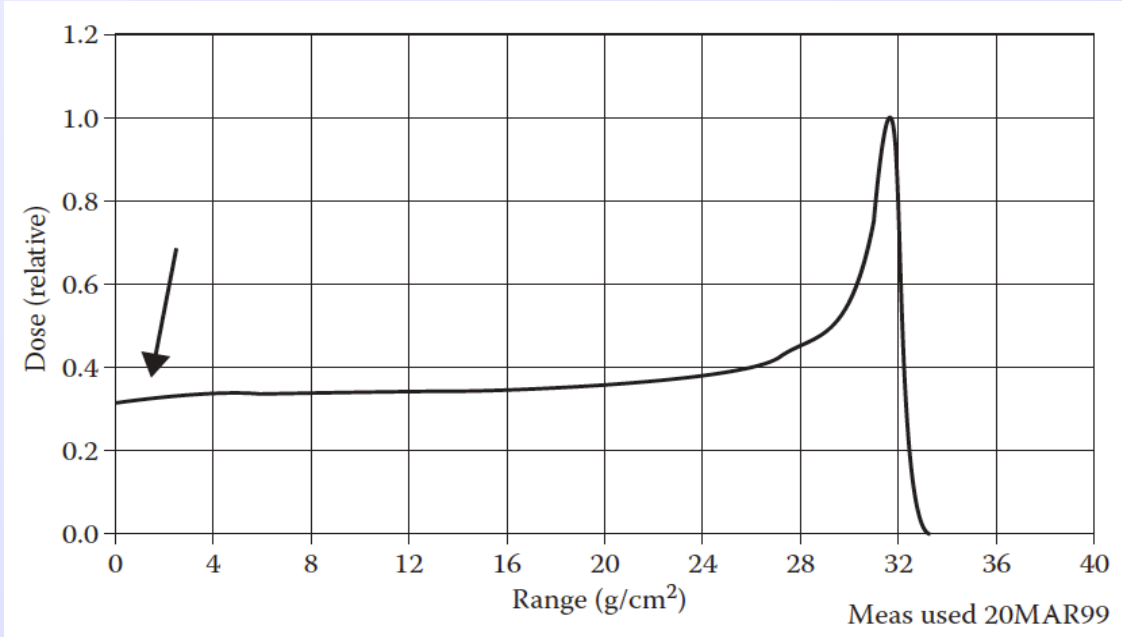

Spectra of Secondary Particles

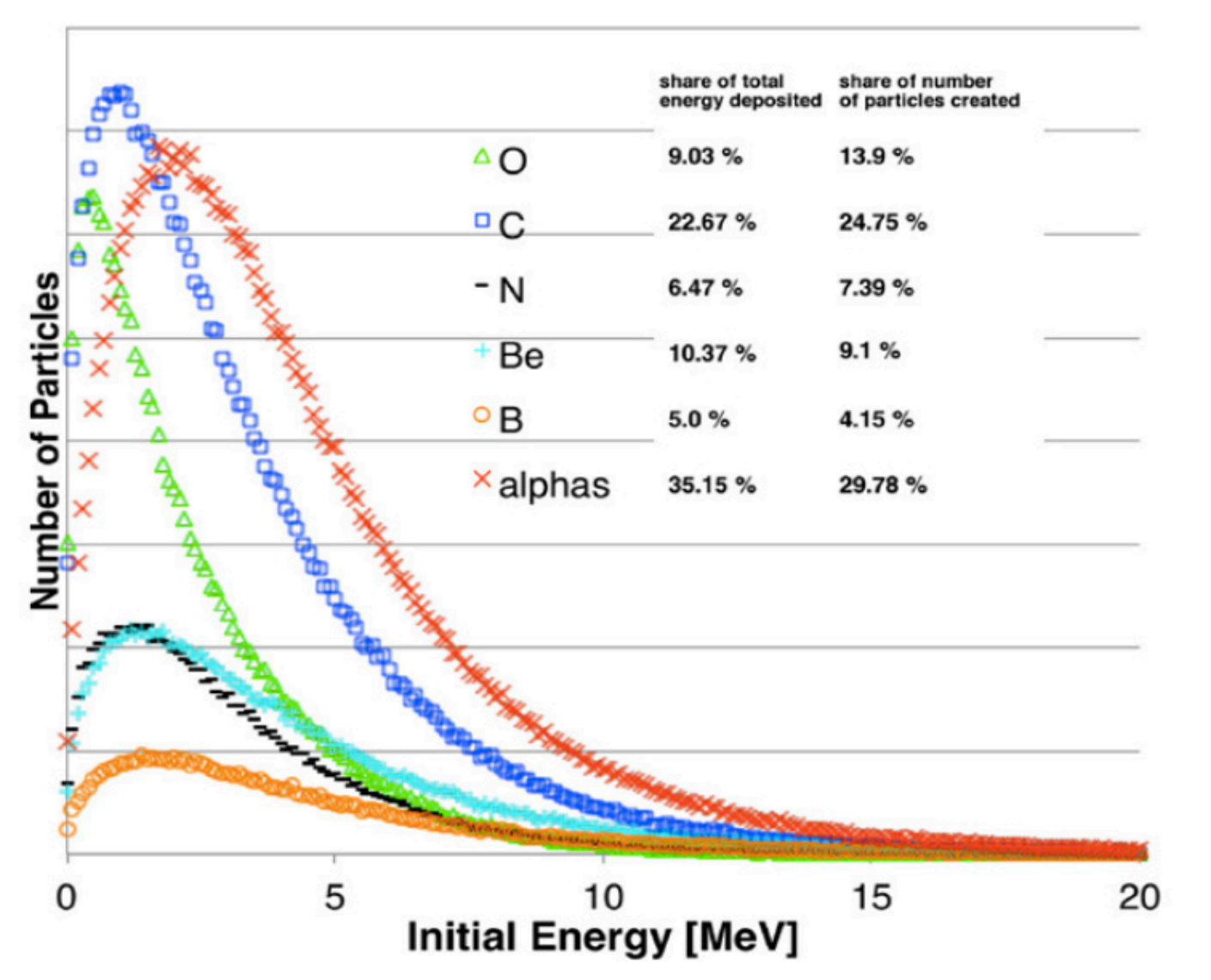

Energy spectra of the prevalent secondary particles (recoils and α-particles) arising from nuclear interactions in a prostate cancer patient irradiated with a 160 MeV proton beam.

[S. España]

Water Equivalent Thickness

- ✓ Measures the thickness of liquid water needed to stop the ion beam in the same manner that a certain thickness of the given material.

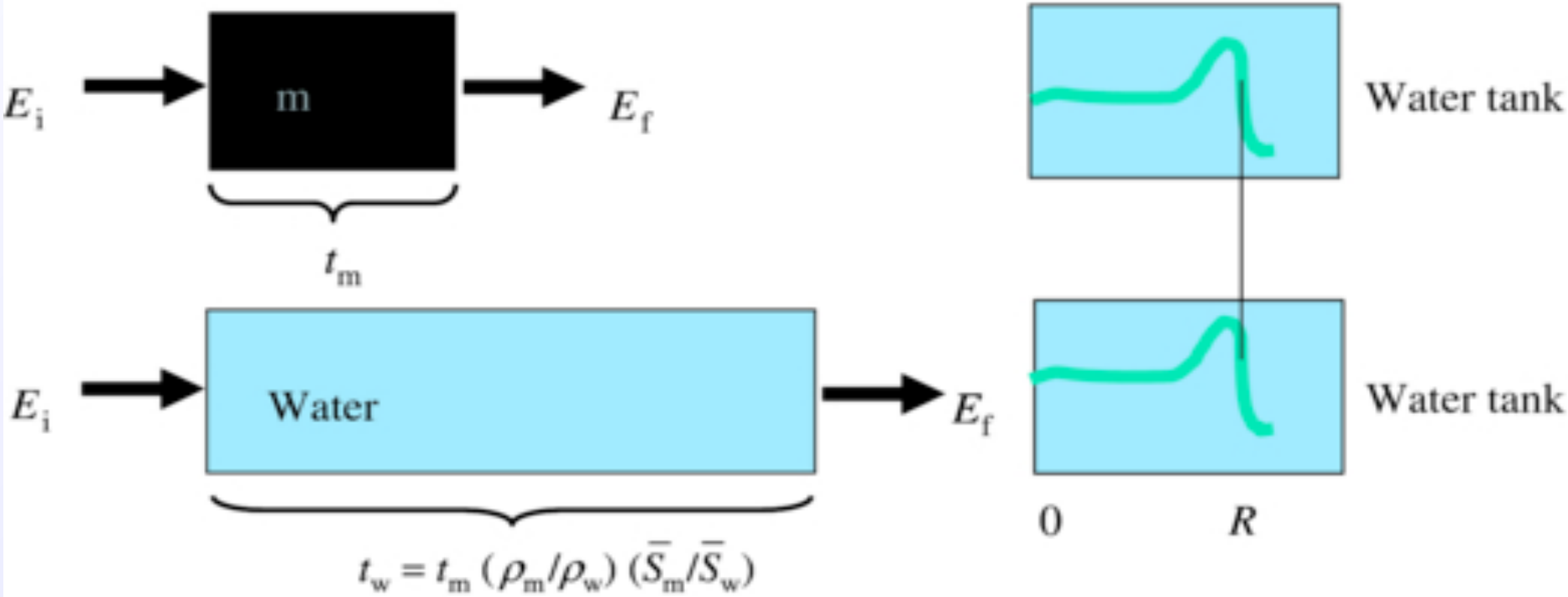

Water Equivalent Thickness

For High-Z material its water equivalent depends on incident energy. The water equivalent of 0.6329 cm Pb is 3.5722 cm at 200 MeV incident but 3.4197 cm at 100 MeV, 1.5 mm less. By contrast, a plastic degrader has the same water equivalent at any radiotherapy energy.

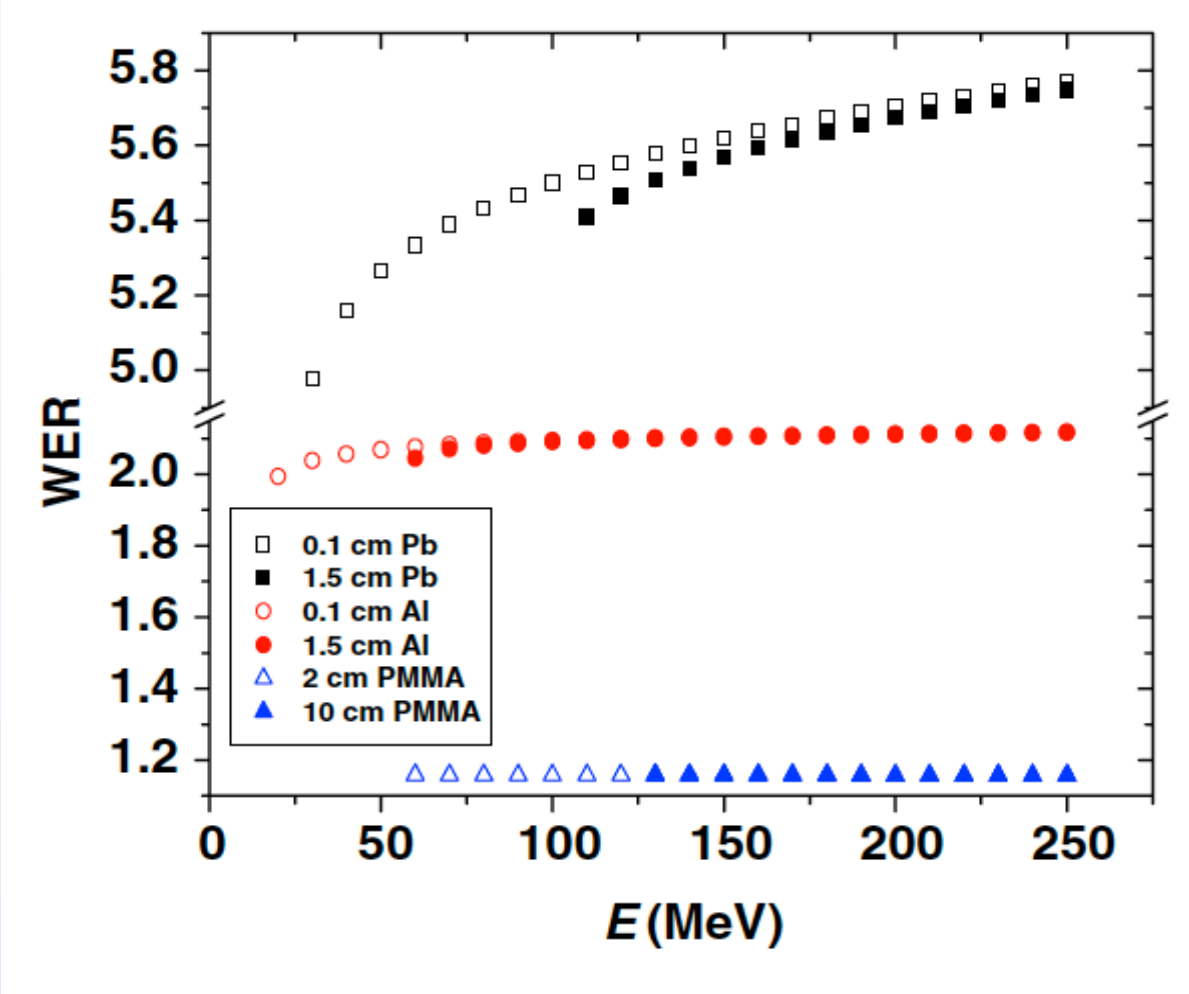

Spread-Out Bragg Peaks (SOBPs)

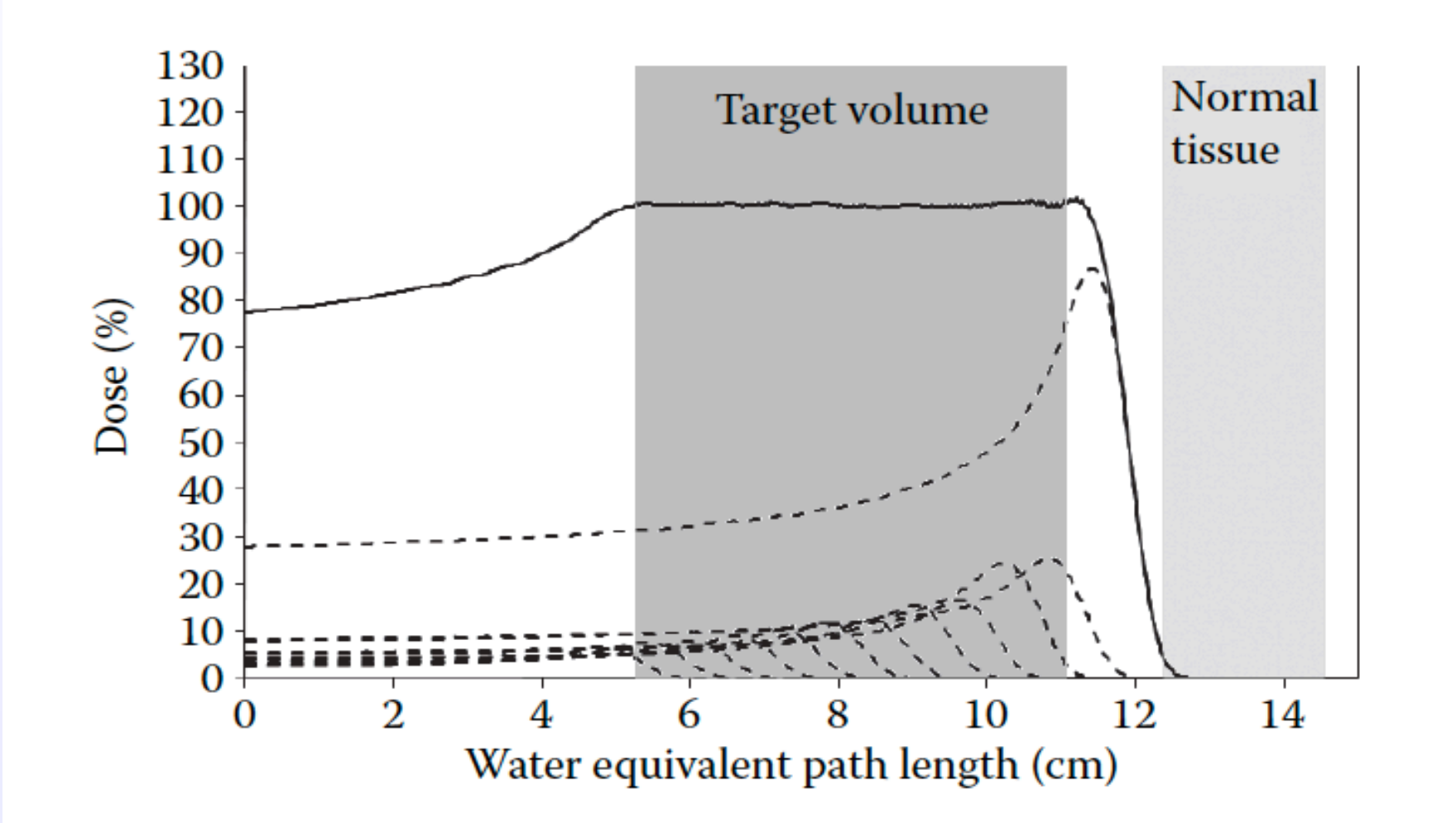

Parameters uses to describe dose distributions

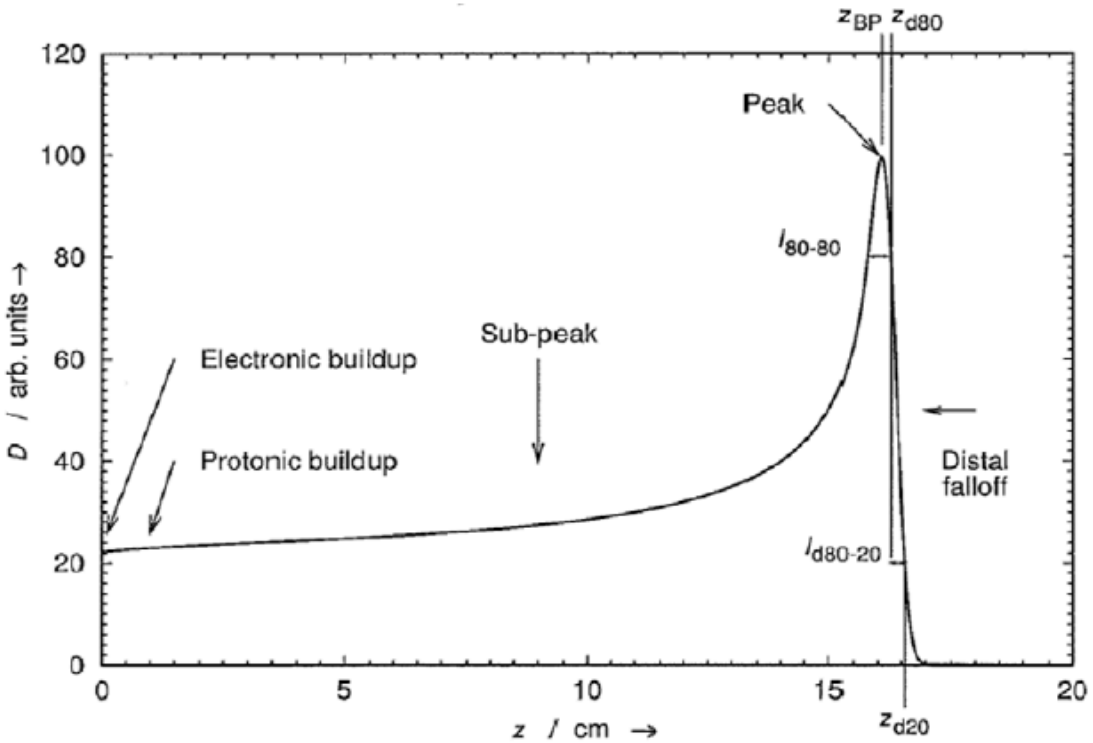

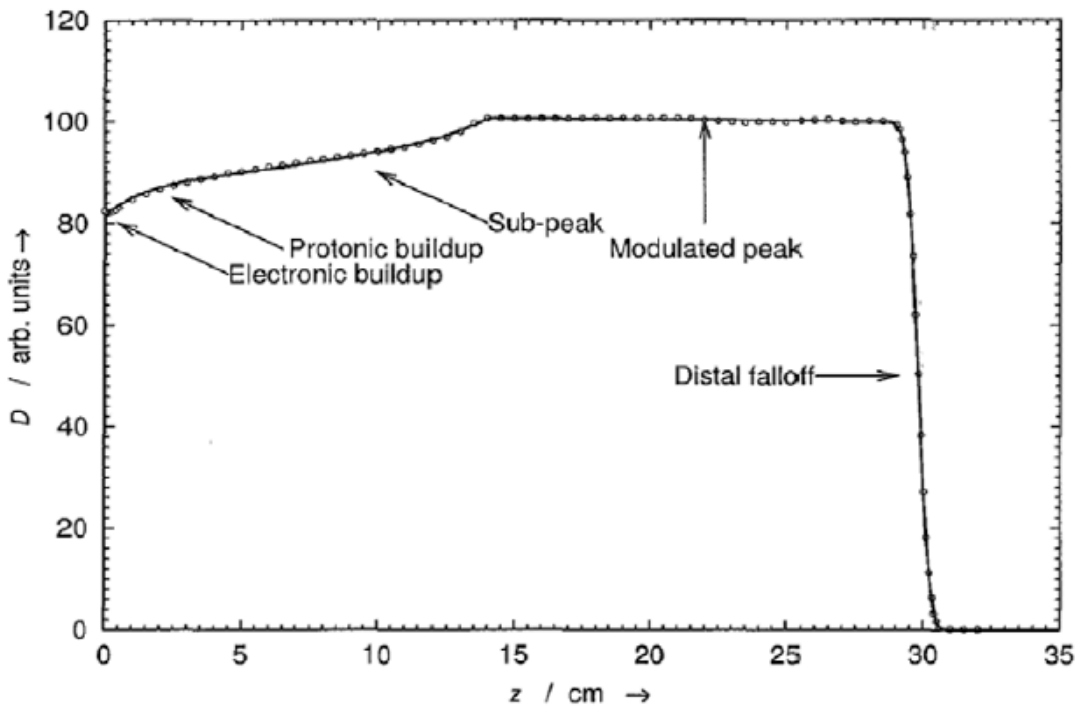

Absorbed dose D as a function of depth z in water from an unmodulated (pristine) proton Bragg peak produced by a broad proton beam with an initial energy of 154 MeV.

L.M. Fraile

Absorbed dose D as a function of depth z in water from a spread-out proton Bragg peak (SOBP)

S. España

Parameters used to describe dose distributions

The beam **range** is defined as the depth of penetration at 90%.
The **modulation** width is defined as the width of the dose plateau

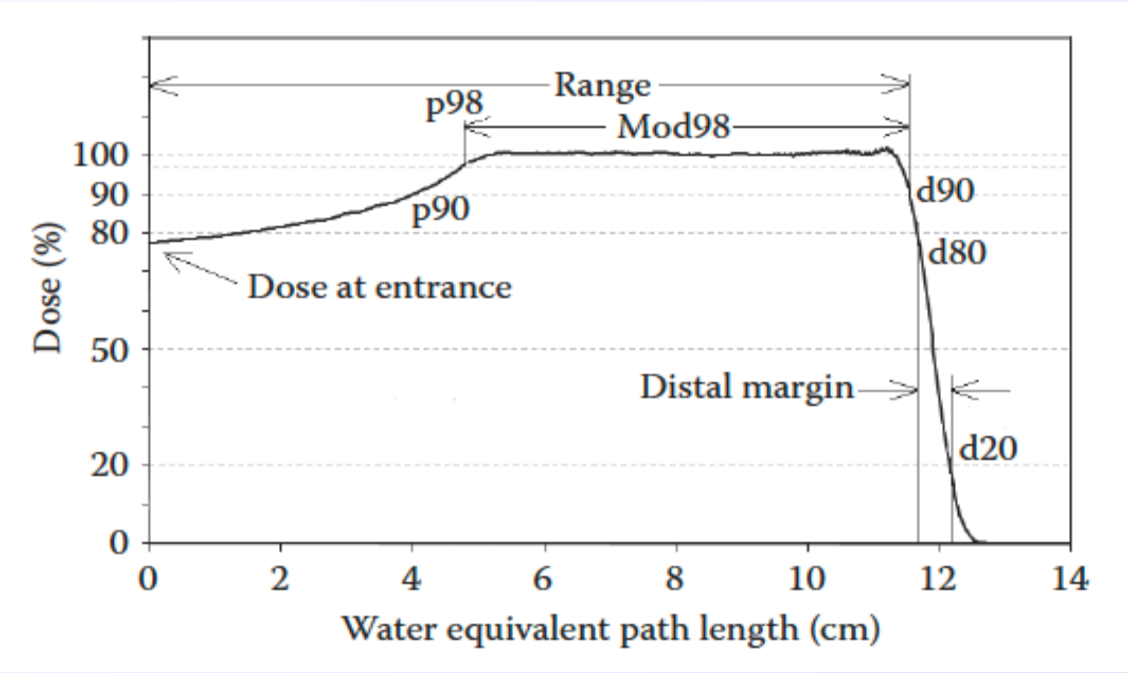

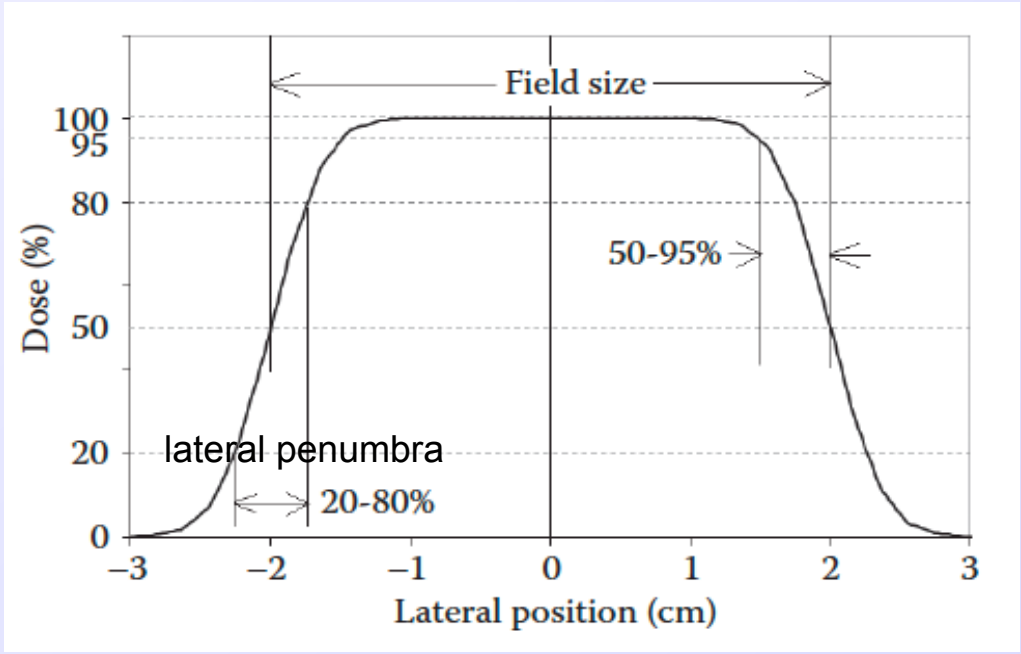

Beam Size: Transverse Equilibrium

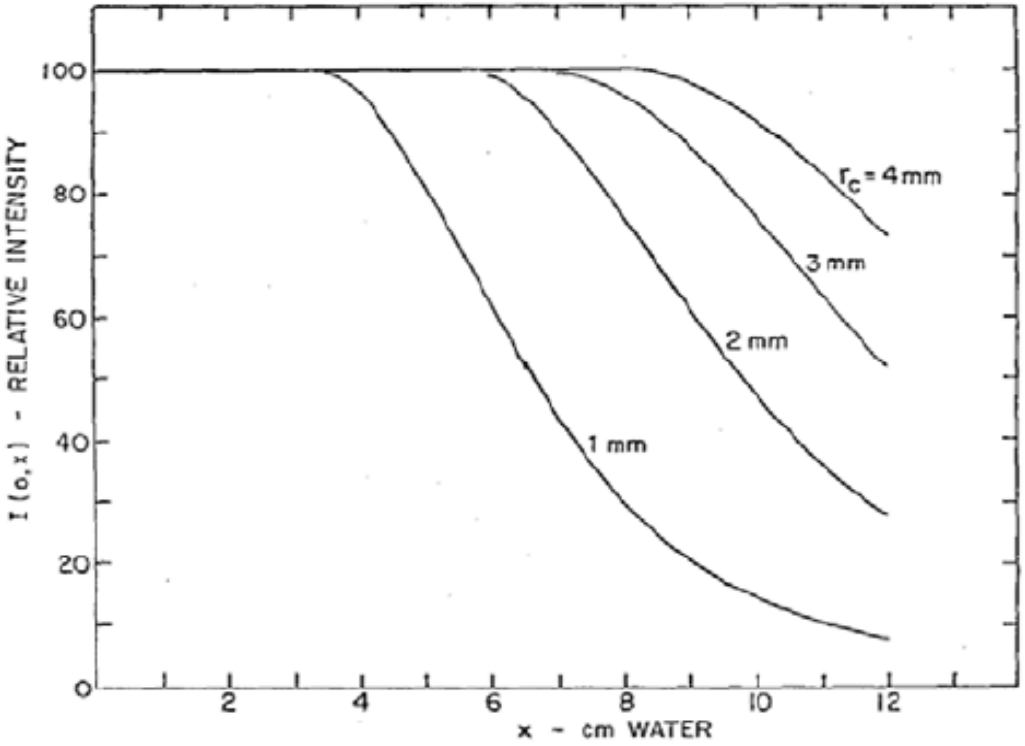

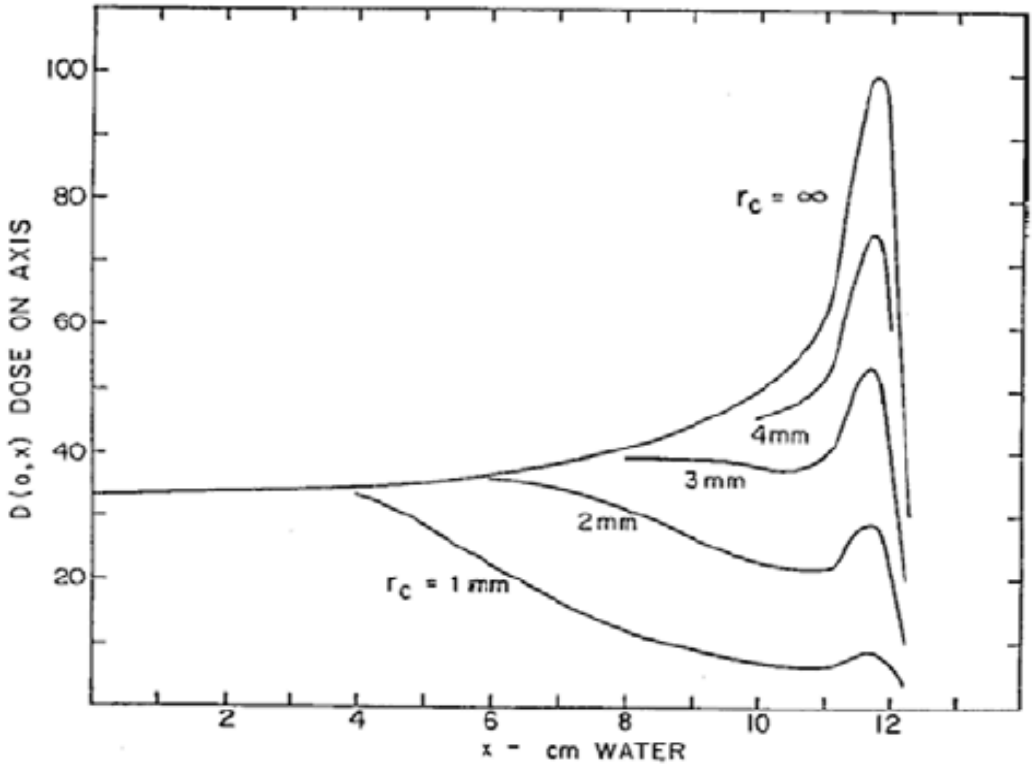

Proton fluence along the beam central axis versus depth x in water. Circular cross sections (r_c) and radii of 1 to 4 mm. Some of the protons are lost because of scattering events that deflect them from the central axis.

The corresponding central-axis absorbed-dose curves. Note how the fluence depletion reduces the absorbed dose at the peak relative to the entrance dose

Lateral Penumbra

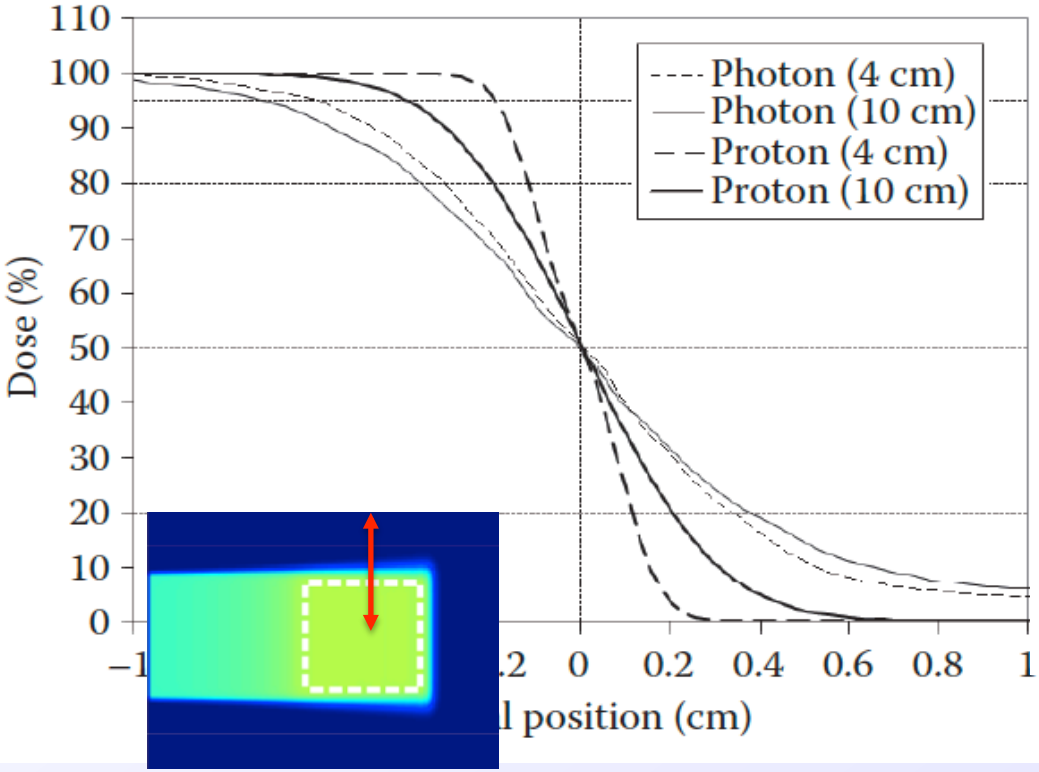

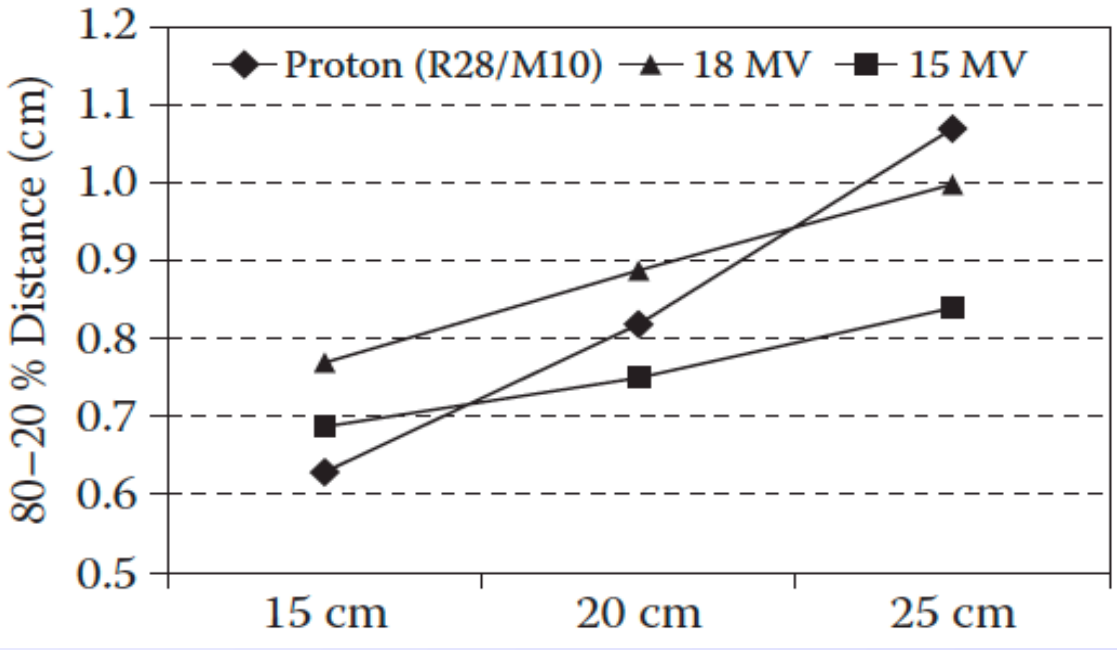

Lateral beam profiles in the penumbra region for scattered beam with range of 14 cm and modulation width of 10 cm at both 4- and 10-cm depths in water. Comparison with 6-MV photon beam.

Proton penumbras are much sharper than the photon counterparts.

Proton penumbra increases drastically as depth increases from 4 to 10 cm, whereas the photon penumbra increase is moderate

Distal Penumbra

- ✓ It increases moderately with energy due to **range straggling** in the patient and also by scattering and range modulation components in the nozzle if scattering is used. From 3.5 to 5.0 mm (20%–80%) over the beam range of 4.8 to 25 cm.
- ✓ When **high-gradient tissue inhomogeneity** present distal penumbra can be degraded distal penumbra substantially.
- ✓ Not always used clinically for tight margin sparing because of **uncertainties in predicting the beam range** in the patient. The range uncertainty issue is managed by **adding an additional amount to the beam range** in treatment planning, usually 3.5% + 1-3 mm, to head off the potential "un

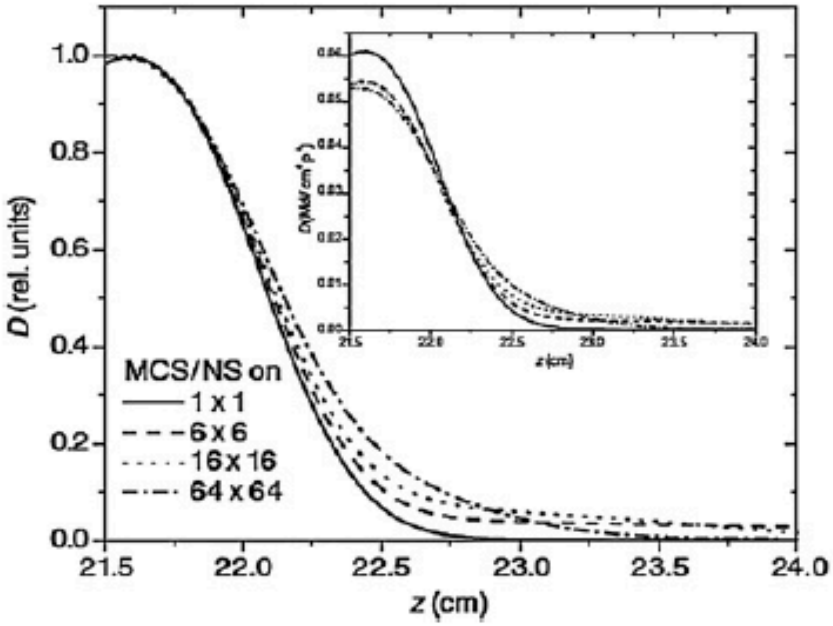

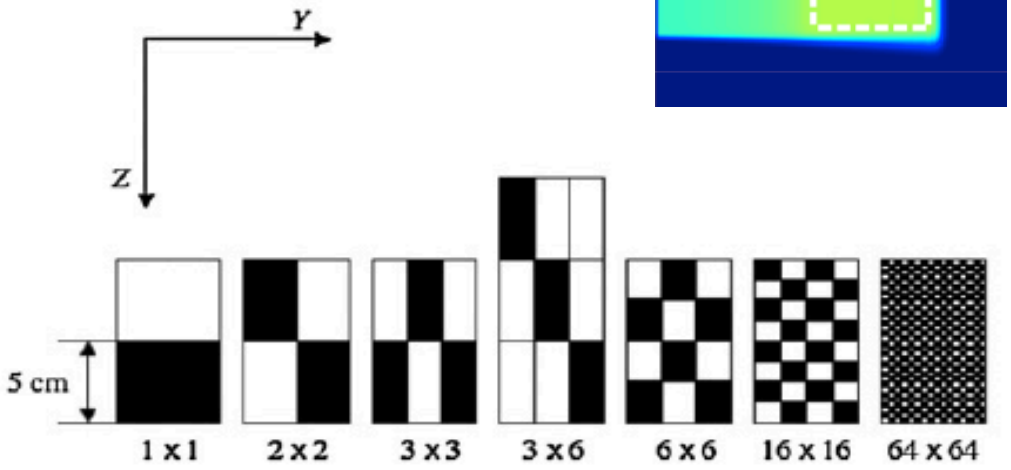

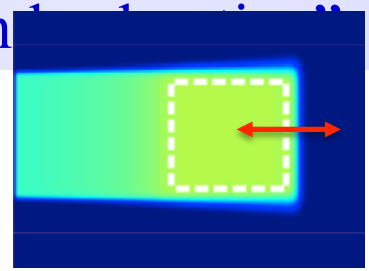

Carbon Ions versus Protons

- ✓ Because of the greater mass of carbon ions, **multiple scattering and range straggling is approximately 3 times less than protons**, resulting in a sharper lateral and longitudinal edge; it is therefore ideal for treatment of deep-seated tumors, where penumbra becomes a limiting factor.

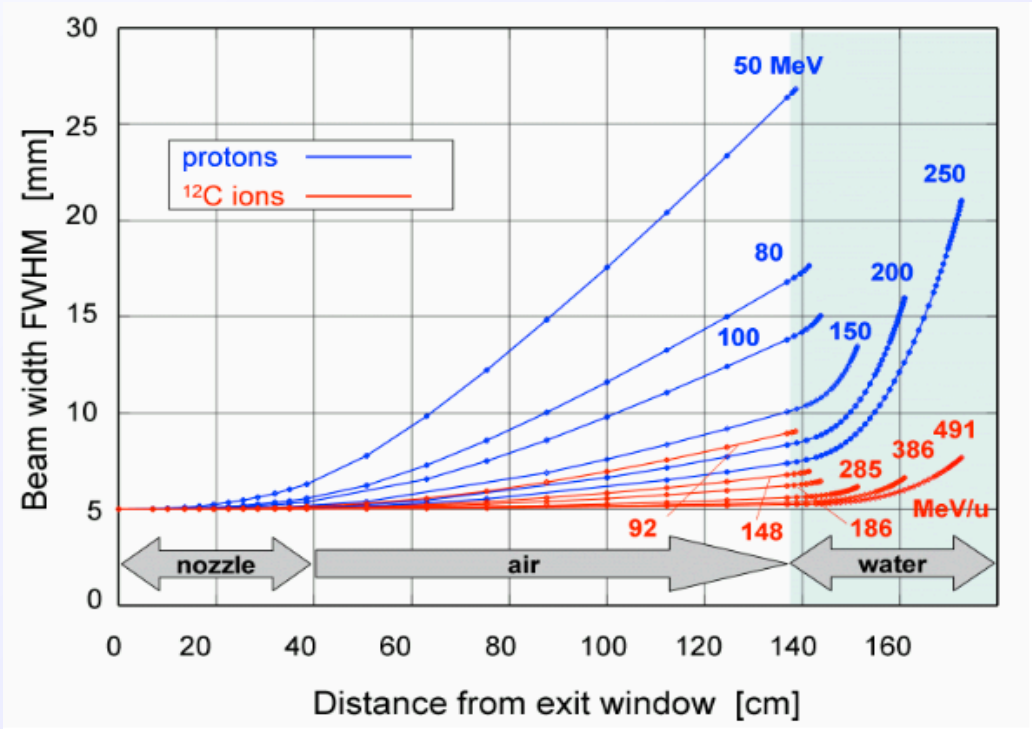

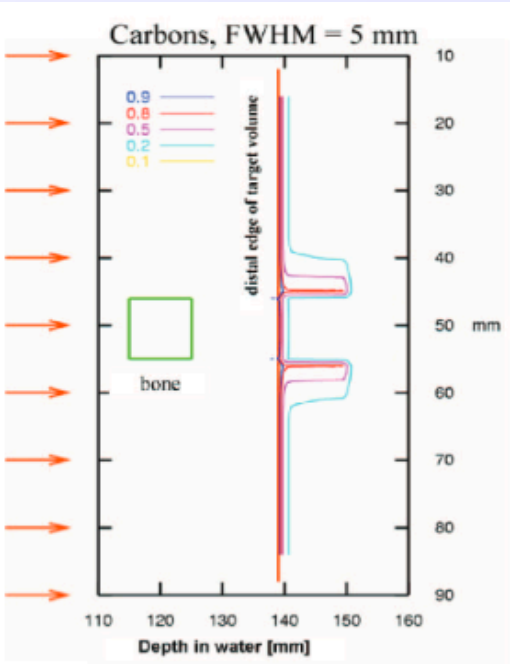

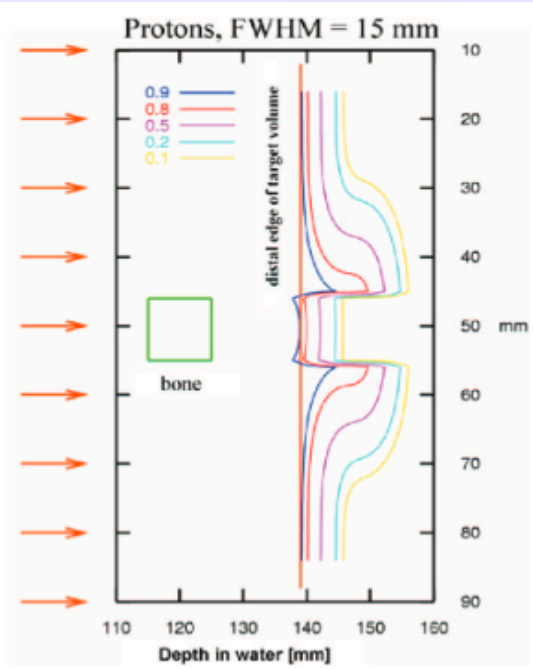

Samuel España

Carbon Ions versus Protons

- Since the **Linear Energy Transfer (LET) in the peak of a carbon beam is larger than that of photon and proton** beams, the Relative Biological Effectiveness (RBE) is 2 to 3 times greater for carbon ions. Therefore, carbon ions have enhanced therapeutic benefits in treating radiation-resistant tumors.
- **Fragmentation of carbon ions produce a tail in the dose distribution after the Bragg peak**.

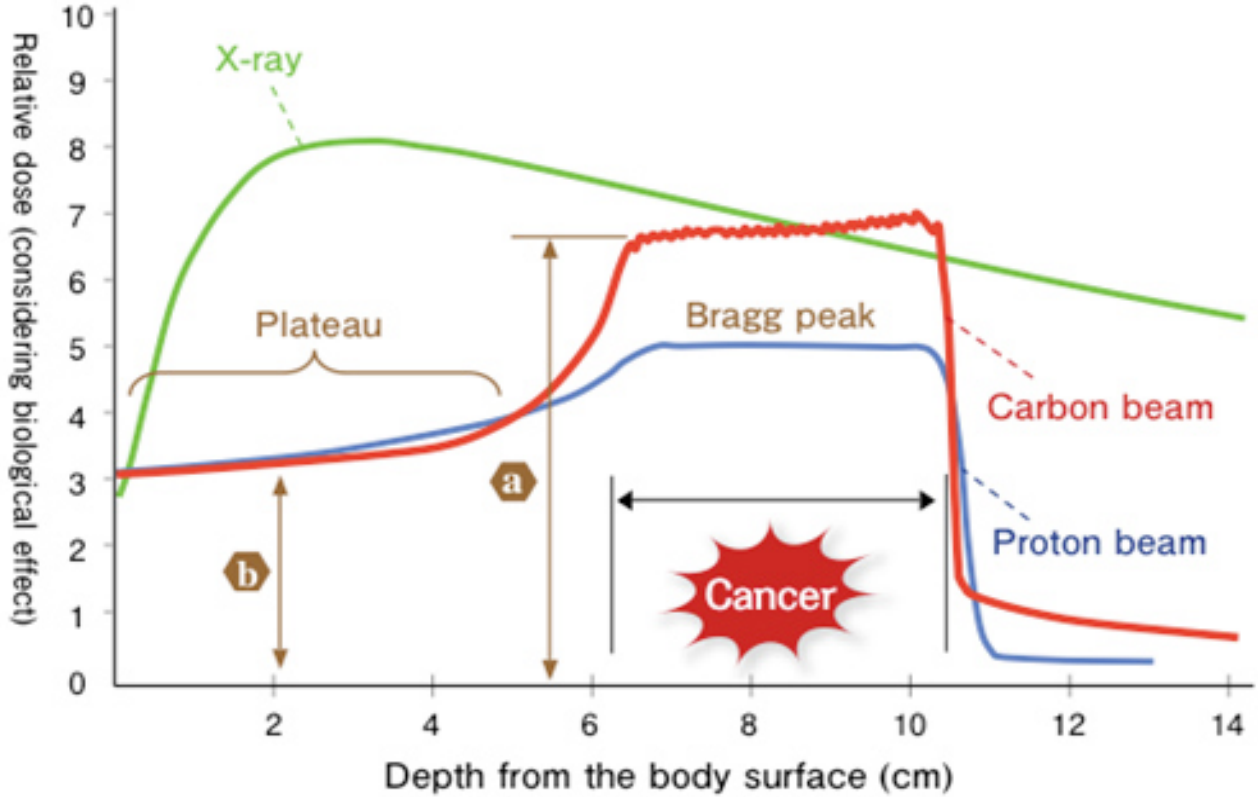

Radiation Therapy

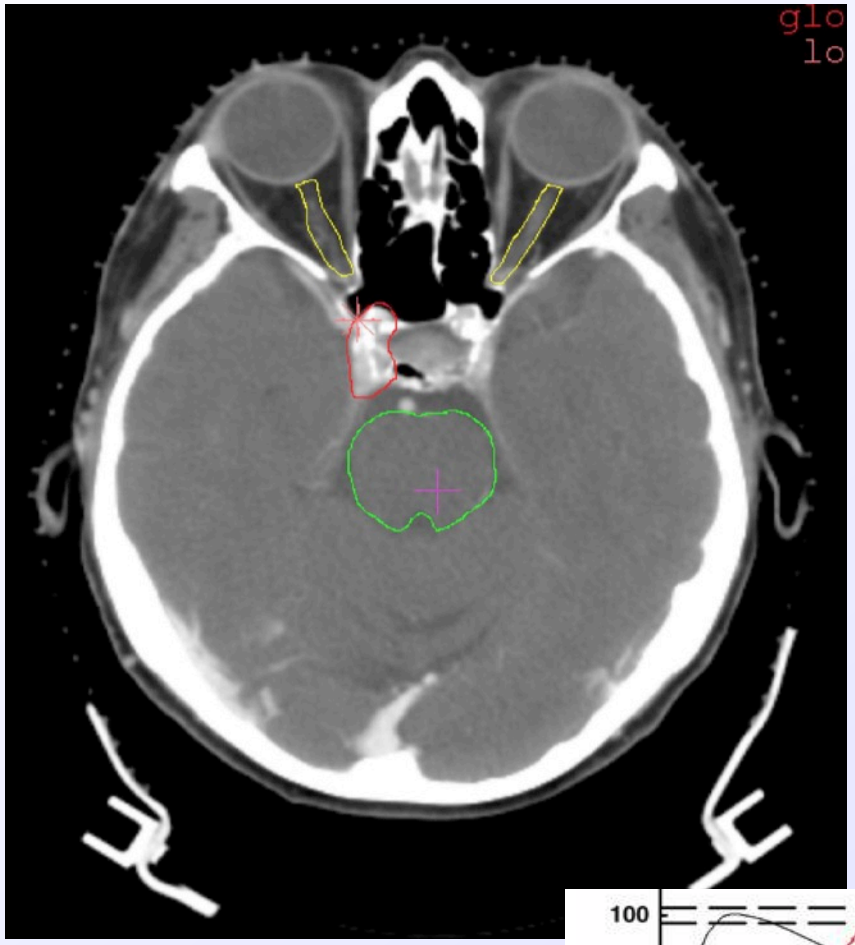

Goal: deliver a uniform prescription dose to the tumor and minimize dose to surrounding healthy tissues.

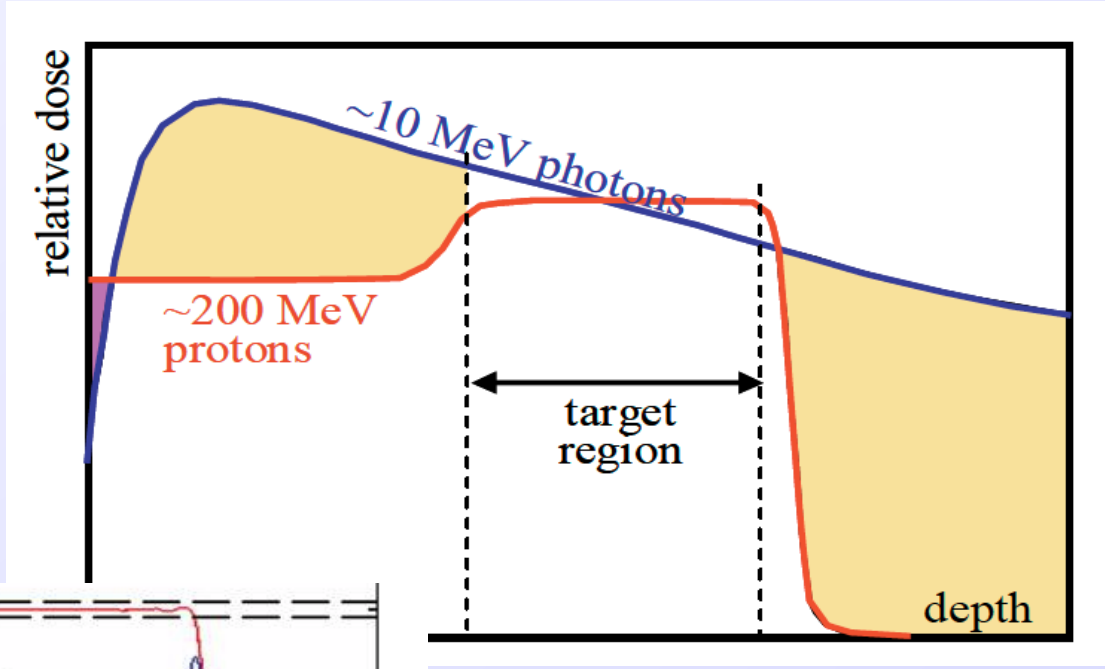

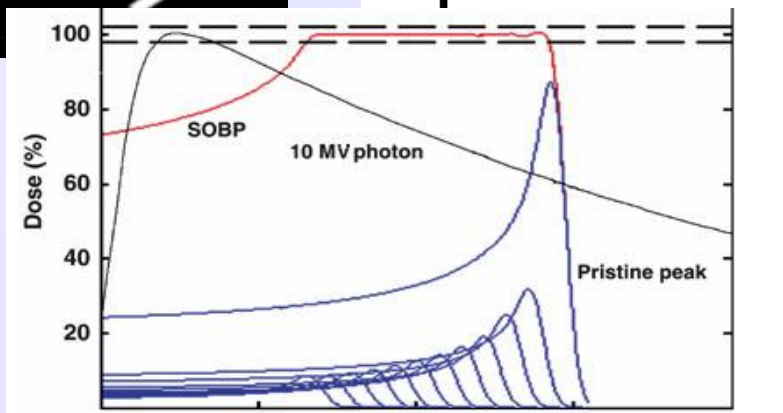

Range Uncertainties

- ✓ Uncertainties in the exact position of the distal dose gradient arise from:
  - →Organ motion.
  - →Setup and anatomical variations.
  - →Dose calculation approximations.
  - →Biological considerations.
- ✓ Treatment planning assumes an uncertainty in the proton beam range of 3.5% of the range plus an additional 1-3 mm.

Protons have the superior advantage of a finite range,

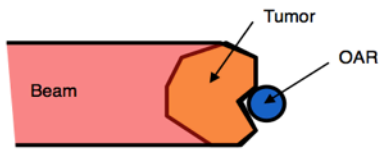

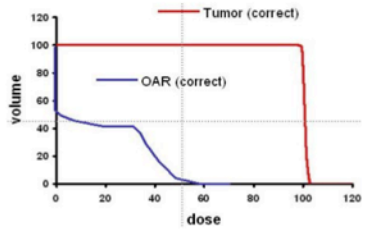

but uncertainties compromise this advantage.

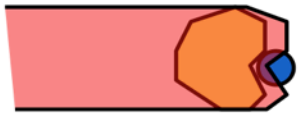

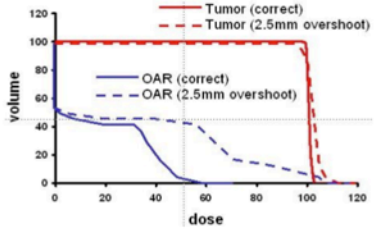

Slight errors may result in severe under dosage of the tumor volume and over dosage of the surrounding critical structures or vice versa.

What is the effect of the proton range?

Source of range uncertainty in the patient	Range uncertainty without Monte Carlo
Independent of dose calculation	
Measurement uncertainty in water for commissioning	±0.3 mm
Compensator design	±0.2 mm
Beam reproducibility	±0.2 mm
Patient setup	±0.7 mm
Dose calculation	
Biology (always positive) ^	+~0.8%
CT imaging and calibration	±0.5%[a]
CT conversion to tissue (excluding I-values)	±0.5%[b]
CT grid size	±0.3%[c]
Mean excitation energy (I-values) in tissues	±1.5%[d]
Range degradation; complex inhomogeneities	−0.7%[e]
Range degradation; local lateral inhomogeneities *	±2.5%[f]
Total (excluding *, ^)	2.7% + 1.2 mm
Total (excluding ^)	4.6% + 1.2 mm

H. Paganetti,
Phys. Med. Biol. 57 (2012) R99

3.5%+3 mm implies 1 cm extra for a tumor at 20 cm depth

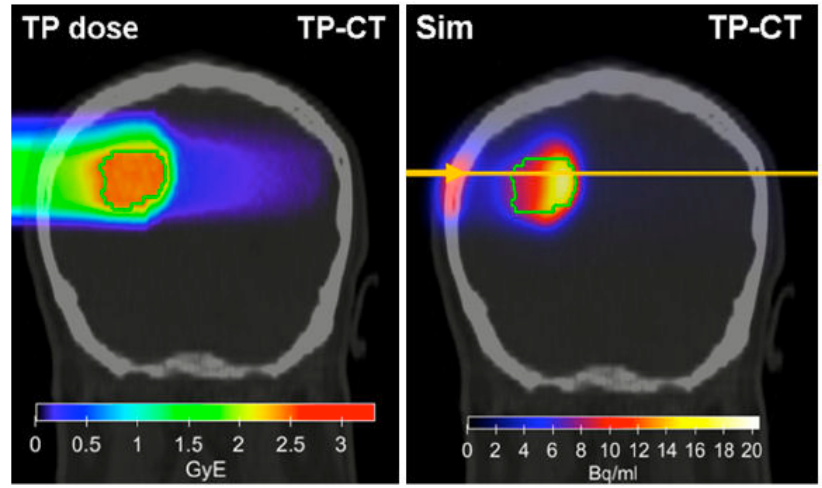

Monte Carlo simulations

Range uncertainties due to multiple Coulomb scattering

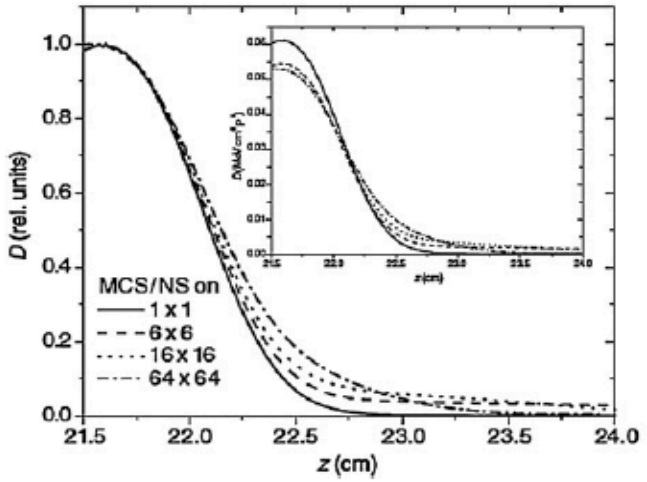

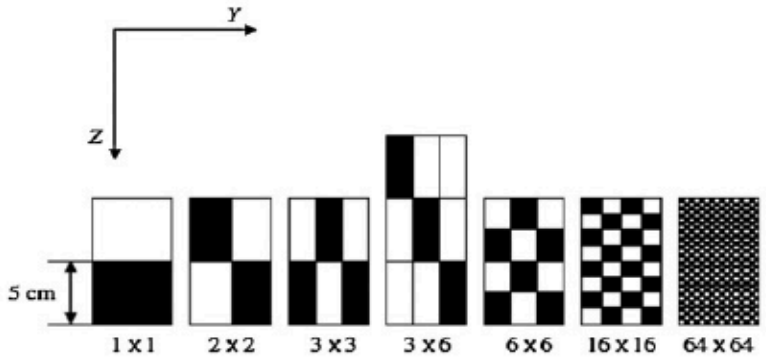

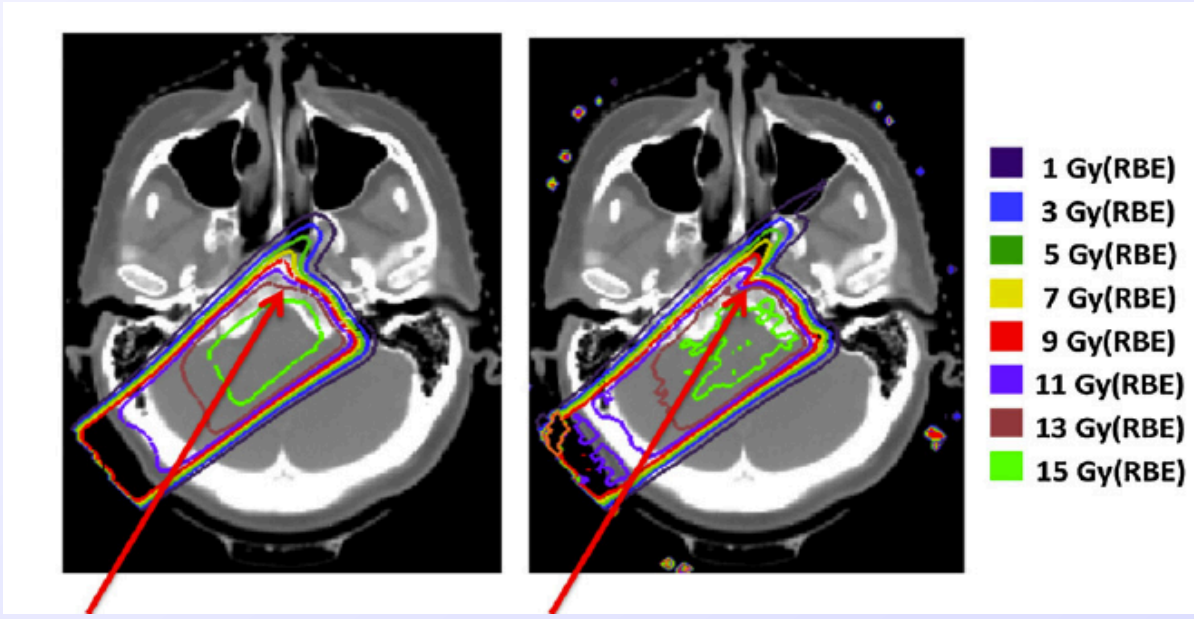

Monte Carlo

Pencil Beam Algorithm

Dose verification

Dose verification in protontherapy

- ✓ CT requires conversion to proton-equivalent stopping power

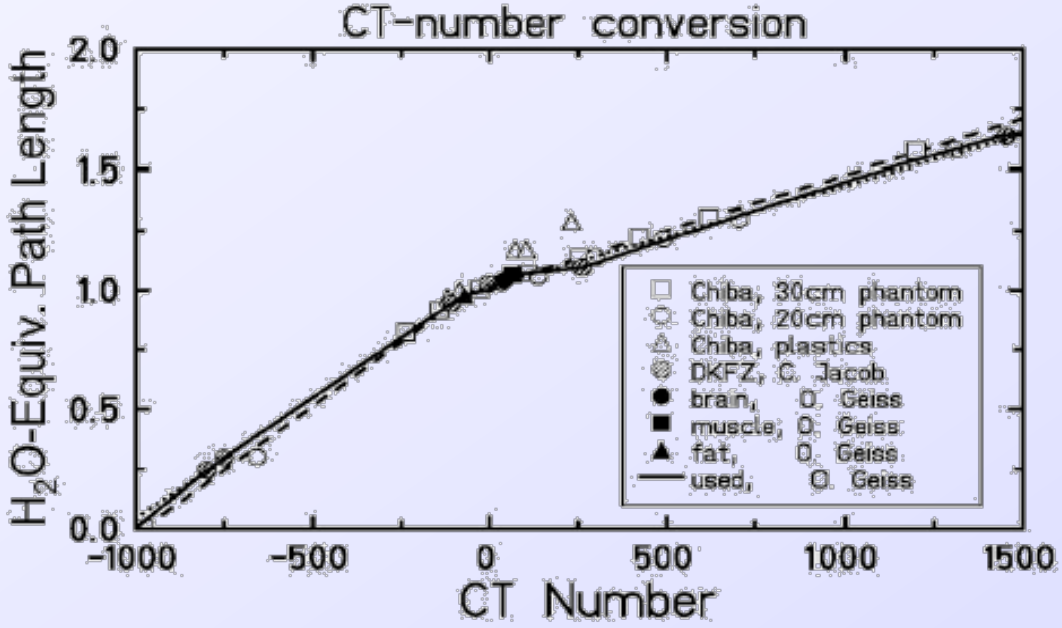

- ✓ Biological washout of produced isotopes: PET emitters

$$Washout(t) = M_f e^{-\lambda_f t} + M_m e^{-\lambda_m t} + M_s e^{-\lambda_s t}$$

- ✓ Proton range needs to be known!

  → uncertainties in range in phantom and controls are of the order of a few mm

PET: Biological Washout Model

$$Washout(t) = M_f e^{-\lambda_f t} + M_m e^{-\lambda_m t} + M_s e^{-\lambda_s t}$$

Table 1. Values used for the fast (*f*), medium (*m*) and slow (*s*) biologic decay properties (*M*: fraction, $T_{1/2,\text{bio}}$: biologic half-life) of different tissue types

	Fast decay		Medium decay		Slow decay	
Tissue type	M_f	$T_{1/2,\text{ bio},f}$ (s)	M_m	$T_{1/2,\text{ bio},m}$ (s)	M_s	$T_{1/2,\text{ bio},s}$ (s)
Hard bone	0.05	20	0.05	300	0.9‡	15,000‡
Soft bone	0.2	15	0.2	250	0.6‡	8,000‡
Fat	0.05	20	0.05	300	0.9‡	15,000‡
Muscle	0.3*	10*	0.15*	195*	0.55*	3,500*
Brain	0.35*	2*	0.3*	140*	0.35*	10,000*

K Parodi et al. Int. J. Radiation Oncology Biol. Phys., Vol. 71, No. 3, pp. 945–956, 2008

In Vivo Range Verification

- ✓ In vivo verification of the delivered range is desirable to understand the true uncertainties and to reduce delivery errors.
- ✓ Use of imaging devices in order to monitor treatment is common practice in photon therapy where each beam penetrates the patient so that exit dose can be utilized.
- ✓ Protons or heavy ions on the other hand stop in the patient and thus imaging can only be based on secondary radiation that is being created by the primary beam.

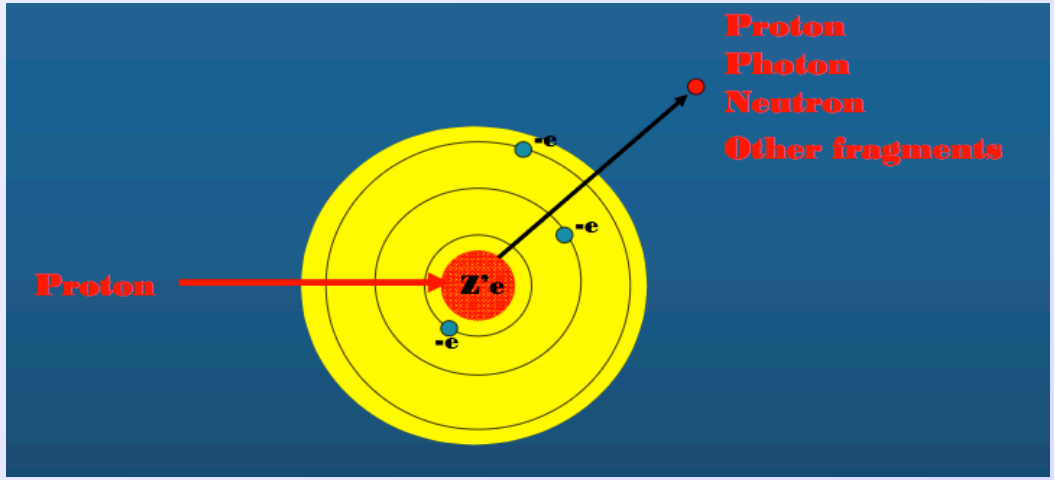

Dose verification

Protoacustics

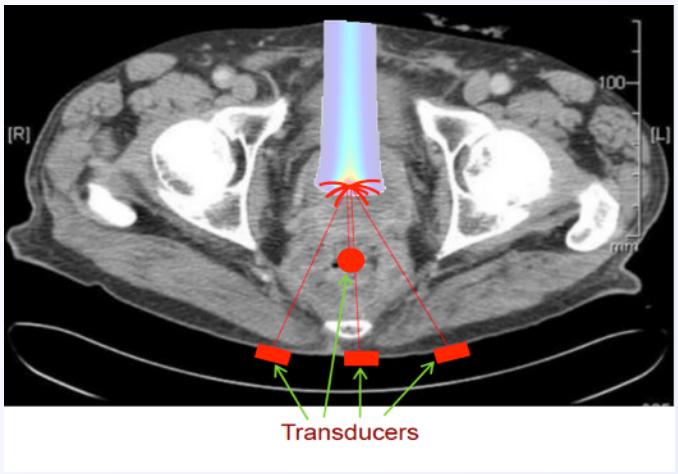

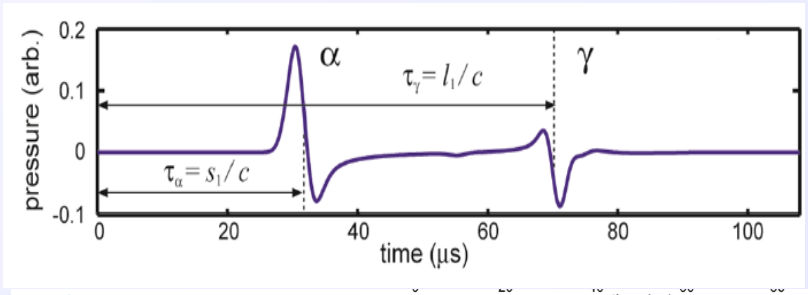

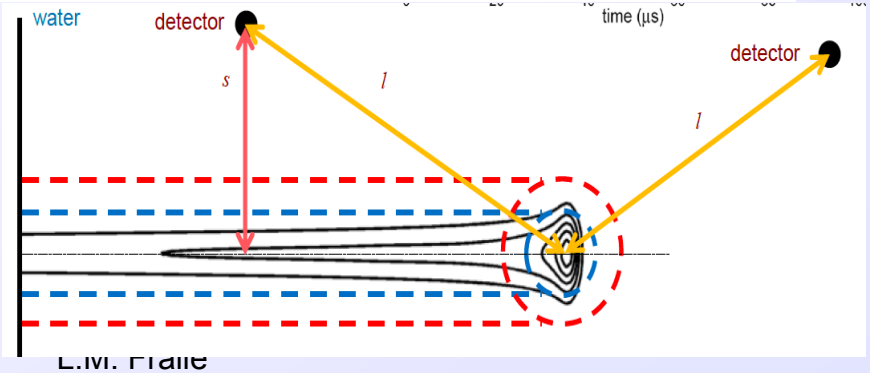

PET, prompt PET

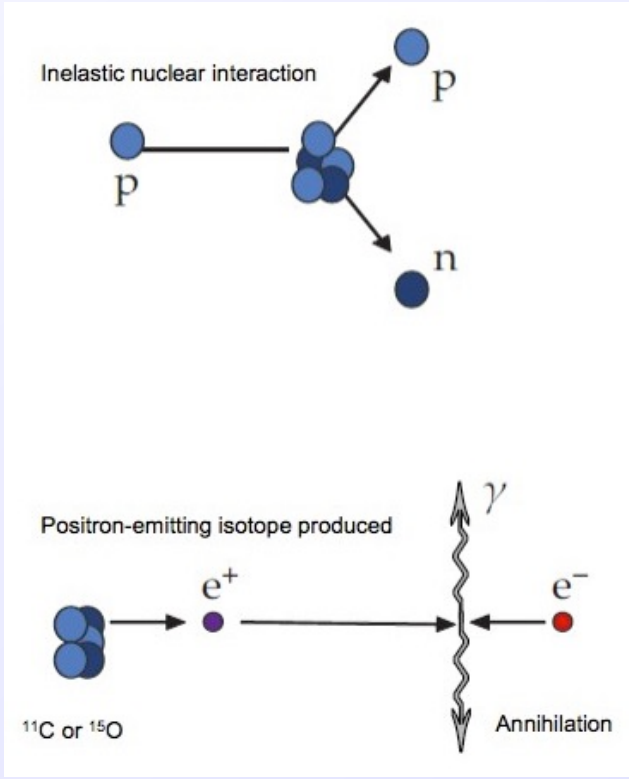

Prompt gamma-rays

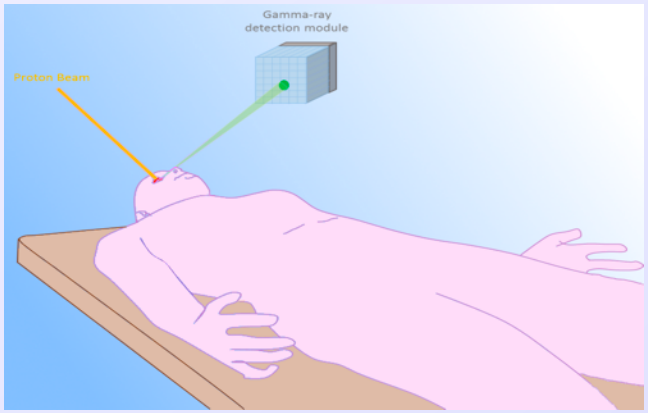

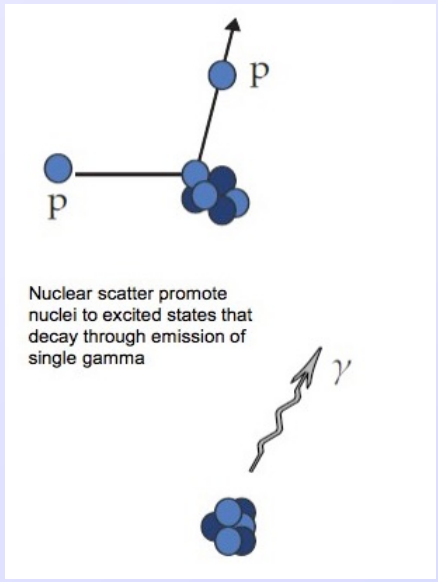

Proton range and techniques

- ✓ Protontherapy
  - → Advantages
  - → Dose vs. nuclei production
  - → PET, PG from nuclear reactions
  - → (Very) small ΔT

Range

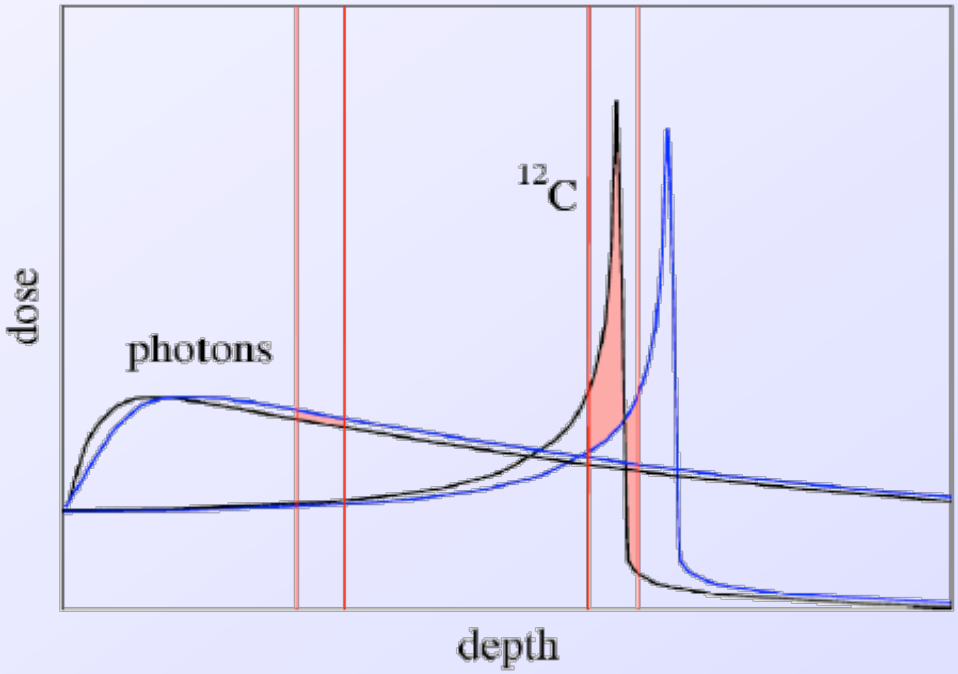

K. Parodi et al., IEEE Trans. Nucl. Science 52 (2005) 778

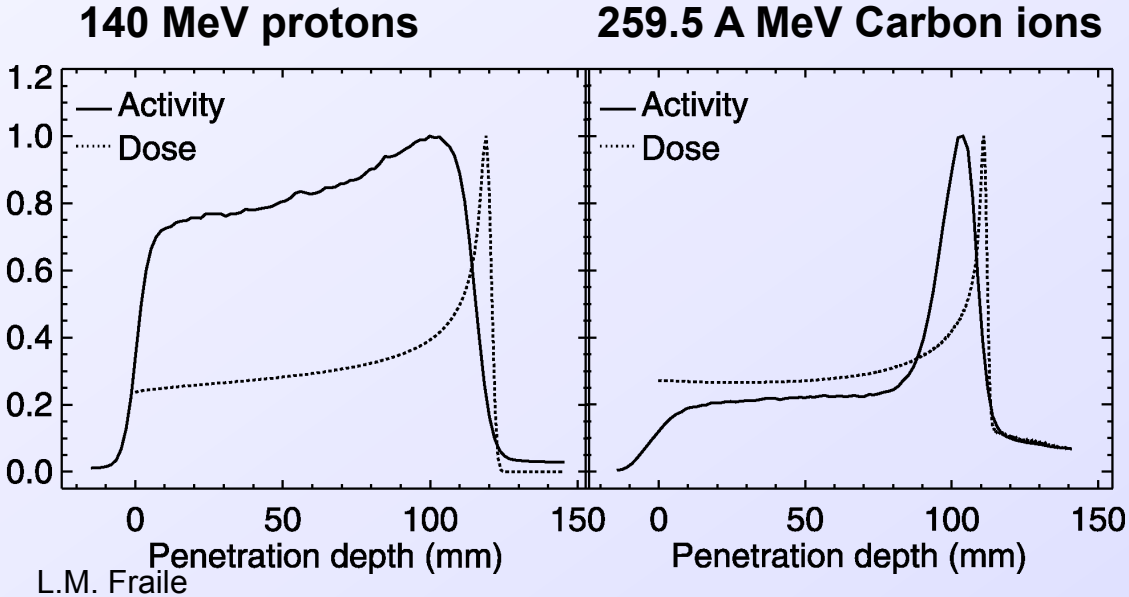

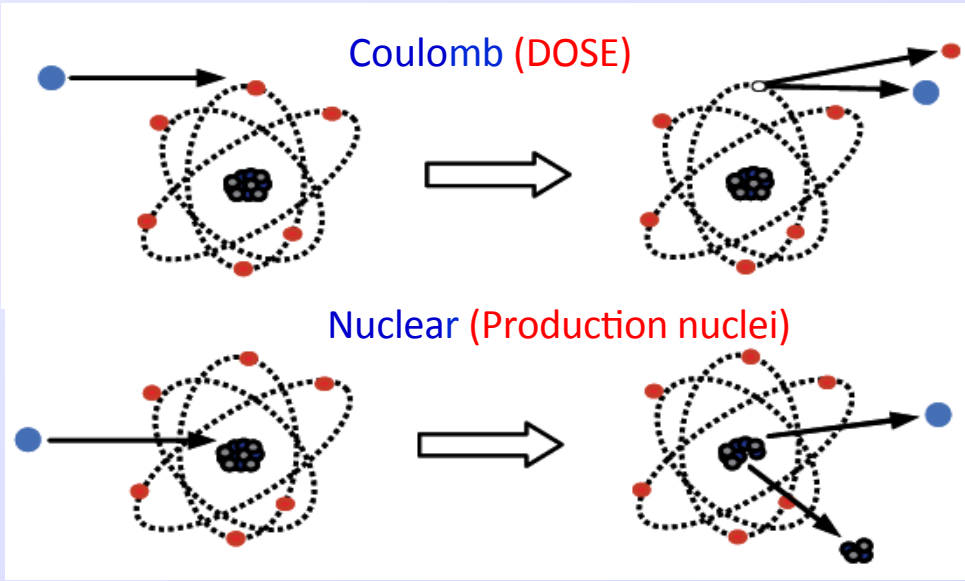

Clinical experience

[S.-Parcerisa]

➢ **PET clinical experience**

- GSI (1997-2004) in-beam, off-spill measurements
- HIT Germany (2013-2017): offline PET/CT after irradiation
  Pending results of clinical trial
- MGH USA (2006-2011): offline PET/CT, in-room neuroPET
  Physical studies, Monte Carlo, cross sections
- NCC Japan (2010): used to monitor changes in daily activity. Short in-room

➢ **Prompt Gamma experience**

- OncoRay (Dresden, Alemania) with Slit Camera by IBA (2016)
- UPenn (Philadelphia, USA) with Slit Camera de IBA (2017)

‘None of the present implementations can be classified as satisfactory’

K. Parodi, Med. Phys. 42:12 (2015) 7153

Slit Camera

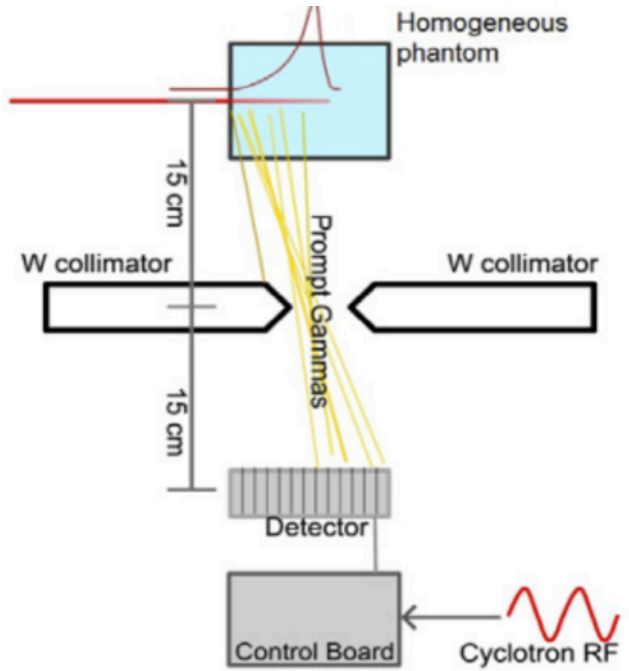

Prompt gamma in vivo

Contents lists available at ScienceDirect

Radiotherapy and Oncology

journal homepage: www.thegreenjournal.com

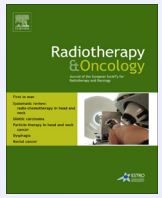

First in man

First clinical application of a prompt gamma based *in vivo* proton range verification system

Christian Richter [a,b,c,d,e,*], Guntram Pausch [a,b,c], Steffen Barczyk [a,b], Marlen Priegnitz [c], Isabell Keitz [a], Julia Thiele [b], Julien Smeets [f], Francois Vander Stappen [f], Luca Bombelli [g], Carlo Fiorini [h], Lucian Hotoiu [f], Irene Perali [h], Damien Prieels [f], Wolfgang Enghardt [a,b,c,d,e], Michael Baumann [a,b,c,d,e]

[a] *OncoRay – National Center for Radiation Research in Oncology, Faculty of Medicine and University Hospital Carl Gustav Carus, Technische Universität Dresden, Helmholtz-Zentrum Dresden – Rossendorf;* [b] *Department of Radiation Oncology, Faculty of Medicine and University Hospital Carl Gustav Carus, Technische Universität Dresden;* [c] *Helmholtz-Zentrum Dresden – Rossendorf;* [d] *German Cancer Research Center (DKFZ), Heidelberg;* [e] *German Cancer Consortium (DKTK), Dresden, Germany;* [f] *Ion Beam Applications SA, Louvain-la-Neuve, Belgium;* [g] *XGLab S.R.L., Milano; and* [h] *Politecnico di Milano, Dipartimento di Elettronica, Informazione e Bioingegneria, Italy*

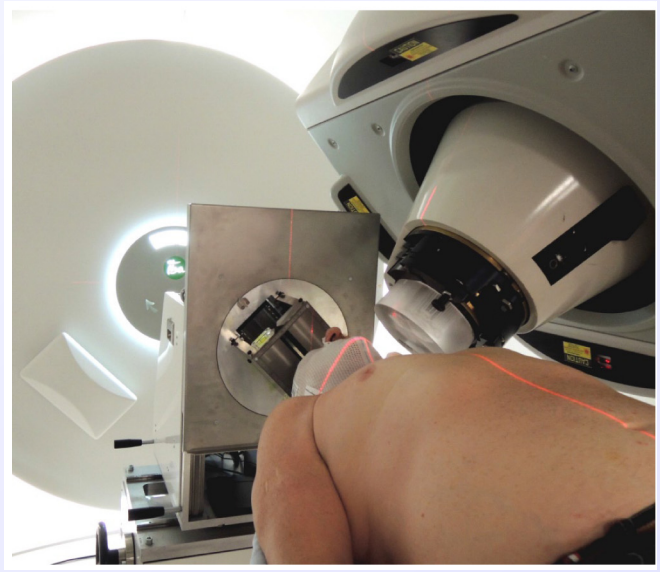

Compared to control CT
Spatial information
+- 2 mm in sum profiles

[absolute range
uncertainty of 6.7 mm]

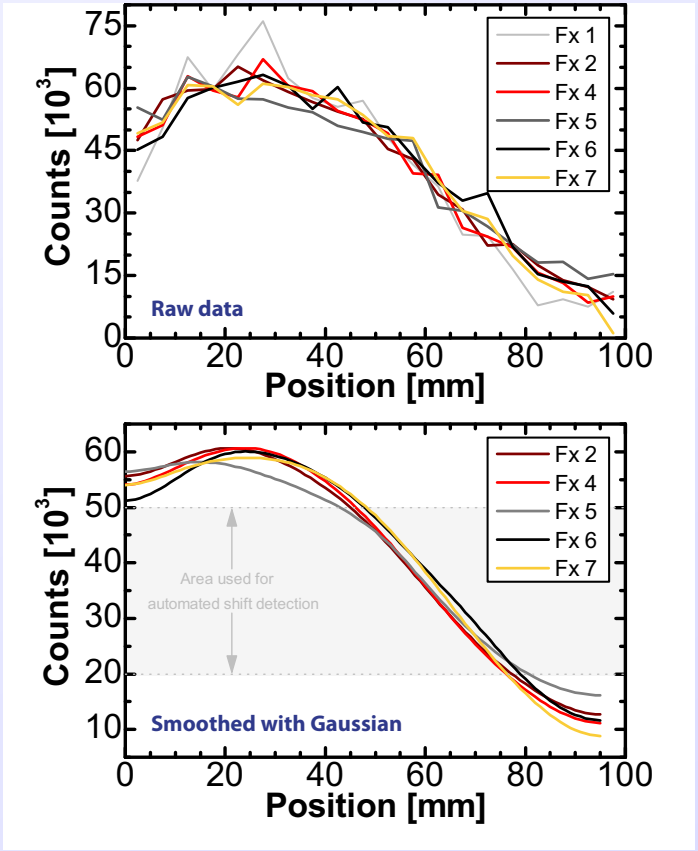

PET

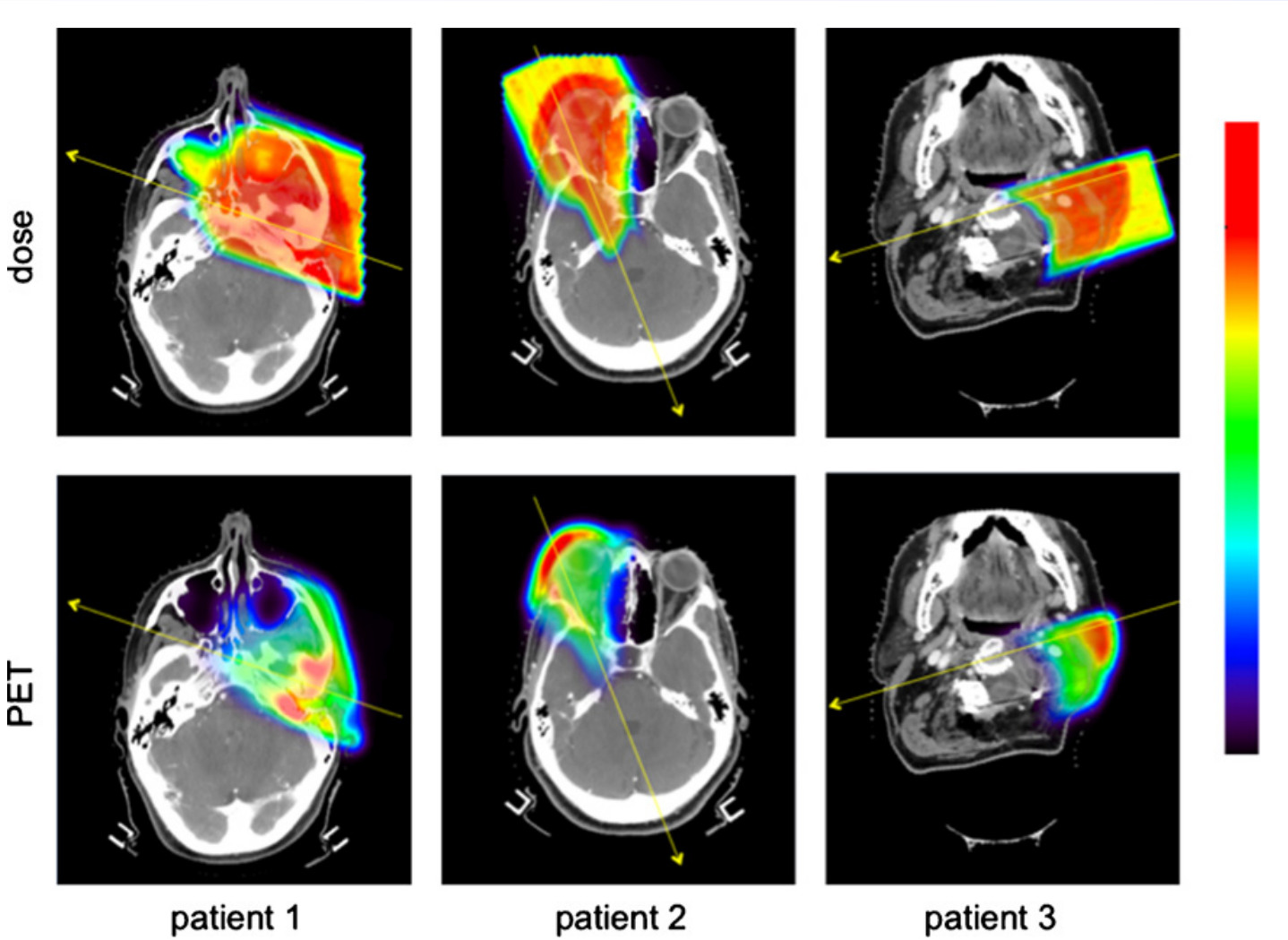

Dose vs. PET based on MC

- Range determination
- Use of Prompt Gammas
- Production of radioisotopes
- Detection techniques
- …

S. España and H. Paganetti
Phys. Med. Biol. 55 (2010) 7557

PET: Nuclear Reaction Cross Sections

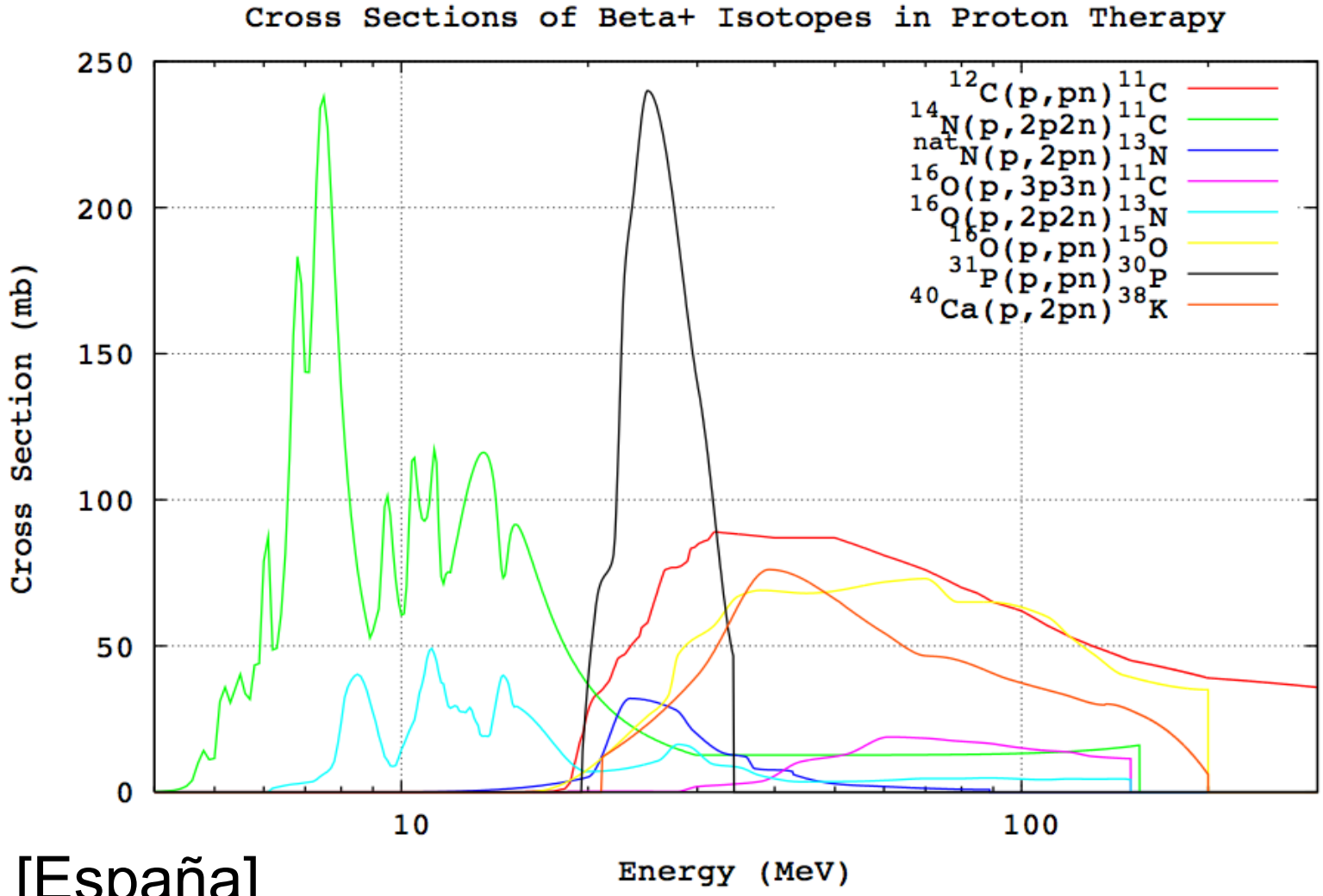

[España]

PET distribution using GEANT4

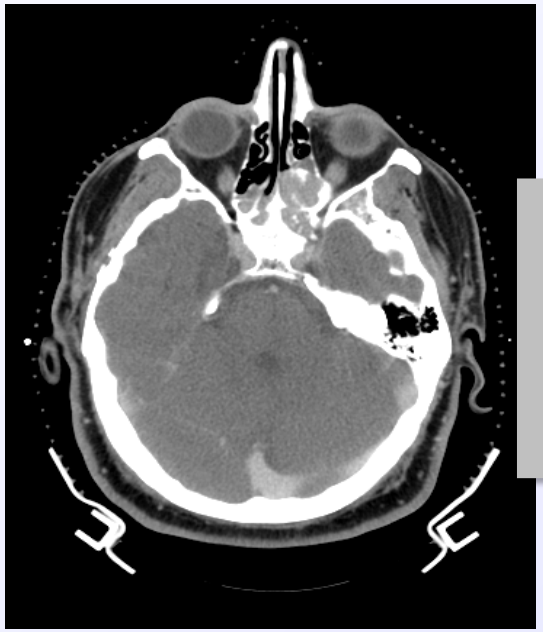

Planning CT
Composition

GEANT4
Fluence
Cross
Sections

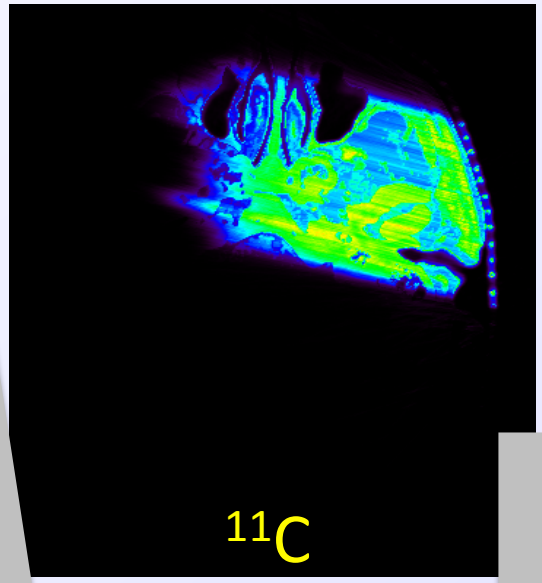

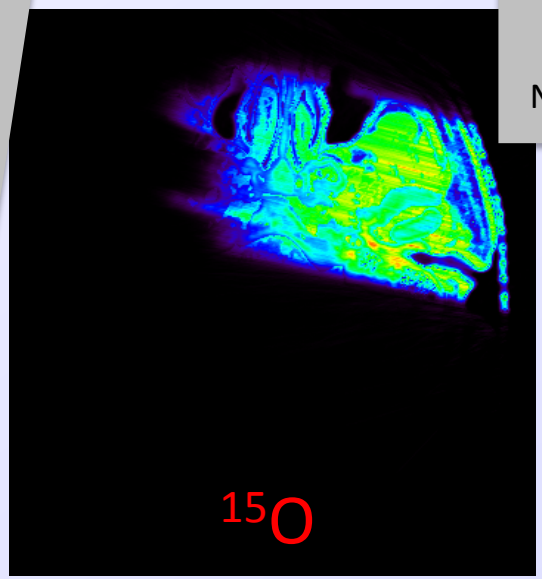

MATLAB
Decay
Washout
Blurrring
Normalization

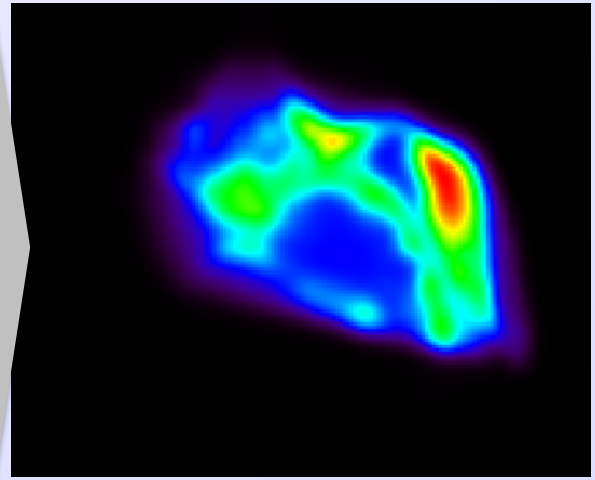

Monte Carlo
PET

PET: In-Beam Protocol

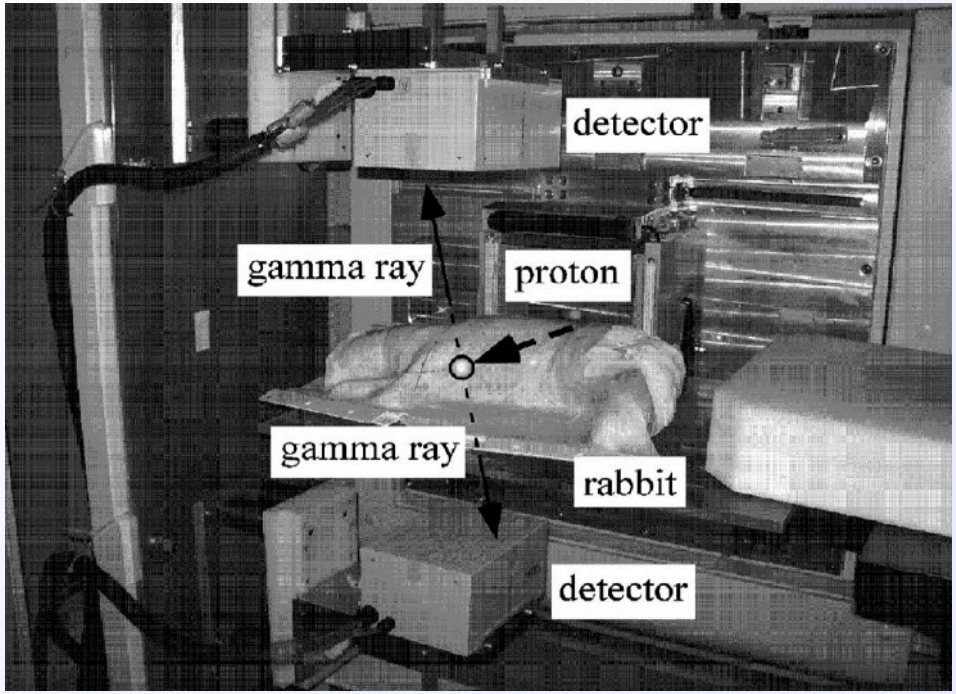

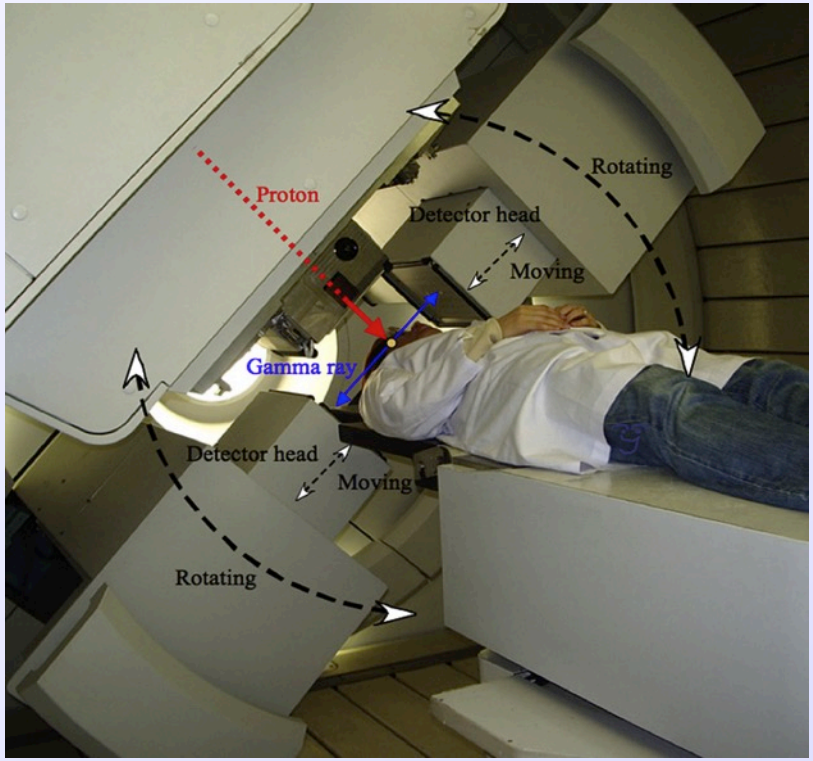

- ✓ **Strong points.**
  - → In-Beam PET with no delay.
  - → Patient movement is minimized.
  - → ^{15}O signal, dominant in soft tissues, is maximized.
- ✓ **Weak points.**
  - → No 3D imaging.
  - → Low Noise to Signal Ratio. Low sensitivity.
  - → No scatter correction.

Measured and Monte Carlo results

S. España and H. Paganetti
Phys. Med. Biol. **55** (2010) 7557

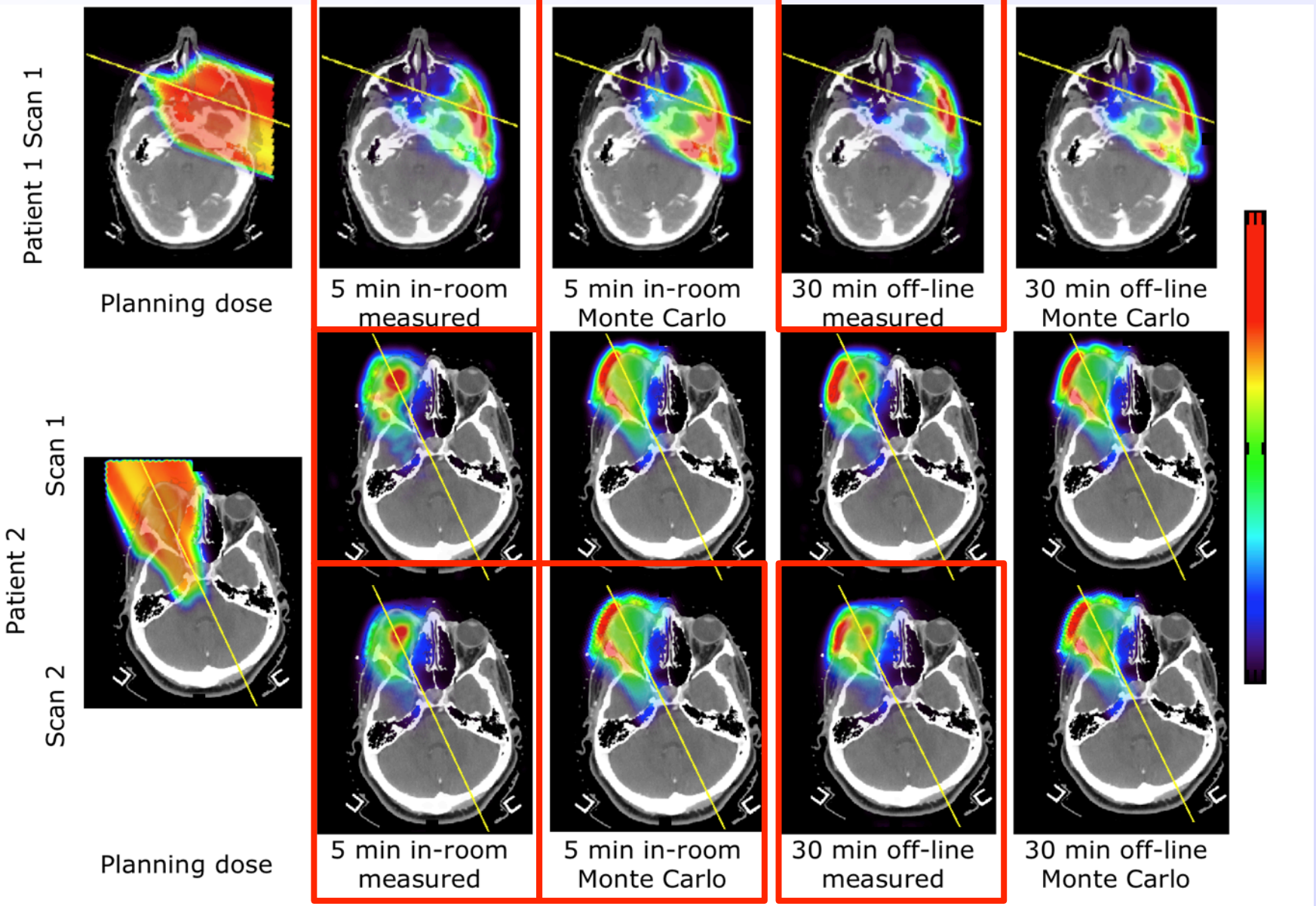

PET profiles

- In room protocol: 2 min delay & 5 min scan.
- ^{15}O ($t_{1/2}$=122.44 s) becomes dominant but ^{11}C ($t_{1/2}$=20.38 min) also contributes among other isotopes.
- Biological washout and spatial resolution are included.

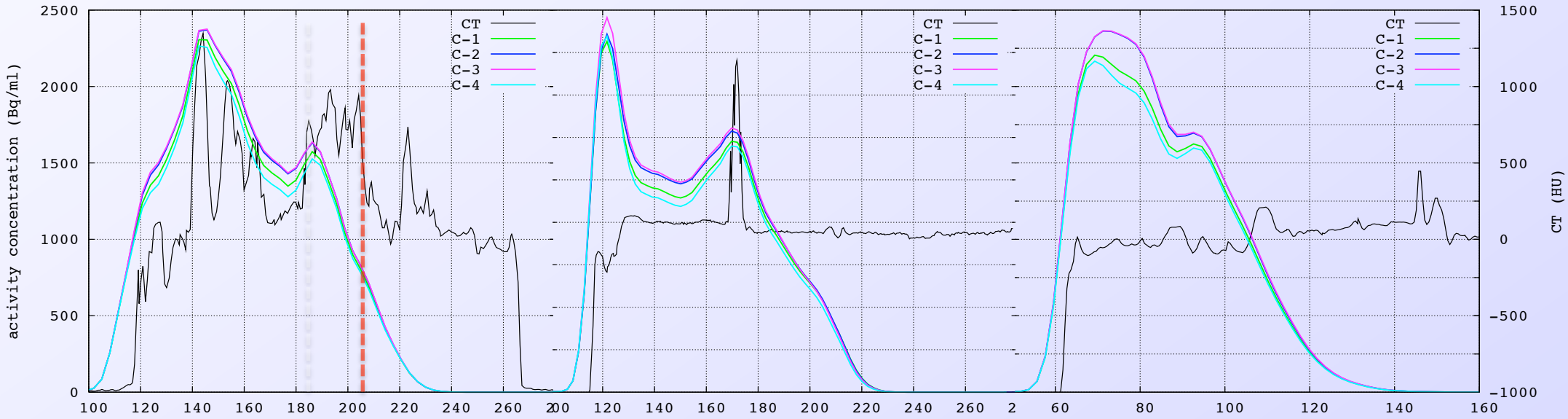

patient 1 patient 2 patient 3

[S. España]

PET range differences

- Range position: 5, 15, 25, 35, 45, 55% of mean activity in the irradiated volume.
- Mean and standard deviation of a few hundred profiles.
- Conversion 1 (C-1) is used as reference calculation and is compared with all other methods.

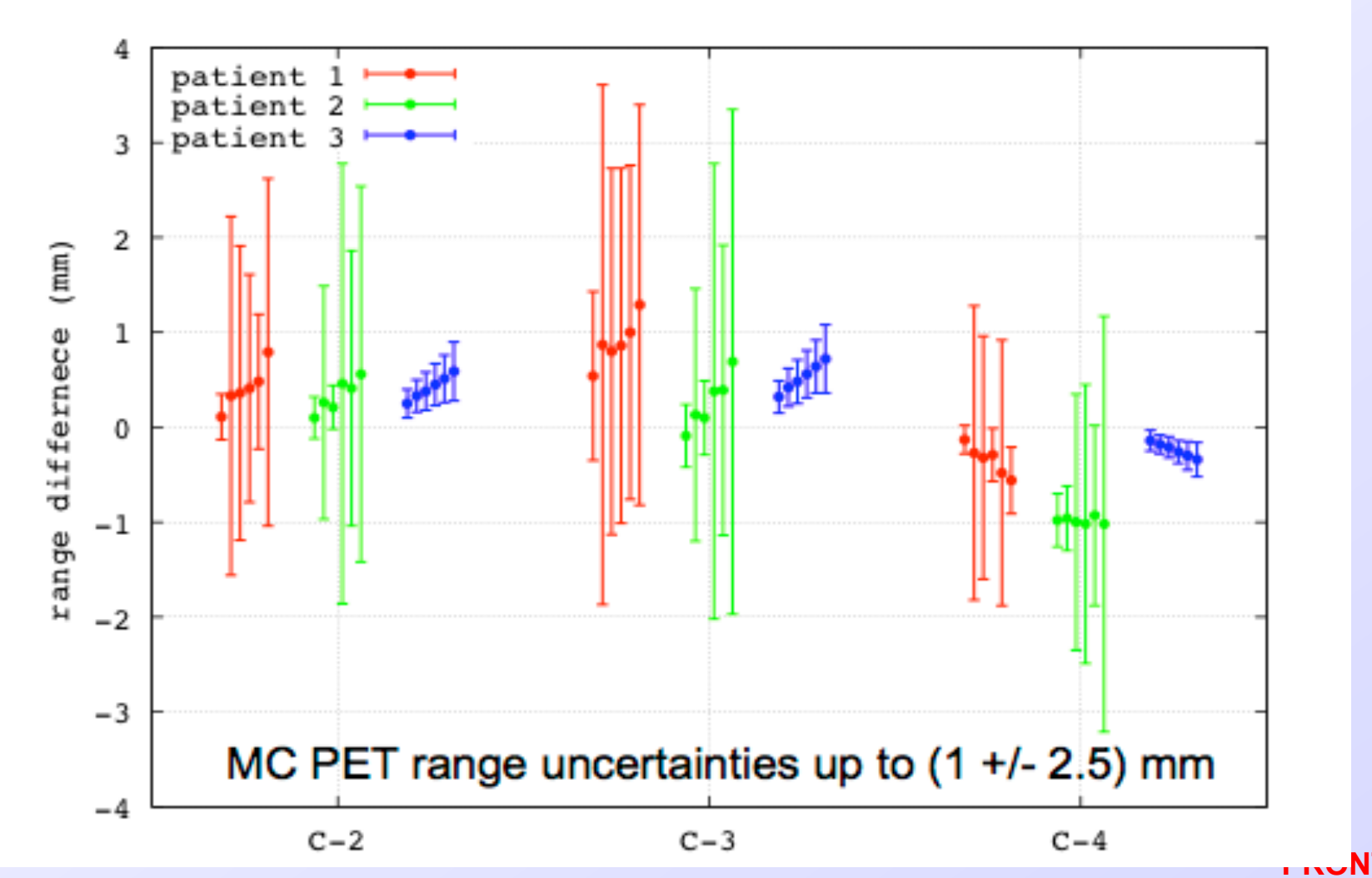

Reliability of nuclear interaction cross section data to predict proton-induced PET images in proton therapy

Which cross sections should be used?

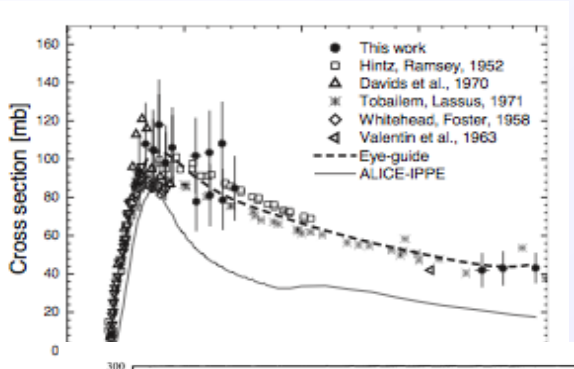

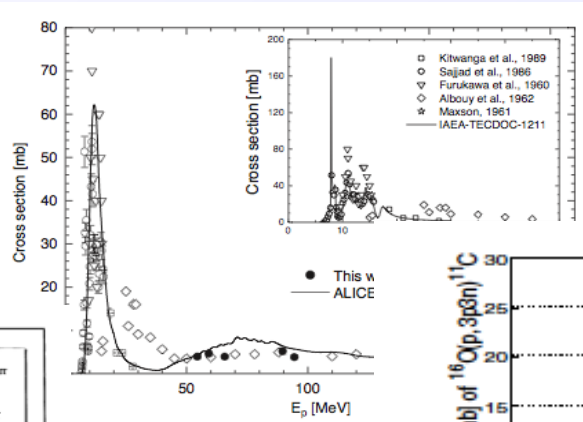

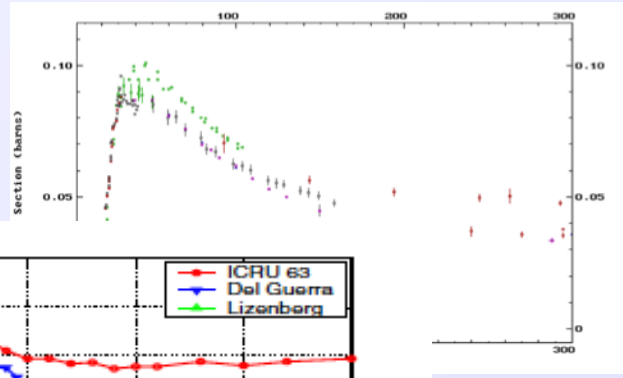

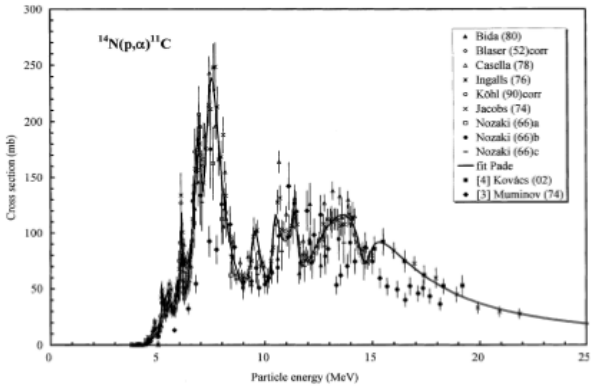

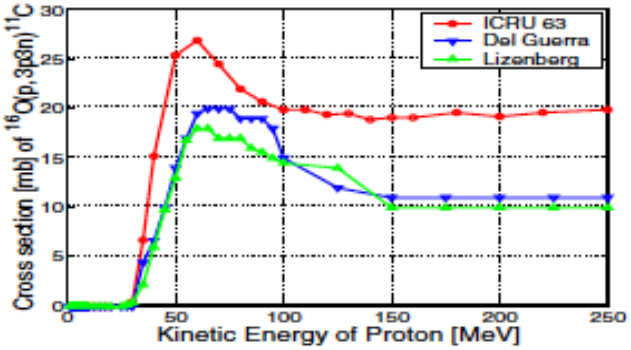

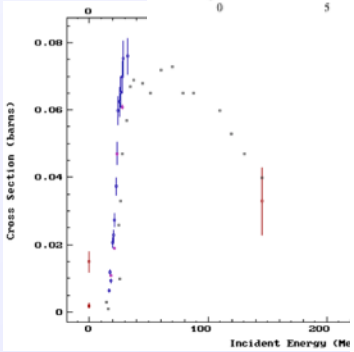

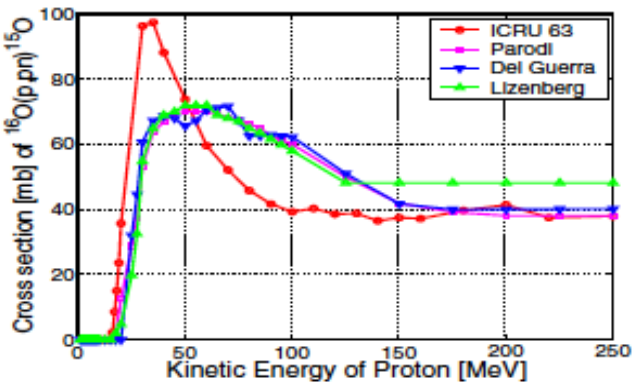

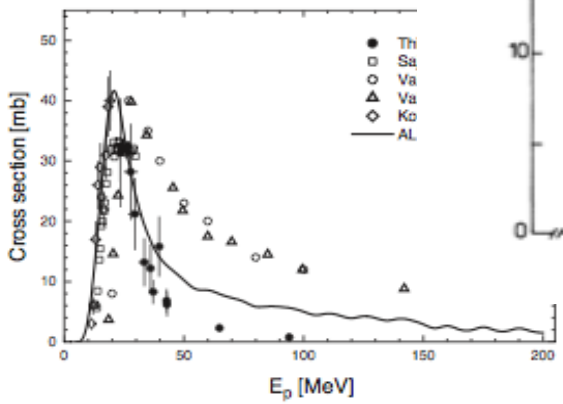

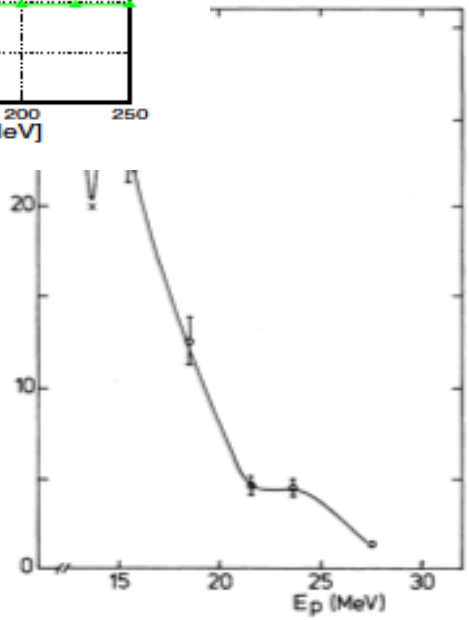

β+ isotope production

S. España

$^{12}C(p,pn)^{11}C$
$^{16}O(p,3p3n)^{11}C$
$^{14}N(p,2p2n)^{11}C$
$^{16}O(p,pn)^{15}O$
$^{16}O(p,2p2n)^{13}N$
$^{nat}N(p,X)^{13}N$
$^{31}P(p,pn)^{30}P$
$^{40}Ca(p,2pn)^{38}K$

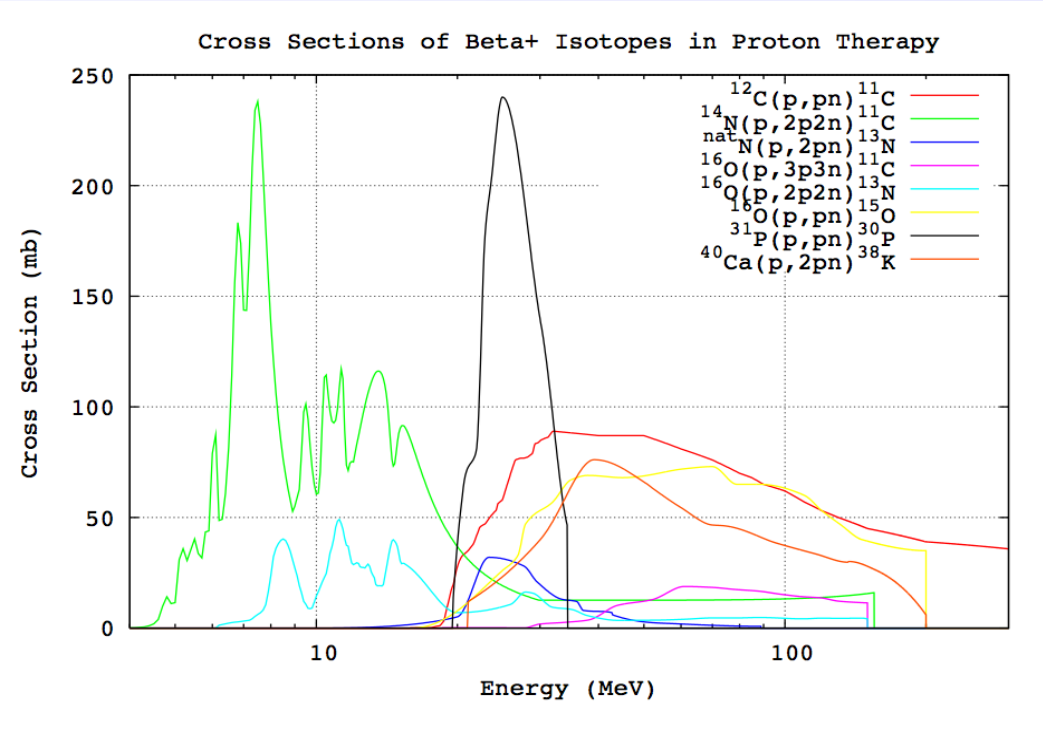

Isotope	Half life (min)
^{15}O	2.03
^{11}C	20.33
^{13}N	9.96

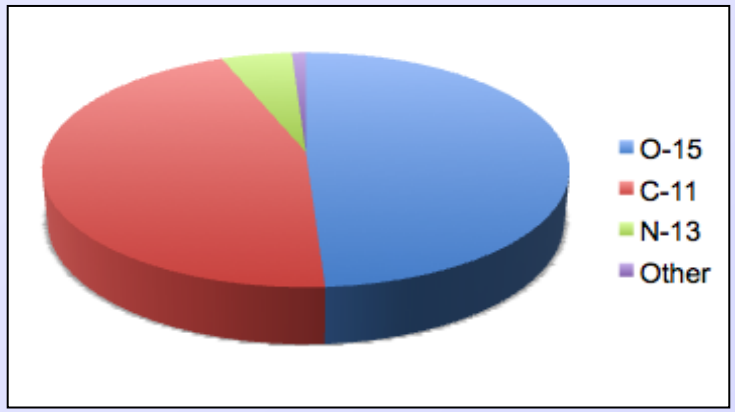

Heterogeneous phantom experiment

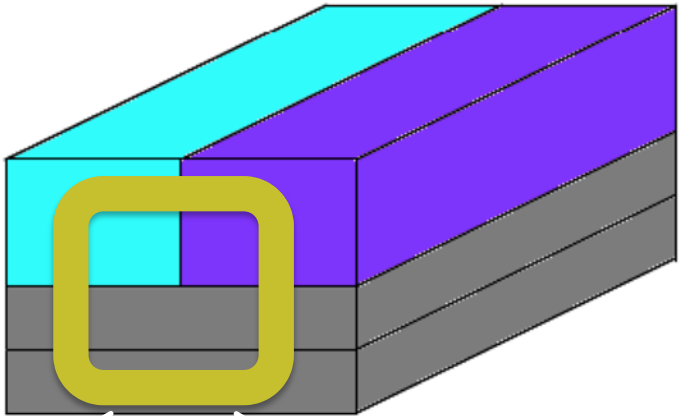

Tissue-equivalent gel

98% water + 2% gelatin

High-density polyethylene

7×7 cm^2 aperture

	C	H	N	O	density
	14.9%	9.6%	1.46%	73.8%	1.13 g/cc
	1.04%	11.03%	0.32%	87.6%	1.01 g/cc
	85.7%	14.3%	0.0%	0.0%	0.95 g/cc

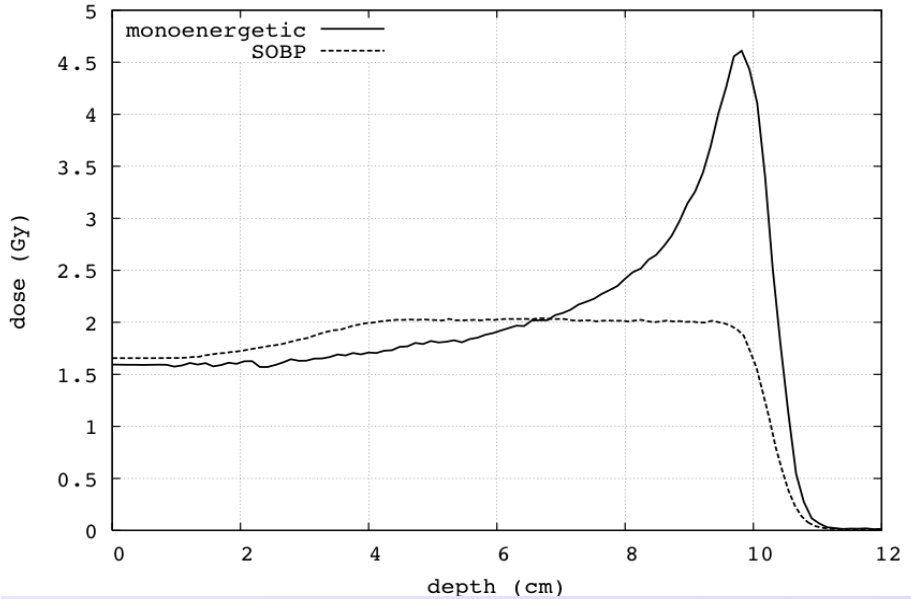

- Monoenergetic 10 cm range
- SOBP 10 cm range, 6 cm modulation

Experimental Setup

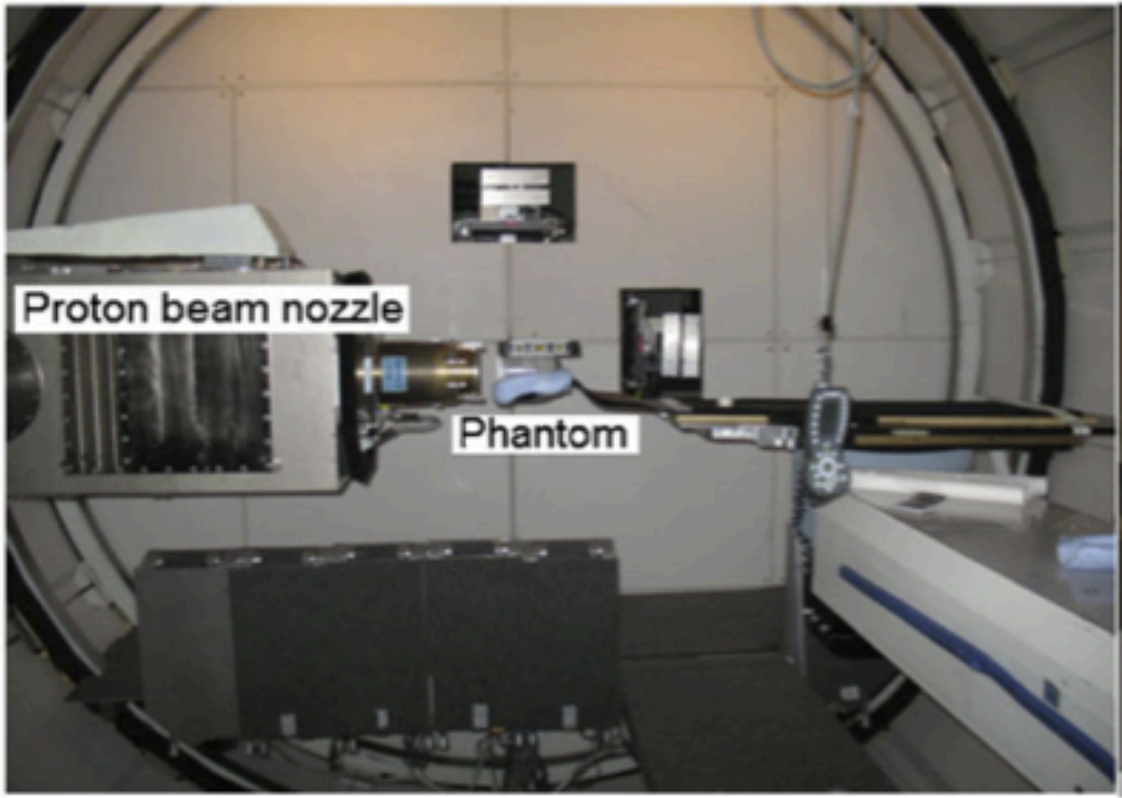

(a) Proton treatment position.

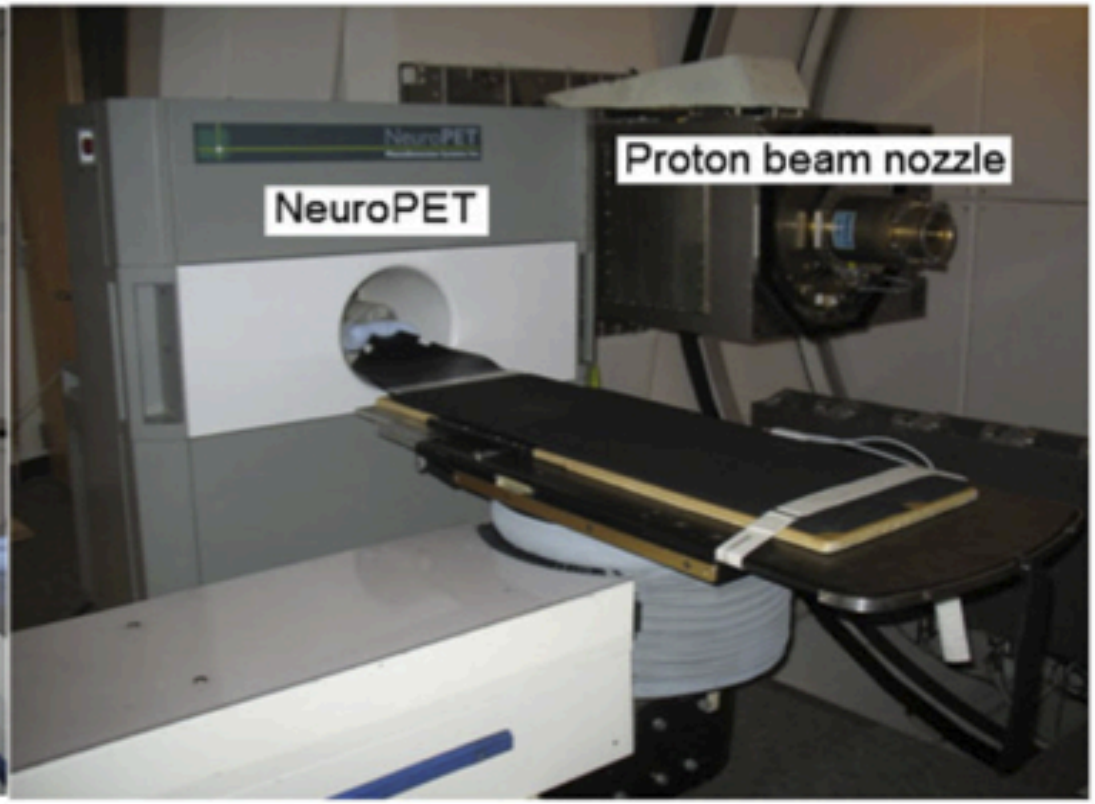

(b) PET scan position.

	C	H	N	O	density
98% water + 2% gelatin	1.04%	11.03%	0.32%	87.6%	1.01 g/cc

& In-room => $^{16}O(p,pn)^{15}O$

$^{12}C(p,pn)^{11}C$

$^{16}O(p,3p3n)^{11}C$

$^{14}N(p,2p2n)^{11}C$

$^{16}O(p,pn)^{15}O$

$^{16}O(p,2p2n)^{13}N$

$^{nat}N(p,X)^{13}N$

$^{31}P(p,pn)^{30}P$

$^{40}Ca(p,2pn)^{38}K$

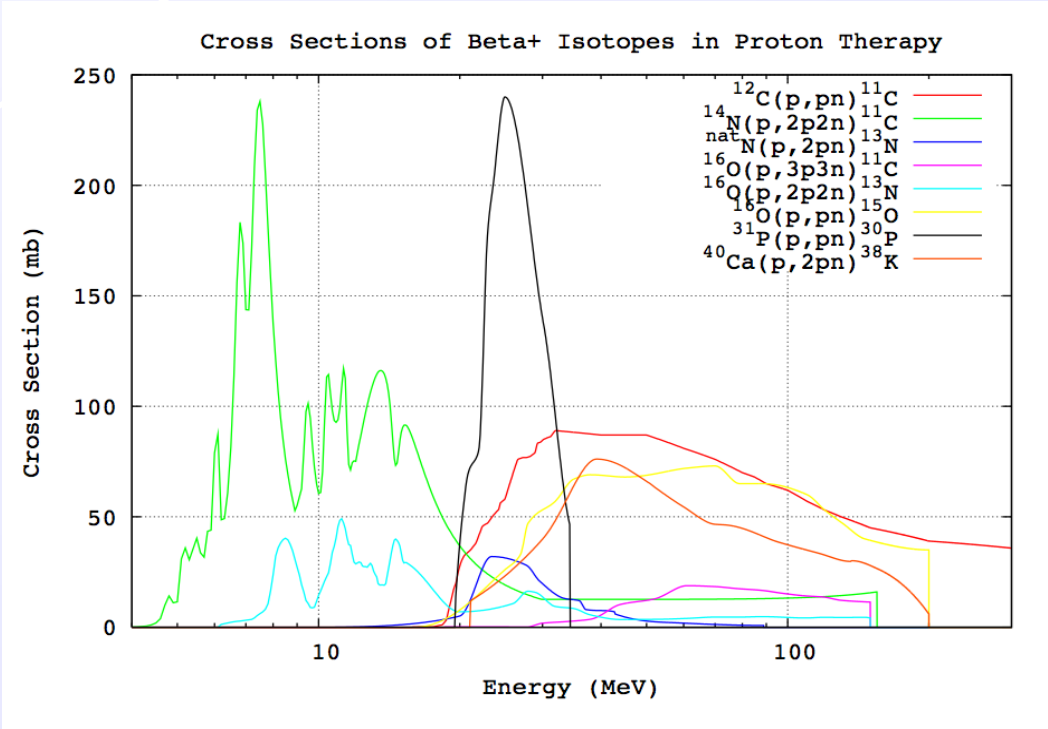

Isotope	Half life (min)
^{15}O	2.03
^{11}C	20.33
^{13}N	9.96

	C	H	N	O	density
Tissue-equivalent gel	14.9%	9.6%	1.46%	73.8%	1.13 g/cc

=> Mixture of channels

monoenergetic

SOBP

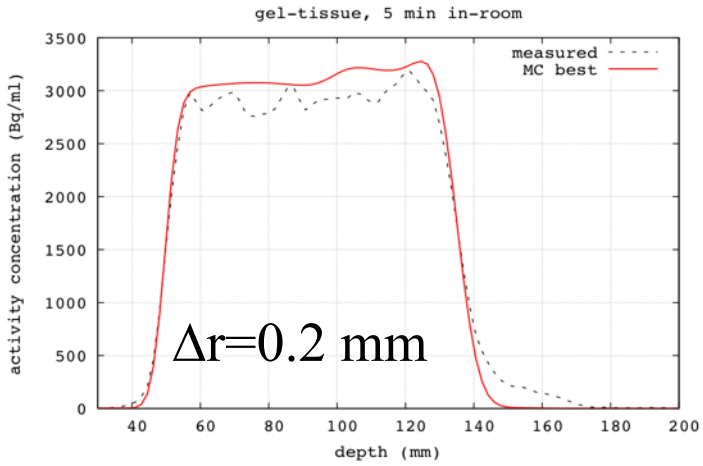

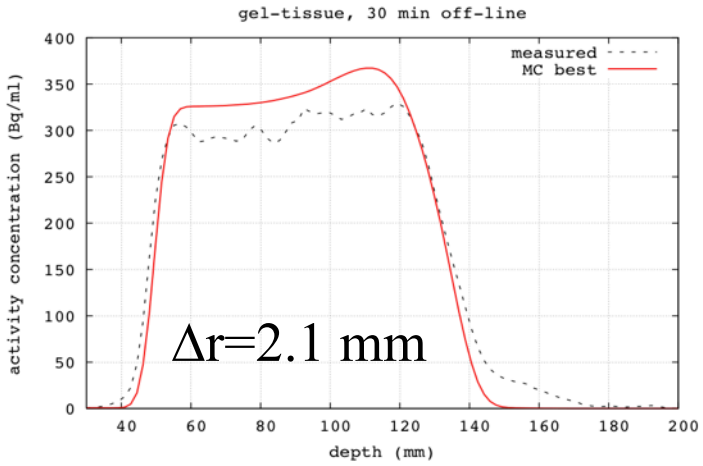

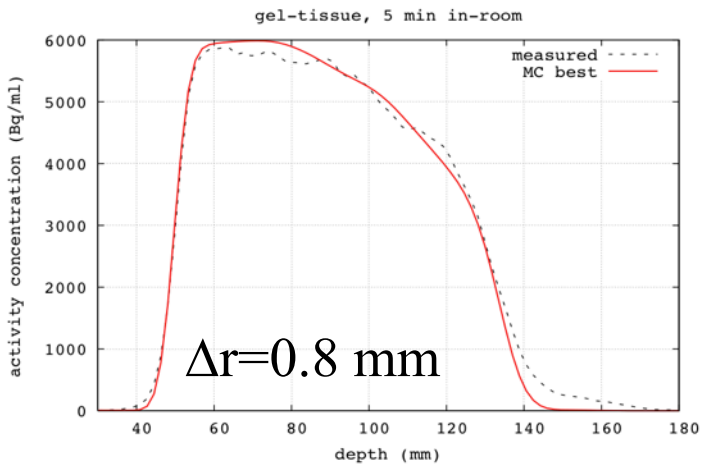

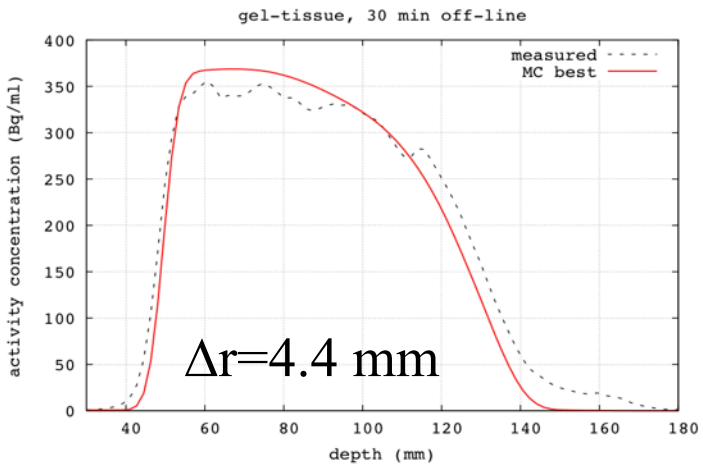

In-room

Off-line

PET: Changes during treatment

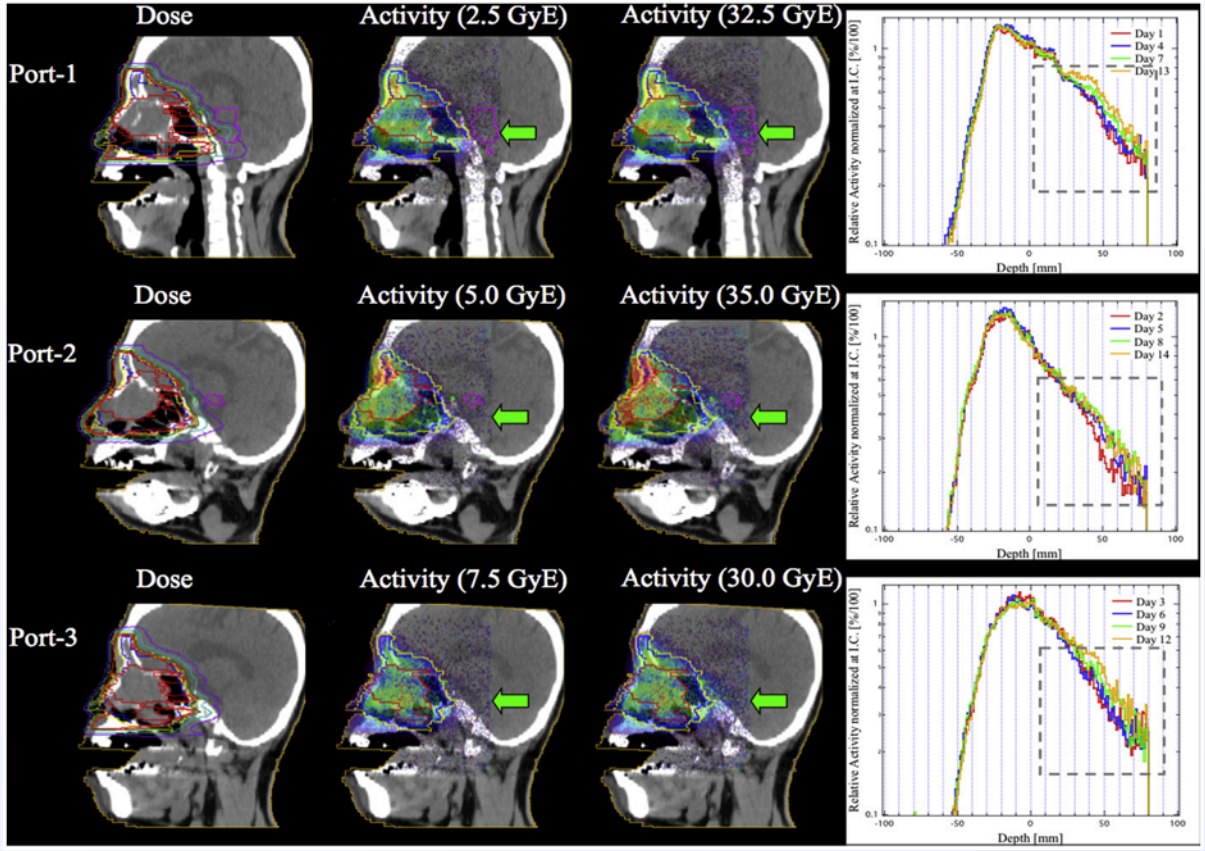

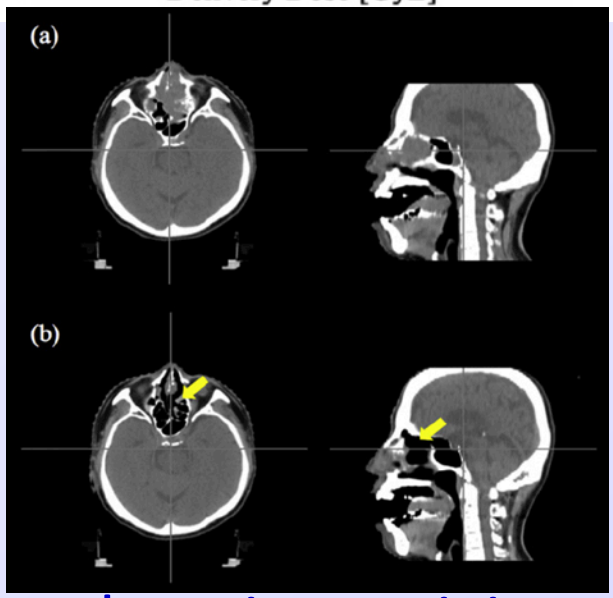

In 3 of 18 clinical cases of the head and neck, the changing activity range of more than 10 mm was observed.

A new CT image acquisition and the retreatment planning .

The reduction of the tumor's volume was more than 100 ml.

PROMPT GAMMA IMAGING

Prompt Gamma Imaging

- ✓ After a nuclear interaction in the patient, nuclei can be left in an excited state. The resulting high-energy (~MeV) gamma radiation emitted shortly (within ~10^{-8} s) after the excitation can be detected.
- ✓ The energy range between 1 and 8 MeV is targeted as it holds the main peaks for oxygen and carbon reaction channels.
- ✓ The disadvantage compared to the PET method is the lack of a two-photon coincidence signal for 3D reconstruction.

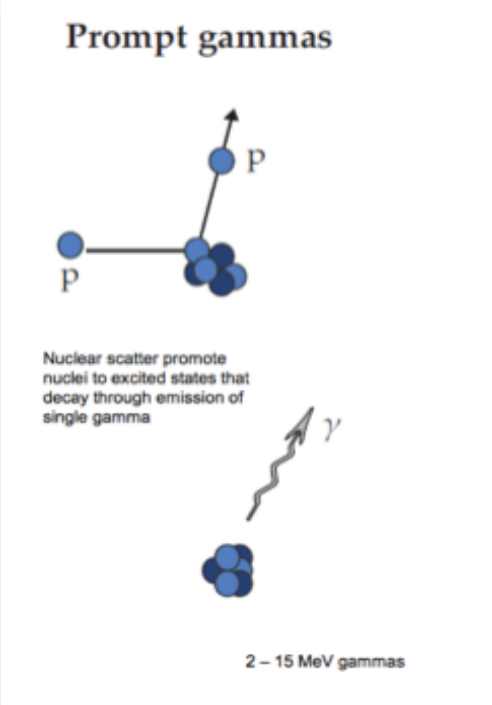

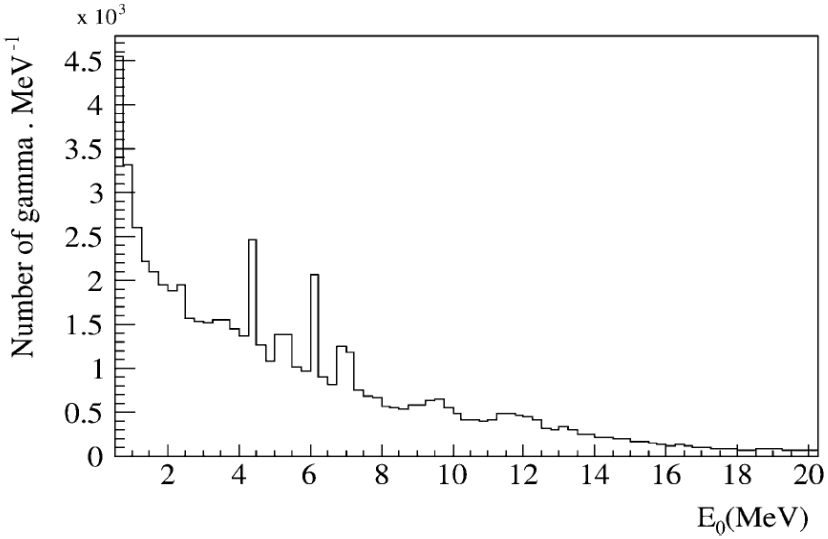

Fig. 3. Emission spectrum (Geant4 simulations) in 4π steradians of prompt γ between 0.5 and 20 MeV obtained with 10^5 ^{12}C at 310 MeV/u in water.

Advantages of Prompt Gamma

- ✓ Prompt gamma method has various advantages compared to PET.
  - →Prompt gammas result in a much higher count rate at production that might even **allow range verification during instead of after dose delivery**
  - →There is **no biological washout**.
  - →The maximum in the nuclear interaction cross sections leading to **prompt gammas appear at a lower energy and thus typically closer to the Bragg peak**. Prompt gamma and dose with the prompt gamma 50% falloff within 1 mm proximal to the dose falloff whereas the PET 50% falloff positions are about 5 mm proximal.

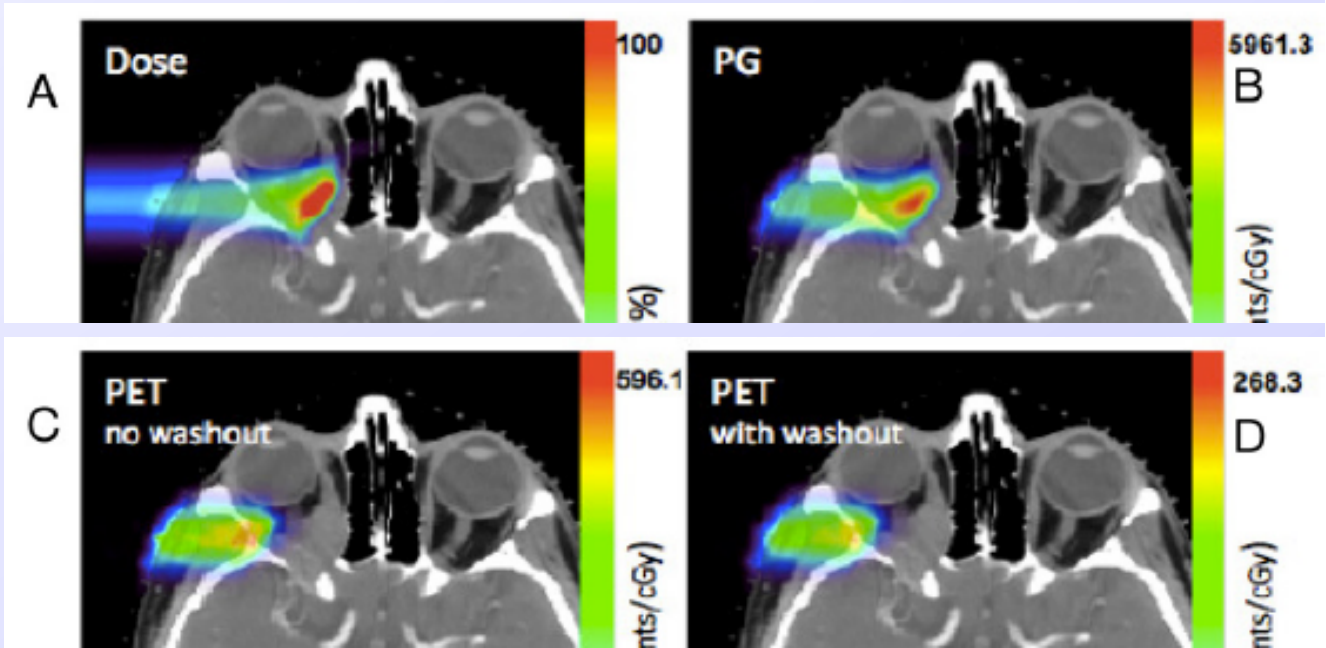

Prompt Gamma: Detector Configurations

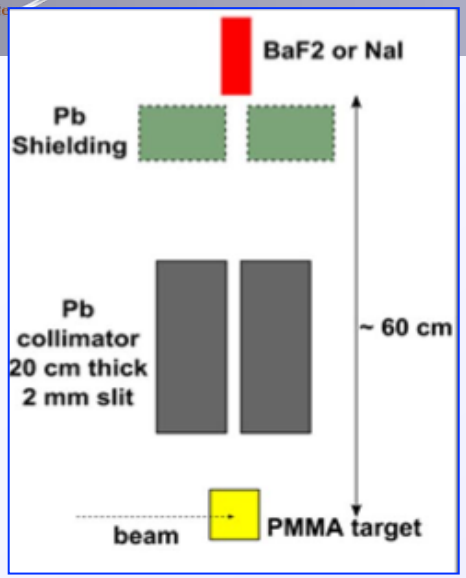

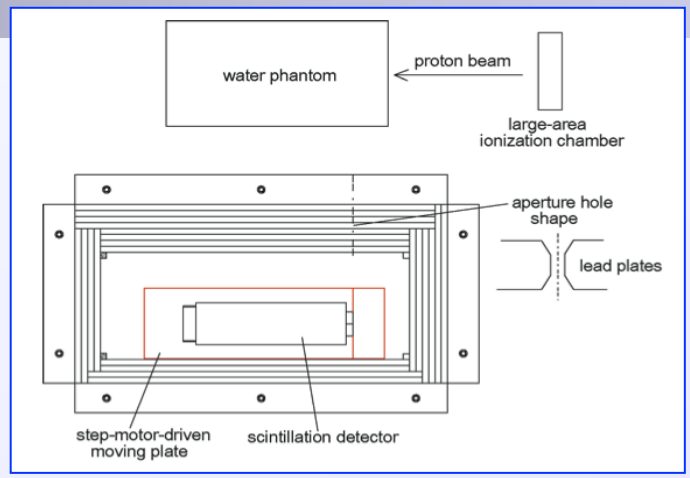

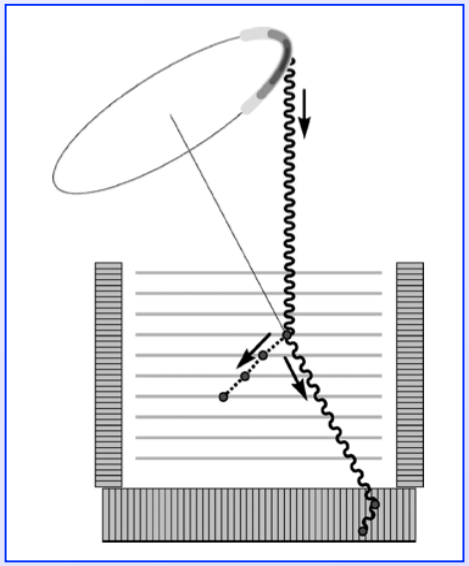

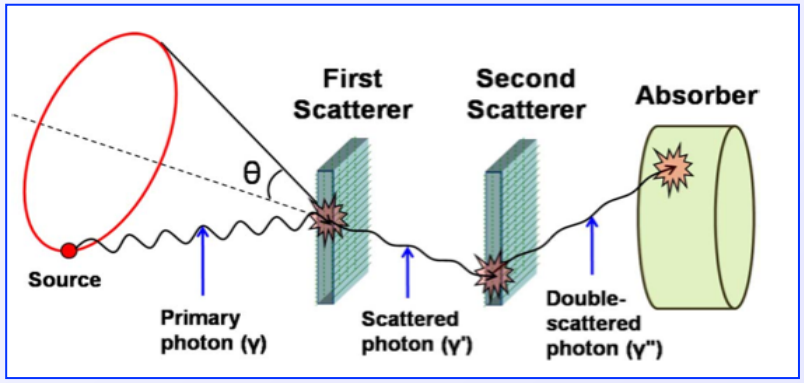

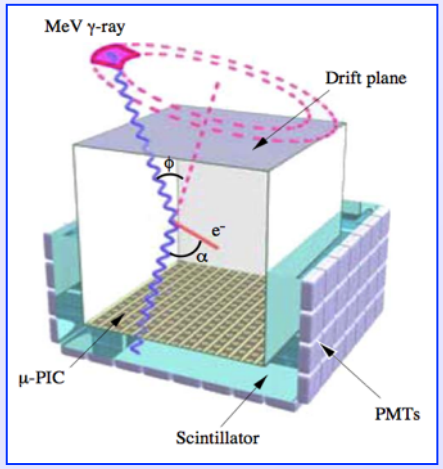

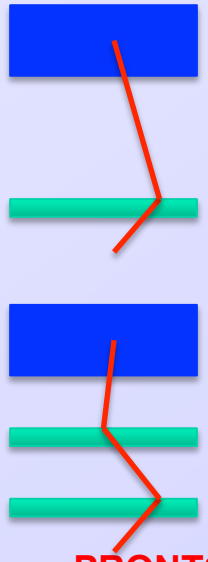

Two-stage Compton camera:

Full absorption to determine inital energy => low efficiency

Three-stage Compton camera:

Not full absorption needed => efficiency X ??

Knife-Edge Slit Camera

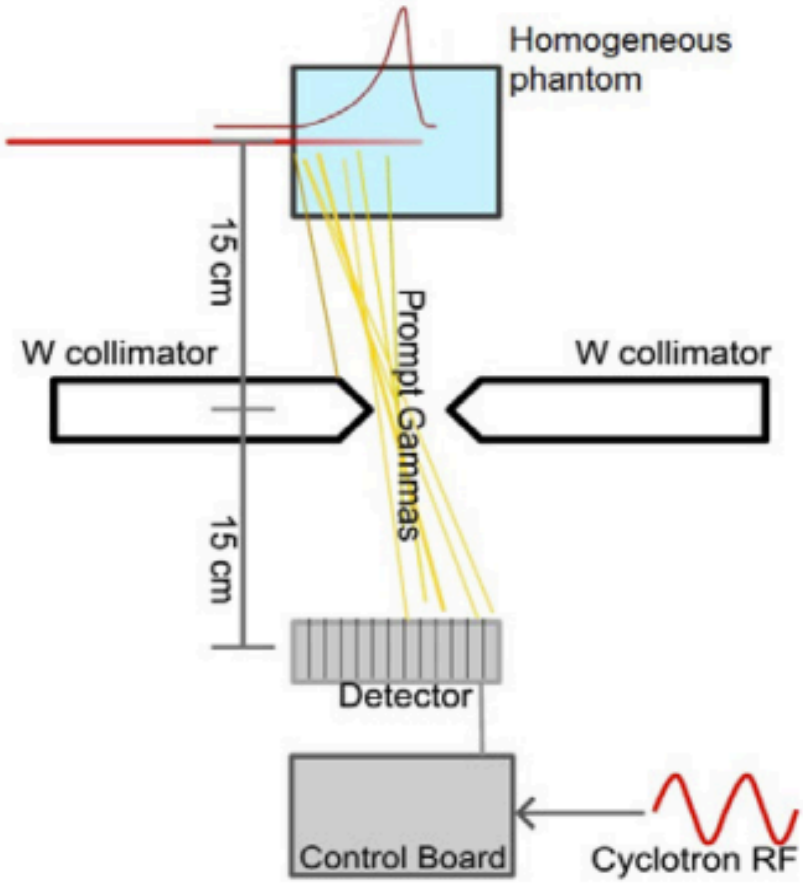

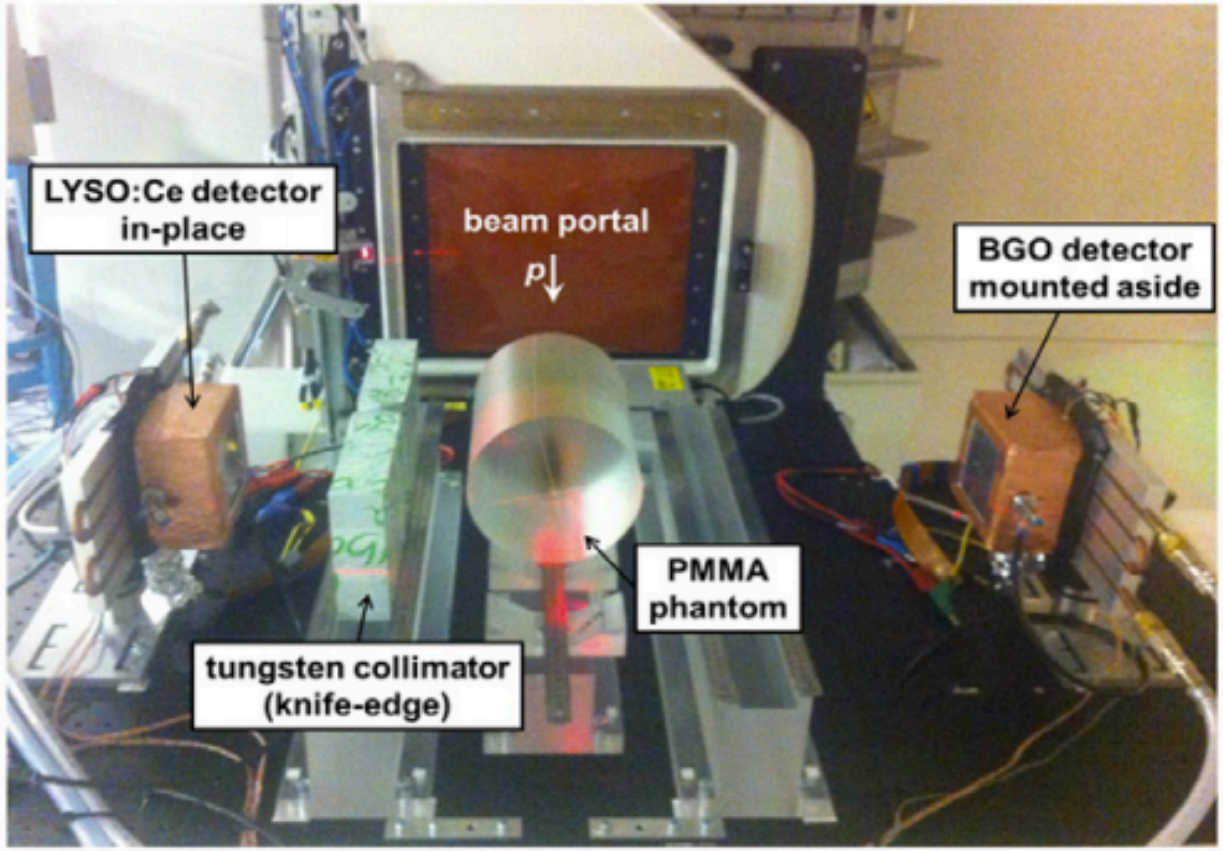

Knife-Edge Slit Camera

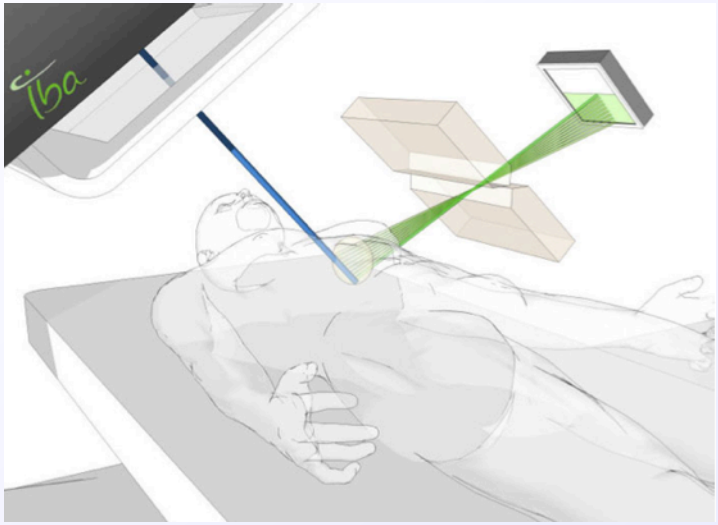

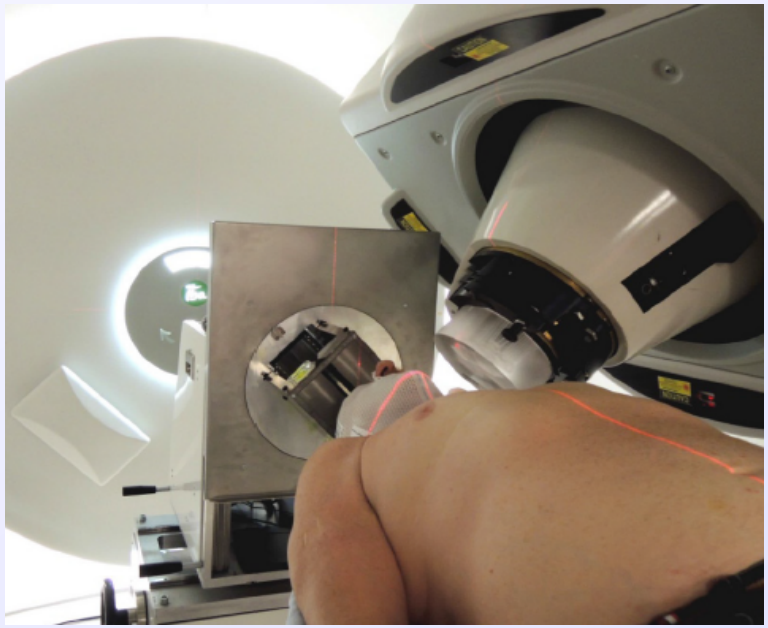

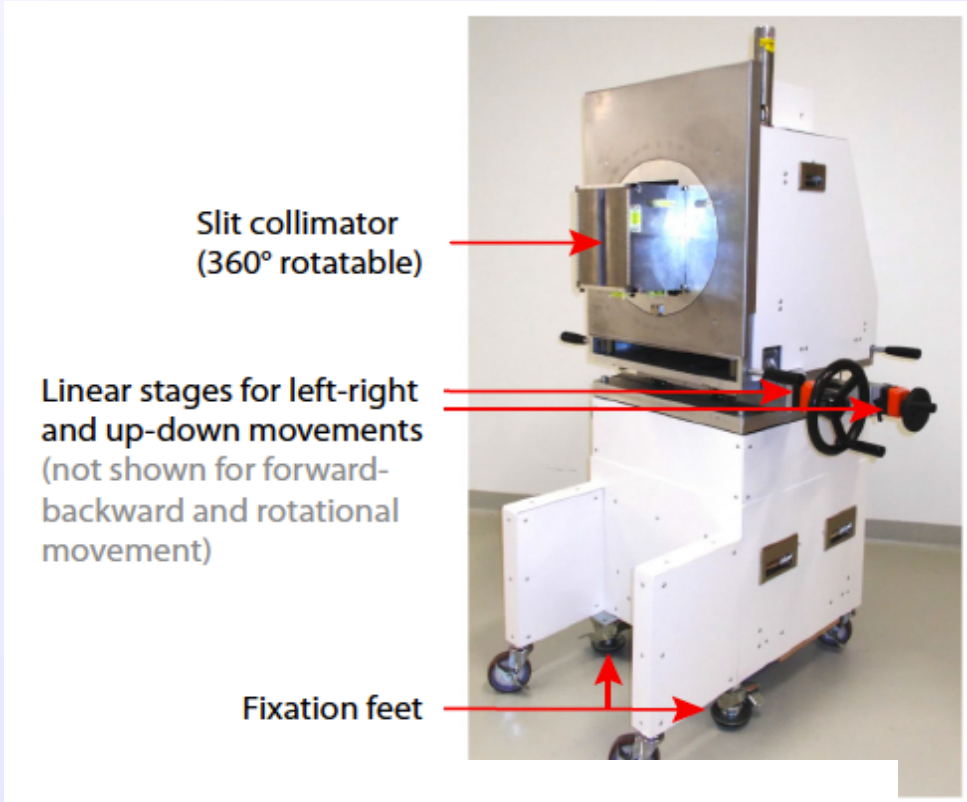

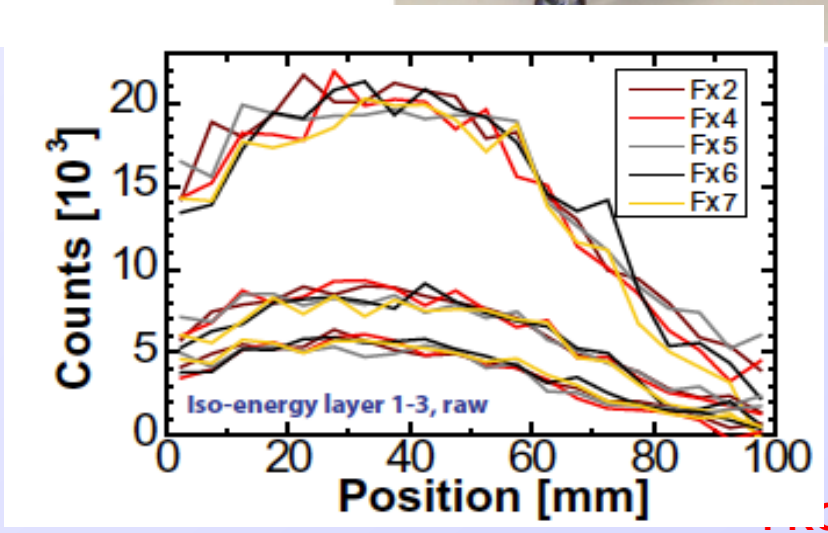

GEMPix for Hadron Therapy

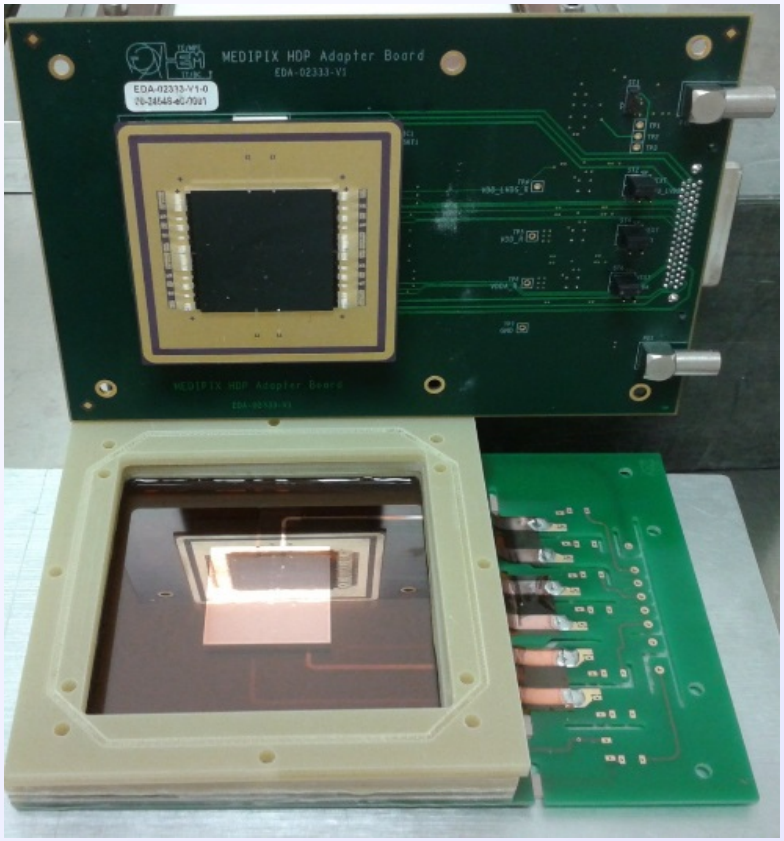

GEMPix detector: 2 x 2 Timepix chips combined with gas detector
8 cm^2 GEM detector read by 55x55μm pixels, 262 000 channels

M. Campbell, EP Department

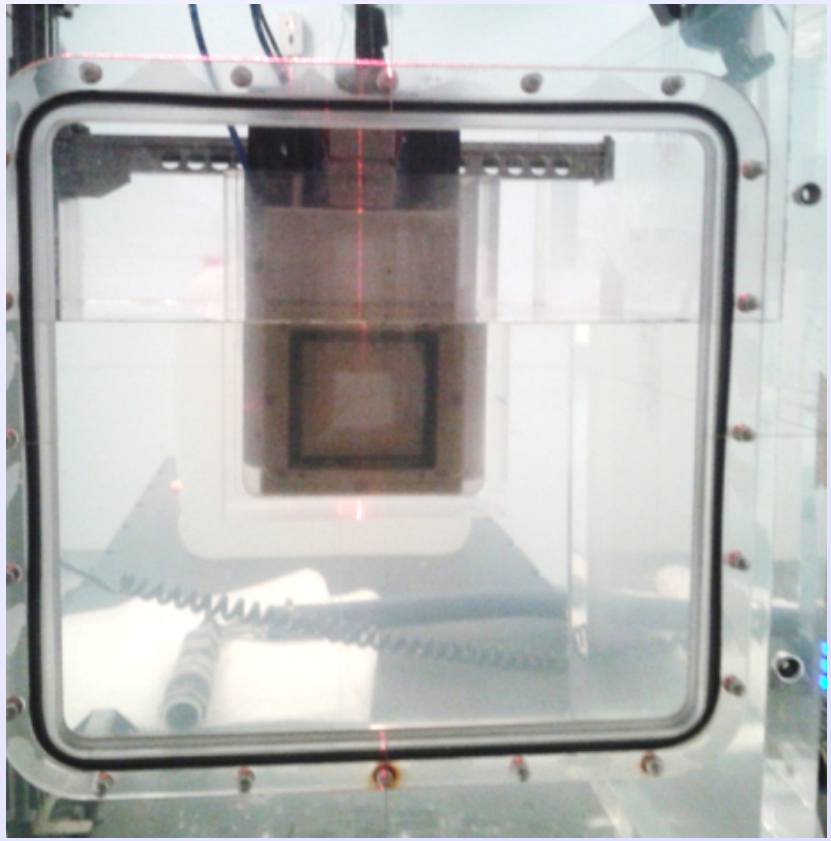

GEMPix placed in phantom

F. Murtas , M. Silari, S. George,
A. Rimoldi, A. Tamborini,
M. Ciocca and A. Mirandola
CERN, INFN, UNIPV, CNAO

Carbon Therapy beam monitoring

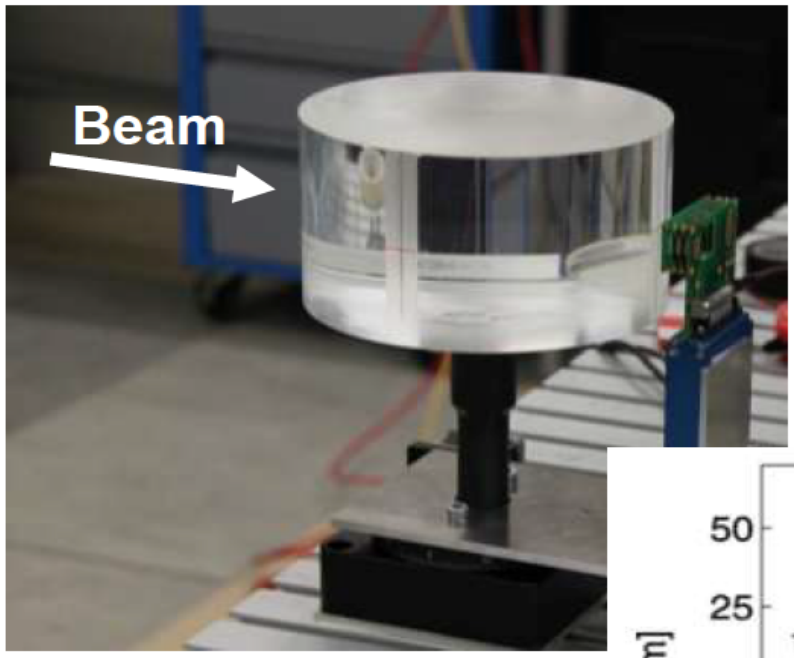

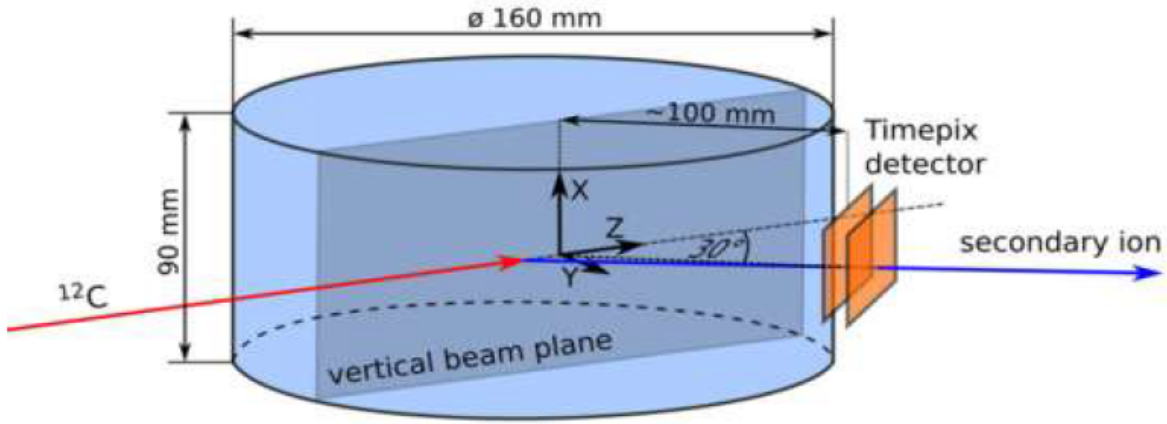

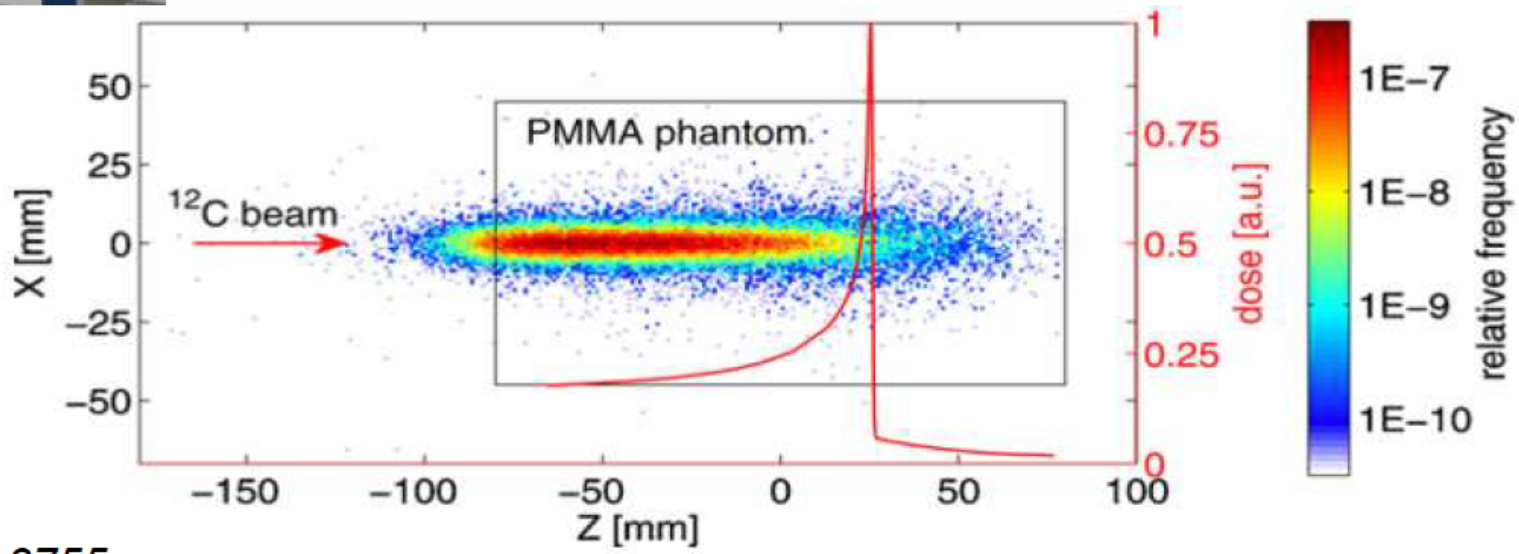

Gwosch et al.: PMB 58 (2013) 3755

M. Martisikova, German Cancer Research Centre, Heidelberg

Proton CT

Range uncertainties are in part caused by translating photon attenuation imaged in CT scanners to relative stopping power for dose calculations. This uncertainty would be minimized if the relative stopping power would be measured directly using a particle beam.

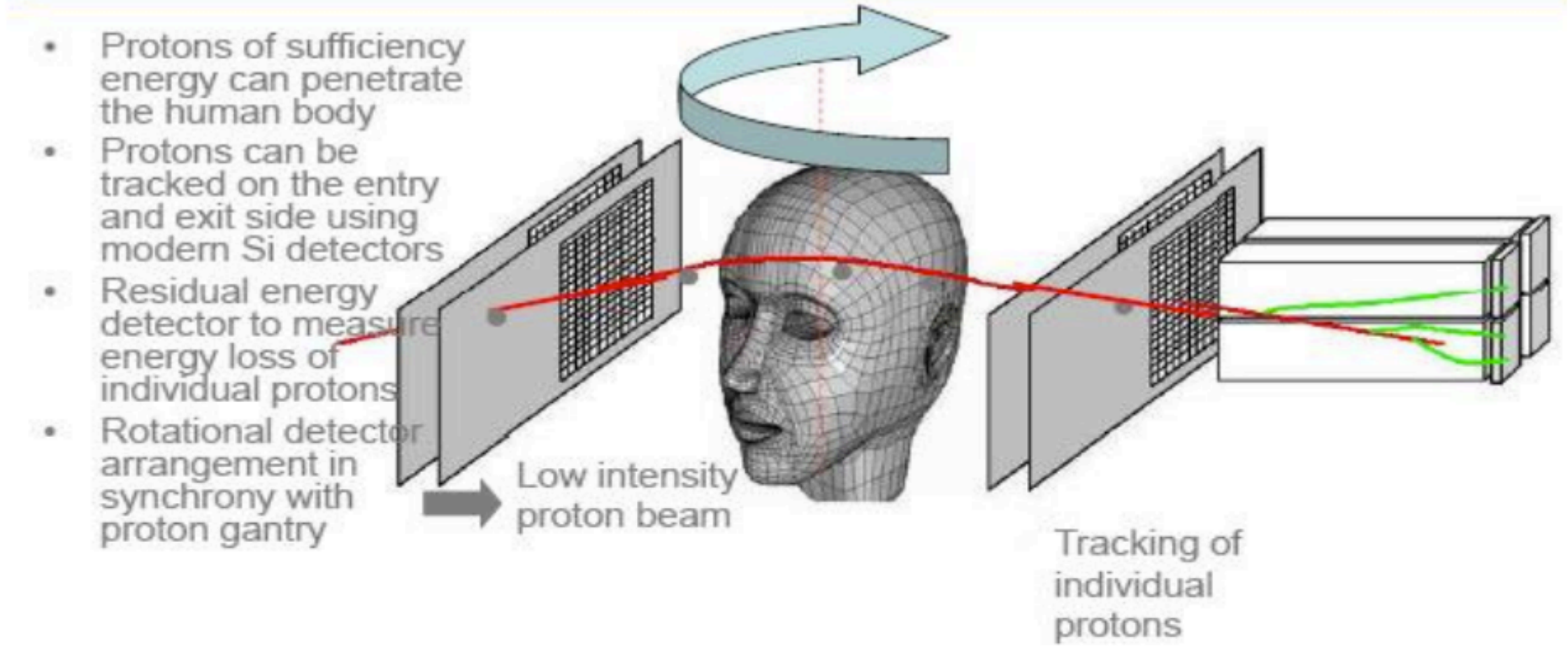

Acvantages of proton CT

- ✓ Reduce range uncertainty from 3% to 1%
  - → better electron map for the planning
  - → better dose accuary to target voluem
- ✓ Avoids CT artifacts arising rom high Z materials
  - → metal/dental implants
- ✓ Lower doe to patient compared to X-ray CT
  - → factor of 3!!
  - → pCT head dose = 1.4 mSv vs. X-ray CT dose = 5.0 mSv
- ✓ pCT imaging able to replace X-ray imaging for alignment prior to treatment

Spatial resolution worse, but density resolution better

RADIOISOTOPE PRODUCTION AND PROOF OF PRINCIPLE

Production of radioisotopes

✓ Cockcroft-Walton 5 MV tandetron accelerator at CMAM

→ 10 MeV proton beam with intensities up to ~1 μA

Natural Ni

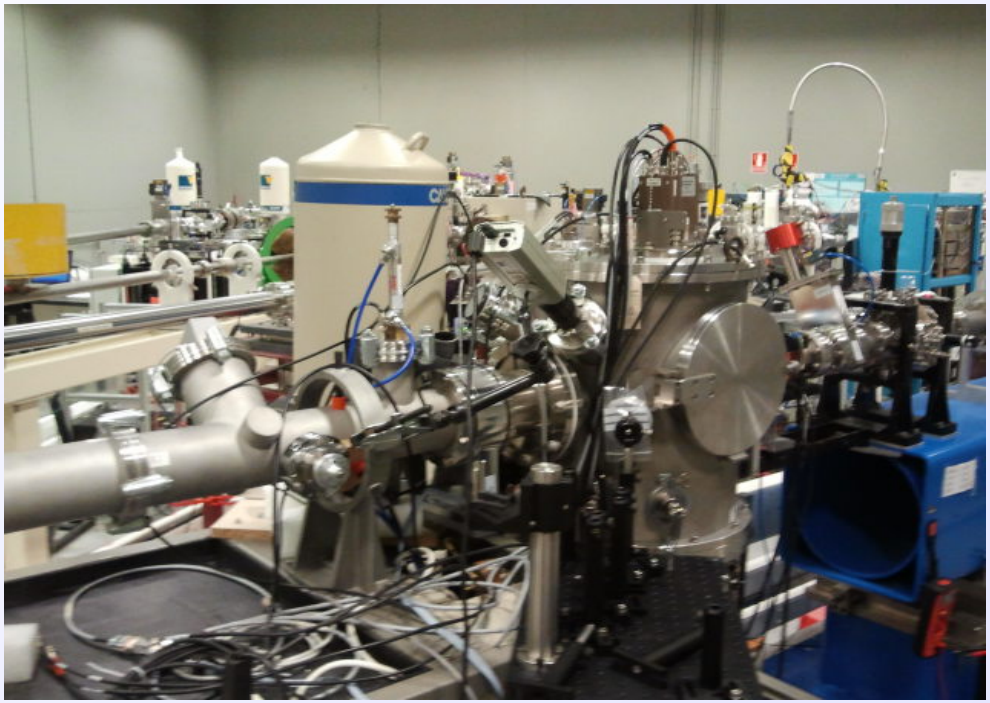

Low activation (<2 μCi) as proof of concept

Solid thin target foils, Ta backing

About 1 min activation

Monitoring by efficiency-calibrated HPGe detector

Natural Mo

Production of ^{60}Cu, ^{52m}Mn and ^{94m}Tc

- ✓ Studied at a linear accelerator (CMAM, Madrid)
  - → mPET: they emit beta-delayed gamma-rays
  - → They can label tracers of interest
  - → Their half-life is suitable for PET studies
  - → Can be produced by proton induced reactions at ~10 MeV
  - → Cross-sections subject to uncertainties at low energy

J. López Herraiz
A. Andreyev et al. PMB 2011
E. Lage et al Med. Phys, 2015
J. Cal-Gonzalez et al. PMB 2015

Isotope	Half-life	β^+ branch (%)	Main Prompt γ (MeV) and Yield (%)	Target	Reaction	Energy threshold (MeV)	Cross – Section (barn) @ 10 MeV
^{60}Cu	23.4 min	93%	1.333 (80%) & 1.760 (52%)	^{Nat}Ni (26.16% ^{60}Ni)	^{60}Ni(p,n)^{60}Cu	6.91	0.25
^{52m}Mn	21.1 min	95%	1.434 (98%)	^{Nat}Cr (83.8% ^{52}Cr)	^{52}Cr(p,n)^{52m}Mn	5.49	0.35
^{94m}Tc	53 min	72%	0.871 (94%)	^{Nat}Mo (9.12% ^{94}Mo)	^{94}Mo(p,n)^{94m}Tc	5.04	0.55

A sample of $\beta^+\gamma$ emitters

	$T_{1/2}$ Half-life	β^+ branching ratio (%)	Main Prompt γ [keV] & intensity [%]	Production
^{82}Rb	1.27 min	95	777 (13%)	Generator
^{52m}Mn	21.1 min	97	1434 (96%)	Generator
^{60}Cu	23.7 min	93	1333 (88%)	Cyclotron
^{94m}Tc	52.0 min	70	871 (96%)	Cyclotron
^{110m}In	1.15 h	62	658 (99%)	Generator
^{120}I	1.35 h	46	560 (72%)	Cyclotron
^{44}Sc	3.97 h	94	1157 (100%)	Generator
^{86}Y	14.7 h	33	1080 (85%)	Large $T_{1/2}$
^{76}Br	16.2 h	26	559 (58%)	Large $T_{1/2}$
^{72}As	1.08 d	88	834 (79%)	Generator
^{124}I	4.18 d	23	602 (51%)	Large $T_{1/2}$

Activation results

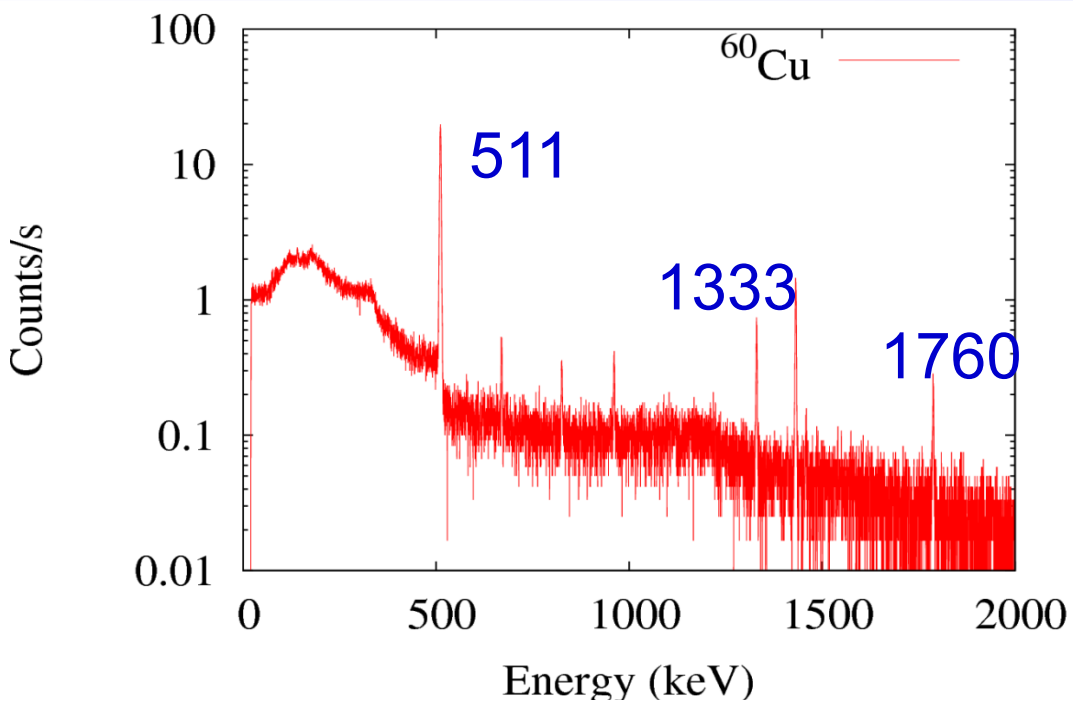

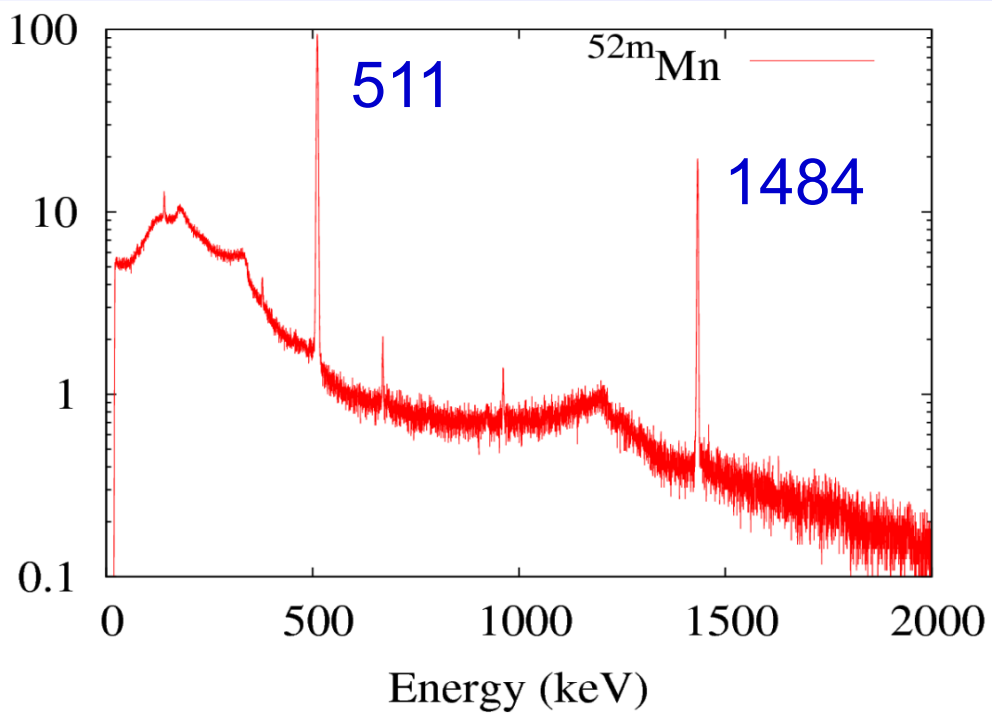

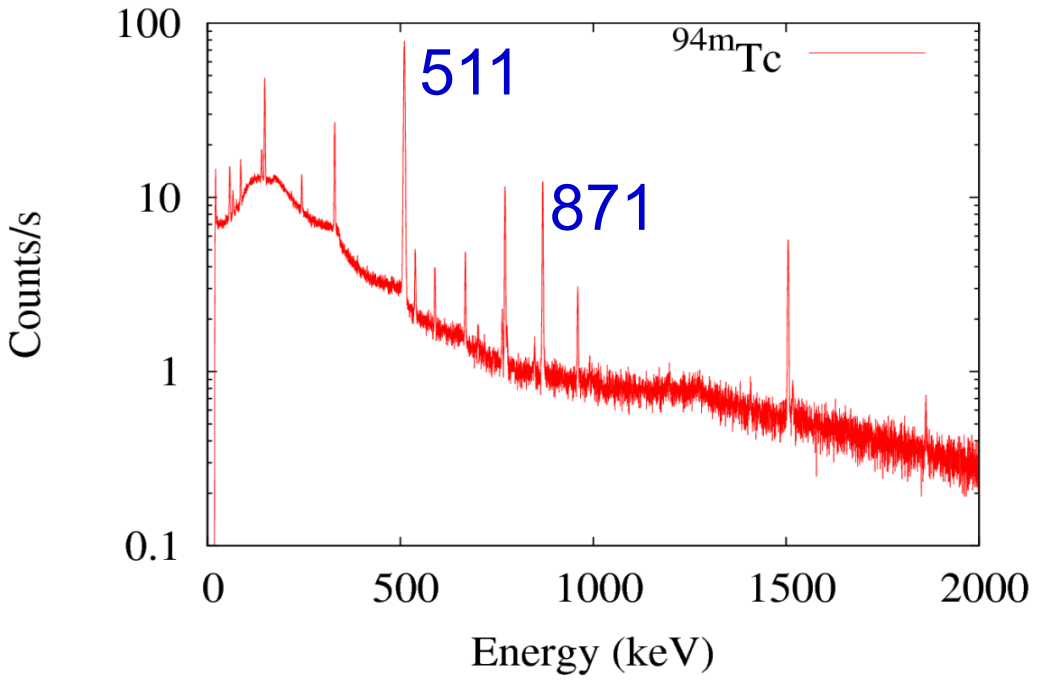

HPGe spectrum of the activated natural Ni, Cr and Mo foils at the end of bombardment

Activation results

- ✓ Expected yields at the end of bombardment (EOB) vs. measured yields:

Target	Thickness (mm)	Total charge (nC)	Irradiation time (s)	Expected yield EOB (mCi/uAh)	Measured yield EOB (mCi/uAh)
^{Nat}Ni	0.200	100.3	10	11.91	**12.11**
^{Nat}Cr	3.175	506.7	10	100.27	**80.35**
^{Nat}Mo	0.100	3000	60	3.63	**5.34**

N. Soppera et al., JANIS Book of proton-induced cross-sections OECD NEA Data Bank
L.P. Szajek et al., Radiochim. Acta 91, 613–616 (2003)
F. Rösch, et al., Radiochim. Acta 62, 115 (1993) and J. Labelled Compd. Radiopharm. 35, 267 (1994)
S.M. Qaim, Nucl. Med. Biol. 27(4) 323 (2000)
D. W. McCarthy et al., Nuclear Medicine & Biology, Vol. 26, 351 (1999)
H. I. West et al., Phys. Rev. C35 (1987)

Imaging: iterative image separation

J.L. Herraiz

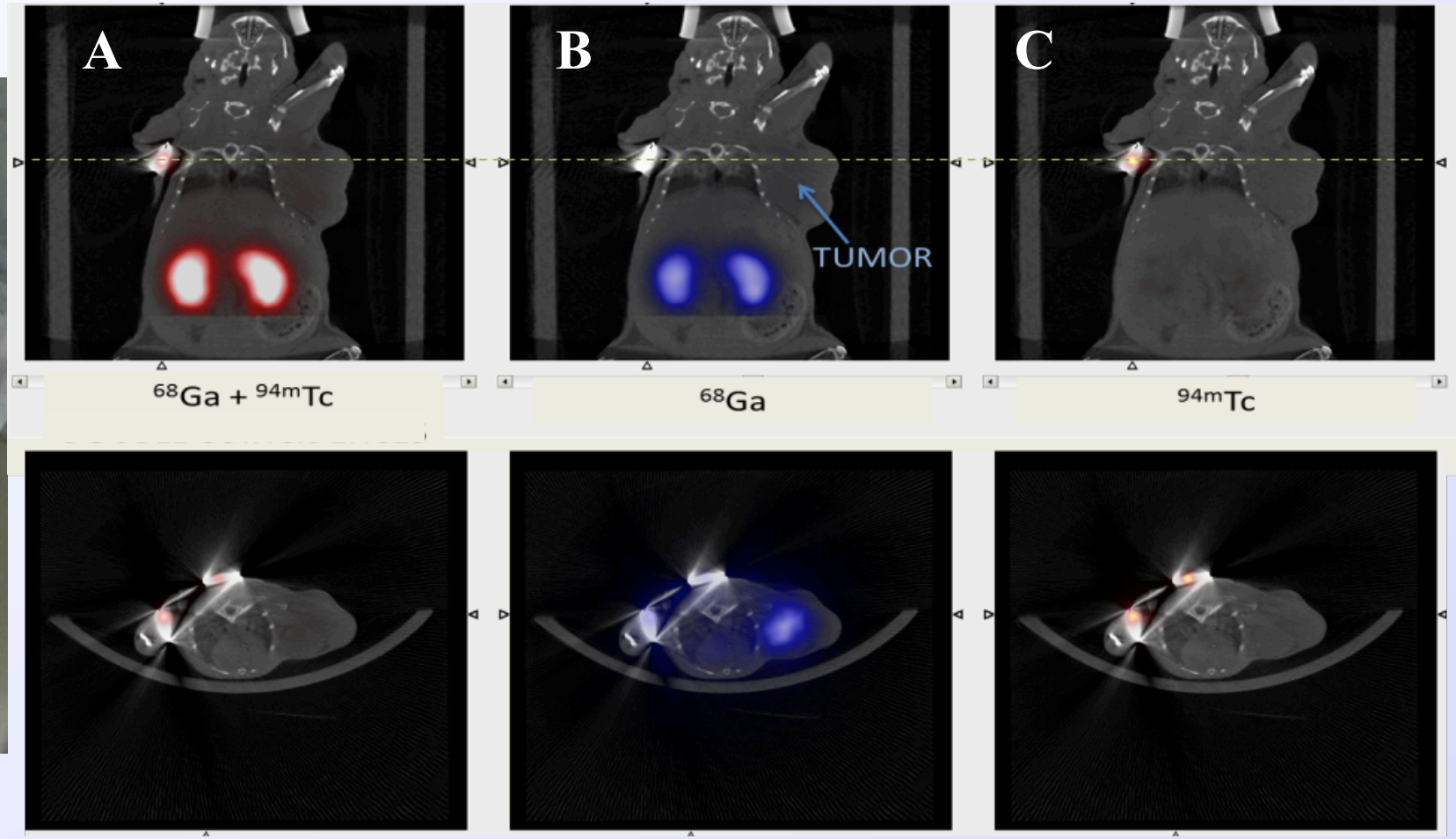

(Left) Mouse in the scanner bed with the foils located in the armpit and on the neck.
(Right) Reconstructed mPET images
(A) Image reconstructed using only double coincidences, standard
(B) (B,C) Reconstructed separated images of ^{68}Ga and ^{94m}Tc using double and triple coincidences, VLOR reconstruction

Ga production and validation

Cross sections, 9 MeV proton beam at CMAM

Nuclear Instruments and Methods in Physics Research A 814 (2016) 110–116

Contents lists available at ScienceDirect

Nuclear Instruments and Methods in Physics Research A

journal homepage: www.elsevier.com/locate/nima

Experimental validation of gallium production and isotope-dependent positron range correction in PET

L.M. Fraile [a,*], J.L. Herraiz [a], J.M. Udías [a], J. Cal-González [a,1], P.M.G. Corzo [a,2], S. España [a,3], E. Herranz [a,4], M. Pérez-Liva [a], E. Picado [a,5], E. Vicente [a,6], A. Muñoz-Martín [b], J.J. Vaquero [c]

[a] Grupo de Física Nuclear, Dpto. Física Atómica, Molecular y Nuclear, Universidad Complutense de Madrid, Spain
[b] Centro de Microanálisis de Materiales, Universidad Autónoma de Madrid, E-28049 Madrid, Spain
[c] Departamento de Bioingeniería e Ingeniería Aeroespacial, Universidad Carlos III de Madrid, Spain

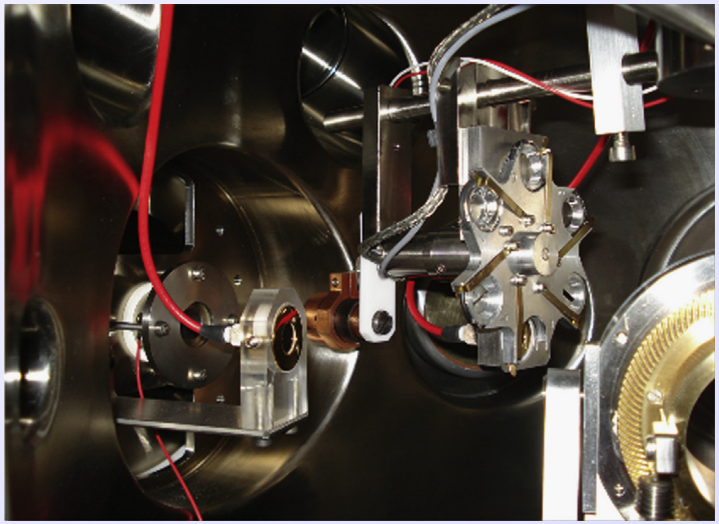

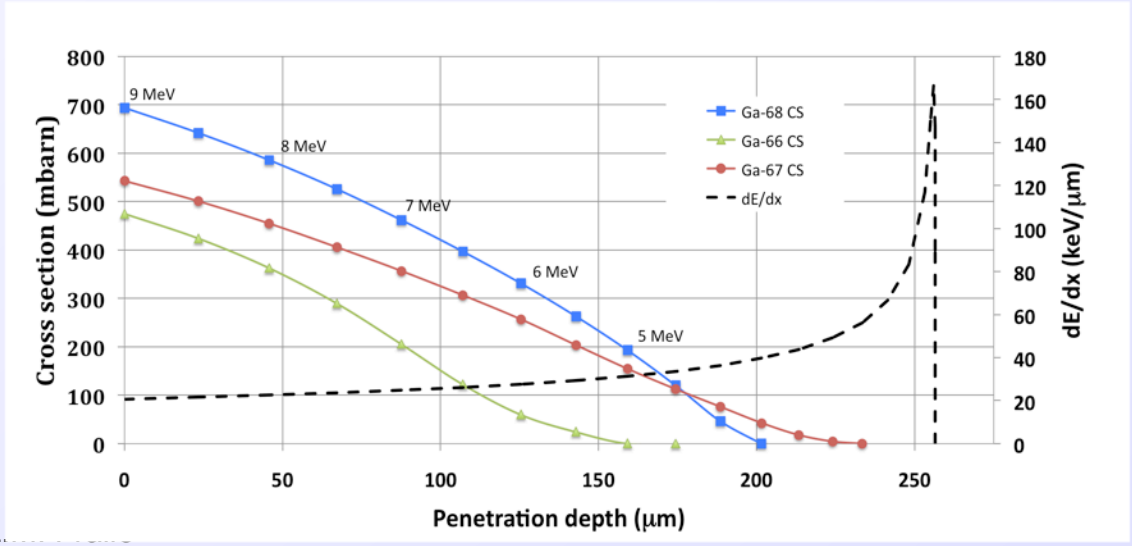

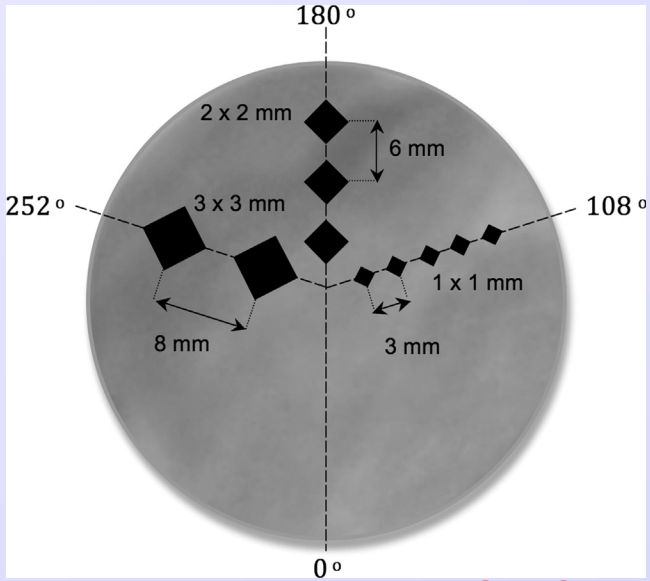

Isotope-dependent range correction

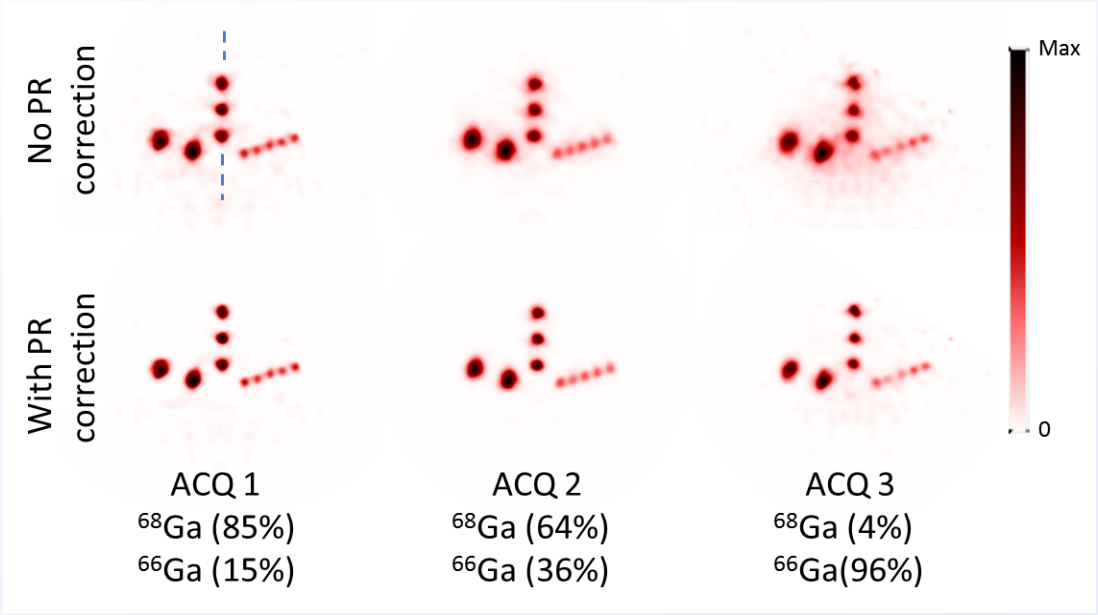

Reconstruction of the Derenzo-like pattern at different times after irradiation

Range correction implemented (lower row)

LMF et al, NIM A814 (2016) 110

Cross-sections as a function of **depth in water**

- ^{68}Ga, ^{67}Ga and ^{66}Ga on Zn scaled to natural abundances
- ^{11}C and ^{15}O

Possibility for Zn contrast in PT?

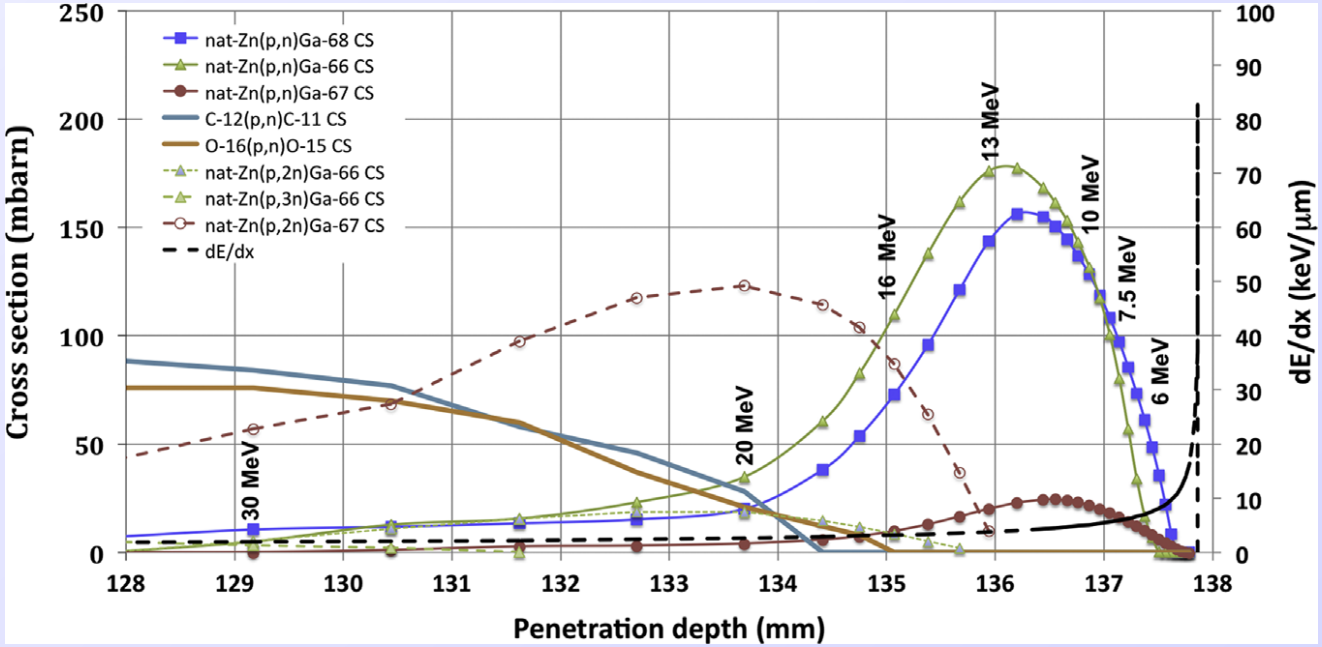

Protontherapy & nuclear techniques for oncology

Pronto
Protontherapy and nuclear techniques for oncology

1. Biophysics simulation package including PET and prompt-gamma activation

2. Exploration of contrast agents for PET and PG

3. Development of new detectors for these imaging modalities

4. Collaboration with clinical partners to eventually include results in clinical protocols

PRONTO

- ✓ Partners
  - → GFN-UCM (coordinator): LMF, S. España, D Sánchez-Parcerisa, JM Udías, J.L. Herraiz
  - → BIOMED-CIEMAT: M.A. Morcillo, E. Romero, N. Magro
  - → FNEXP-IEM-CSIC: E. Nácher, M.J.G. Borge, O. Tengblad
- ✓ Associates
  - → Sedecal Molecular Imaging
  - → CUN: clinical beam (+patients)
  - → Justesa Imagen: radiopharmaceuticals
  - → CMAM: low energy beams
- ✓ Funded for 4 years (2018-2021) by

Comunidad de Madrid

Objectives

- ✓ Biophysics simulation package
  - → Study of existing MC packages: PeneloPET, GATE, TOPAS…
  - → Cross sections
  - → Inclusion of PET/PG isotope activation in FoCa / matRad
  - → Washout models
  - → Experimental validation, phantoms, tissues: CMAM + …
- ✓ Development of contrasts
  - → ex. Zn for several Ga β^+ emitters (channel open at low E)
  - → What concentration can we provide? In which form?
  - → Apart from radiation, what other biological effects can appear?
  - → Other isotopes for PET?
  - → PG isotopes

Objectives (2)

- ✓ Detector developments
  - → PG detector based on FATIMA technology
    - comparison with SEDECAL design
    - Fast and efficient detectors
  - → Adapt CEPA detector for proton range verification
    - Protons and gamma-rays
    - Good energy range
- ✓ Clinical application
  - → Guide research by realistic ojectives and utility for future practice
    - Contact with facility and oncologists

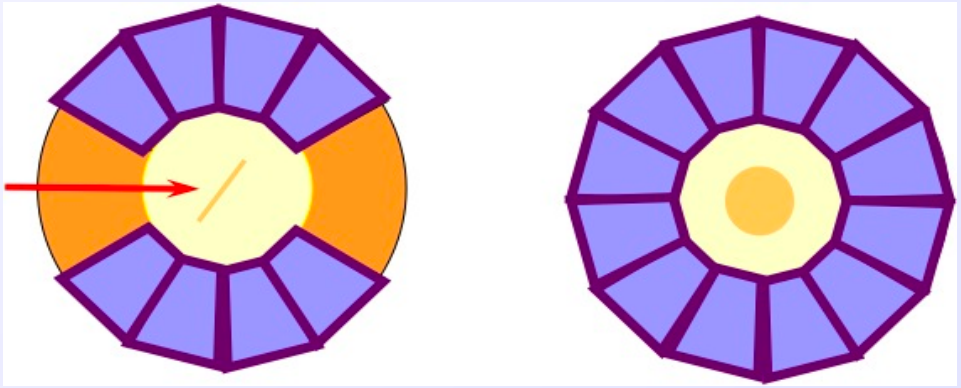

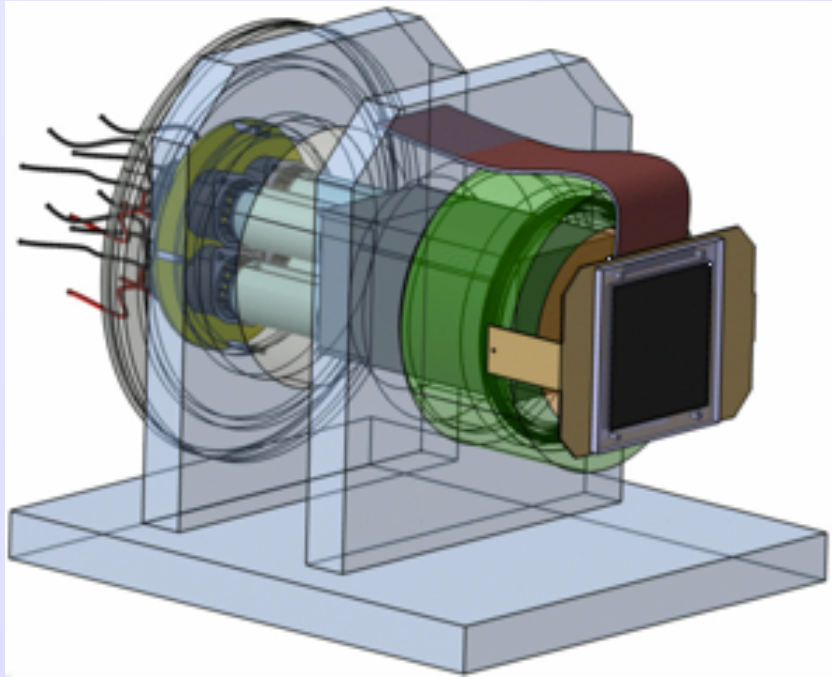

Acknowledgements

Comunidad de Madrid

UNION EUROPEA
FONDO EUROPEO DE DESARROLLO REGIONAL
"Una manera de hacer Europa"

Grupo de Física Nuclear

Thank you!

B2017/BMD-3888
Programas de I+D en Biomedicina 2017

Pronto
Protontherapy and nuclear techniques for oncology

Madrid-MIT m+VISIÓN CONSORTIUM

MARIE CURIE ACTIONS

CSIC
Consejo Superior de Investigaciones Científicas

Ciemat
Centro de Investigaciones Energéticas, Medioambientales y Tecnológicas

campus MONCLOA

FPA2015-65035-P

GOBIERNO DE ESPAÑA
MINISTERIO DE CIENCIA, INNOVACIÓN Y UNIVERSIDADES